This dissertation has been
microfilmed exactly as received

67-8234

CRAIG, James Arthur, 1937-

A STUDY OF THE FREE ENERGIES OF FORMATION OF URANIUM MONOCARBIDE AND URANIUM DICARBIDE.

The University of Michigan, Ph.D., 1966
Engineering, chemical

University Microfilms, Inc., Ann Arbor, Michigan

A STUDY OF THE FREE ENERGIES OF FORMATION OF URANIUM MONOCARBIDE AND URANIUM DICARBIDE

James Arthur Craig

A dissertation submitted in partial fulfillment
of the requirements for the degree of
Doctor of Philosophy in the
University of Michigan
1966

Doctoral Committee:

Associate Professor Richard E. Balzhiser, Chairman
Doctor David V. Ragone (General Atomic/Division of General Dynamics)
Associate Professor Robert D. Pehlke
Professor Maurice J. Sinnott
Professor Edgar F. Westrum, Jr.

ACKNOWLEDGEMENTS

The author would like to express his sincere gratitude to Dr. David V. Ragone whose interest and guidance helped immeasurably in the completion of this work. He is also indebted to Professor Richard E. Balzhiser for serving as Chairman of his Doctoral Committee. The other members of the Doctoral Committee, Professor Robert D. Pehlke, Professor Maurice J. Sinnott, and Professor Edgar F. Westrum, Jr., are acknowledged for their contributions. Appreciation is extended also to Dr. Lee O. Case for his advice at the beginning of the thesis work.

The author would like to express his appreciation to the many members of the staff of General Atomic for their help during the course of this work. In particular, thanks are extended to Messrs. Robert Coburn and Henry Bothman for their help with the experimental apparatus; to Mr. William Tozer for his help in construction and repair of special glassware; to Messrs. Gordon Rankin and Robert Morrissey for their help with chemical analysis; and to Mr. Dwight Smith for his contributions to the experimental program.

Also, the author's thanks are extended to his wife, Beverly, for her patience and encouragement during his doctoral program.

The author acknowledges with sincere gratitude the generous financial support afforded this work by General Atomic/Division of General Dynamics Corporation.

TABLE OF CONTENTS

		Page
ACKNOWLEDGEMENTS		ii
LIST OF TABLES		vi
LIST OF FIGURES		vii
LIST OF APPENDICES		x
LIST OF SYMBOLS		xi
ABSTRACT		xii
I.	INTRODUCTION	1
II.	LITERATURE SURVEY	5
	Uranium Carbides	5
	Alloys	20
III.	EXPERIMENTAL PROGRAM	22
	Equipment	23
	Samplers	28
	Materials	32
	Bismuth	32
	Cadmium	32
	$UC_2 + C$	34
	$UC + UC_2$	35
	Flux	37

TABLE OF CONTENTS (cont'd)

		Page
	Procedure	37
	$(UC_2 + C)$ + Bismuth	37
	$(UC_2 + C)$ + Cadmium	41
	$UC + UC_2$	41
	Sampling	45
IV.	RESULTS	47
	$UC_2 + C$	47
	Bismuth	48
	Cadmium	50
	$UC + UC_2$	55
V.	DISCUSSION OF RESULTS	63
VI.	SUMMARY	72
	APPENDICES	77
	BIBLIOGRAPHY	114

LIST OF TABLES

Table		Page
I	Heats of Formation for Uranium Carbides	10
II	Properties of Porous Carbon	30
III	Properties of UC_2 + C Carbide	34
IV	Properties of UC + UC_2 Carbide	36
V	(UC_2 + C) + Bi Equilibrium Data	51
VI	(UC + UC_2) + Bi Equilibrium Data	60
VII	Comparison of $\Delta G_f^\circ(UC)$ with $\Delta G_f^\circ(UC_2)$	65
VIII	Uranium Activities	73
IX	Free Energy of Formation of Uranium Dicarbide . .	74
X	Free Energy of Formation of Uranium Monocarbide .	75

Appendices

C-I	Summary of X-Ray Diffraction Inspection	87
D-I	Eifect of the Change in Sample Weight When Using Strontium as an Internal Standard	102
D-II	Reproducibility and Accuracy of the Determination of Uranium. Comparison of X-Ray Analysis Data to Known Values	103

LIST OF FIGURES

Figure		Page
1	Tentative Phase Diagram of the Uranium-Carbon System	6
2	Heat Capacities of UC_2 and U_2C_3	8
3	Heat Capacity of UC	9
4	Vaporization Data for UC_2	13
5	Free Energy of Formation of UC_2 using Rauh & Thorn's Uranium Vaporization Data	16
6	Free Energy of Formation of UC_2 using Drowart, Pattoret and Smoes' Uranium Vaporization Data	17
7	Free Energy of Formation of UC using Rauh & Thorn's Uranium Vaporization Data	18
8	Free Energy of Formation of UC using Drowart, Pattoret and Smoes' Uranium Vaporization Data	19
9	Schematic of Experimental Equipment	24
10	Schematic of Reaction Chamber	26
11	Stirrer and Coil	29
12	Samplers	29
13	Pyrex Filtering Apparatus	33
14	Cutaway of Equilibrium Chamber Showing Bismuth Position at Start of Run	39
15	Sample Rod	42
16	Carbide Addition Tube	42

LIST OF FIGURES (cont'd)

Figure		Page
17	Crucible Lid for Cadmium Experiments	43
18	Concentration of Uranium in Bismuth in Equilibrium with $UC_2 + C$	52
19	Activity of Uranium in the Two-Phase Region UC_2+C	53
20	Free Energy of Formation of UC_2	54
21	Concentration Uranium in Bismuth for Run Bi-26 . .	57
22	Concentration Uranium in Bismuth for Run Bi-32 . .	58
23	Activity of Uranium in the Two-Phase Region $UC+UC_2$	61
24	Free Energy of Formation of UC	62
A-1	Graphite Die and Tungsten Filters	80
A-2	Schematic of Tungsten Coating Apparatus	81
A-3	Coating Arrangement for Samplers	82
B-1	Schematic of Solenoid Power Supply	85
C-1	Microstructures in the Uranium-Carbon System . .	88
C-2	Microstructure of $UC_2 + C$ (4094 DC)	91
C-3	Microstructure of $UC + UC_2$ (5000 DC)	92

LIST OF FIGURES (cont'd)

Figure		Page
C-4	Microstructure of Arc-Melted UC + UC_2 (AM-11) .	93
C-5	Microstructure of Arc-Melted UC + UC_2 (AM-12) .	94
C-6	Microstructure of Carbide in Residue of Bi-32 . . .	95
D-1	Representative Calibration Curve	104

LIST OF APPENDICES

Appendix		Page
A	Tungsten Filters and Samplers	78
B	Stirrer	83
C	Characterization of Carbides	86
D	Chemical Analysis	96
E	Data	105

LIST OF SYMBOLS

a	Thermodynamic Activity
C_p	Heat Capacity
g	Grams
$\bar{G}^{xs}$	Excess Partial Molar Free Energy
$\Delta G°$	Standard Free Energy of Reaction
$\Delta G_f°$	Standard Free Energy of Formation
$\Delta H°_{298}$	Standard Heat of Formation at 298°K
$\log_{10}$	Common Logarithm
ln	Natural Logarithm
mg	Milligram
mls	Milliliter
ppm	Parts Per Million
R	Gas Constant
T	Temperature
x	Mol Fraction
γ	Activity Coefficient
μ	Micron
σ	Standard Deviation
σ^2	Variance

ABSTRACT

The free energies of UC_2 and UC were determined by measuring the activities of uranium in the two-phase regions $UC_2 + C$ and $UC + UC_2$ of the uranium-carbon system at temperatures 1015-1165°K. Each activity was determined by measuring the concentration of uranium in a bismuth melt at equilibrium with the two-phase mixture of interest, $UC_2 + C$ or $UC + UC_2$. From the concentration data, the activity of uranium in the melt can be obtained using the activity coefficient data of Pehlke, Tien and Guion. The activities of uranium in the two regions are summarized below.

URANIUM ACTIVITIES

Temperature (°K)	Uranium Activity* $UC + UC_2$	Uranium Activity* $UC_2 + C$
1165	3.27×10^{-5}	3.1×10^{-5}
1115	2.09×10^{-5}	1.91×10^{-5}
1065		1.14×10^{-5}
1015		6.43×10^{-6}

*Standard State - pure, solid uranium.

From the activity of uranium in the $UC_2 + C$ region, the free energy of formation of UC_2 was computed and is listed below.

FREE ENERGY OF FORMATION OF URANIUM DICARBIDE

Temperature (°K)	$\Delta G_f^\circ(UC_2)^*$ (kcal/mol)
1160	-24.03 ± 0.48
1115	-24.07 ± 0.46
1065	-24.08 ± 0.44
1015	-24.11 ± 0.42

*Standard State - pure, solid uranium and pure, solid carbon.

Using the $\Delta G_f^\circ(UC_2)$ and the activity of uranium in the UC + UC_2 region, the free energy of formation of UC was computed. The calculated values are shown below.

FREE ENERGY OF FORMATION OF URANIUM MONOCARBIDE

Temperature (°K)	$\Delta G_f^\circ(UC)^*$ (kcal/mol)
1165	-23.97 ± 0.36
1115	-23.97 ± 0.33

*Standard State - pure, solid uranium and pure, solid carbon.

The free energy of formation of UC_2 determined in this work agrees very well with the "agreed upon values" of the IAEA Panel of 1962 (Vienna).

The free energy of formation of UC determined in this work is only different from the "agreed upon values" of the IAEA Panel by less than one kilocalorie per mol.

CHAPTER I

INTRODUCTION

Much interest has been shown in the uranium carbides in recent years because of their potential as nuclear fuels. As nuclear reactor operating temperatures have been raised to increase thermal efficiency, new fuels have been required. The uranium carbides are of interest because of their high melting points >2000°C, high thermal conductivity, and resistance to irradiation damage.

The manufacture and handling of uranium carbides are aided by a knowledge of their stability and reactivity under various conditions. In this regard the thermochemical properties of the carbides; i.e., heat capacity, heat of formation, free energy, etc., are particularly important.

A great amount of work has recently been done on the thermodynamics of the uranium-carbon system. Unfortunately, however, there has not been good agreement among the various investigations. The low temperature heat capacity measurements (0 - 350°K) and the heat of formation measurements, ΔH°_{298}, do not agree well with the high temperature (2000-3000°K) effusion studies. It was felt that an investigation of the free energies of formation of uranium monocarbide

and dicarbide at intermediate temperatures (1100-1200°K) would be useful.

It is noted that in the temperature range of this investigation (1100-1200°K), the thermodynamically stable phase in equilibrium with graphite is U_2C_3, not UC_2. However, U_2C_3 is stable only under extremely low oxygen and nitrogen pressures. Uranium dicarbide, although metastable, exists under almost all conditions of manufacture and use from below room temperature to temperatures in excess of 2000°C.

The approach taken in this study of the free energies of formation of UC and UC_2 was to measure the thermodynamic activities of uranium in the two-phase regions $UC_2 + C$ and $UC + UC_2$. In the two-phase region $UC_2 + C$, the activities of UC_2 and C are unity, and in the two-phase region $UC + UC_2$, the activities of UC and UC_2 are unity. Thus, by determining the activity of uranium in each region, the free energies of formation of UC_2 and of UC can be calculated.

$$\Delta G_f^\circ(UC_2) = -RT \ln \frac{a_{UC_2}}{a_C^2 \, a_U(UC_2+C)}$$

and

$$\Delta G_f^\circ(UC) = \tfrac{1}{2}\Delta G_f^\circ(UC_2) + \tfrac{1}{2} RT \ln \frac{a_{UC_2} \, a_U(UC + UC_2)}{a_{UC}^2}$$

The equations are developed more fully in Chapter IV of this treatise.

At the temperatures of interest in this investigation, the vapor pressure of uranium in the two-phase mixture $UC_2 + C$ is too low for a determination of the activity by vapor pressure techniques. The method used was to equilibrate one of the two phase mixtures, $UC + UC_2$ or $UC_2 + C$, with bismuth and to determine the activity of the uranium in the liquid bismuth. The activity of uranium in the two-phase mixture was then known since at equilibrium the activity in the liquid must be equal to the activity in the solid two-phase mixture. The activity of uranium in the bismuth was determined by measuring the concentration of uranium in the liquid phase. The activity coefficient of uranium in bismuth has been determined by others (42).

In order to measure the concentration of uranium in the liquid bismuth, it was necessary to sample the liquid while excluding the solid $UC_2 + C$ or $UC + UC_2$. This was done by filtering the liquid through a porous carbon filter into a graphite cup for the $UC_2 + C$ equilibrations. For the equilibrations with $UC + UC_2$, a tungsten filter and cup were employed.

The values of the free energies of formation of UC and UC_2 obtained during this investigation agree well with the values which

were "agreed upon" by the Vienna Panel (IAEA, 1962), which assessed the thermochemical data of the uranium-carbon system available at that time (43).

CHAPTER II

LITERATURE SURVEY

Uranium Carbides

Interest in the uranium-carbon system dates back many years. In 1896, Moissan (30) reported a carbide of uranium to which he assigned the formula U_2C_3. Lebeau (23) later showed that a carbide made in the manner described by Moissan should have the formula UC_2. In 1943, investigators at Iowa State College (22, 50) identified the monocarbide. Mallett, Gerds and Vaughn (29) prepared and identified the sesquicarbide, U_2C_3 in 1951, and Mallett, Gerds and Nelson (28) published a tentative constitutional diagram of the U-C system. However, the constitutional diagram is still not well established. Storms (41) gives the diagram shown in Figure 1, with some of the lines left out, indicating a lack of information about the phase relationships in those areas. It has been well established that the dicarbide phase is not the equilibrium phase below 1500°C unless it is stabilized by oxygen or nitrogen (18). However, U_2C_3, the stable phase, requires very low oxygen and nitrogen potentials (18) and under most conditions of manufacture and handling, UC_2 and not U_2C_3 will be the phase present.

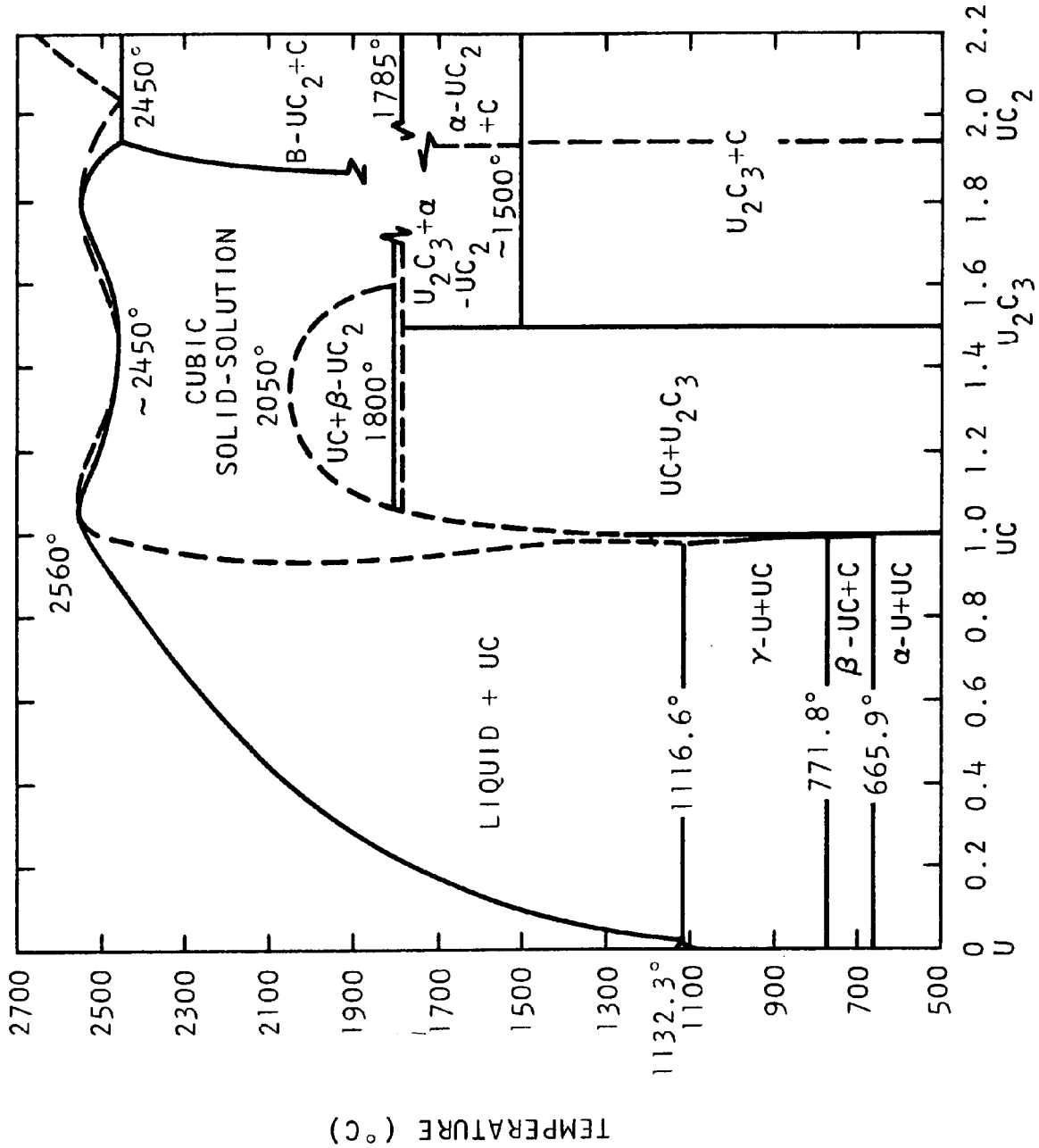


Figure 1. Tentative Phase Diagram of the Uranium-Carbon System

In an effort to better understand the phase relationships in the uranium-carbon system, there have been numerous investigations of the thermochemical properties of the uranium carbides. The heat capacities of UC_2, U_2C_3 and UC have been measured at low temperatures by Westrum and co-workers (14, 49, 48). Combarieu, et al. (8), and Martin and co-workers (43) have also measured the low temperature heat capacity of UC. At intermediate temperatures Makaibo, et al. (31, 32, 43) have measured the heat capacities of UC and UC_2. Harrington and Rowe (16) have measured the C_p of UC from 300°C to 1200°C. Levinson (25) has determined the heat capacity of UC_2(1200-1750°C). Boettcher and Schneider (6) report values of heat capacity of UC at 125° and 250°C. The reported values of these investigations are summarized in Figures 2 and 3.

The heat of formation of UC has been measured by Farr, et al. (13) and Droege and co-workers (11). Huber and Holley (20, 19) report the heats of formation of UC_2 and U_2C_3 from heat of combustion measurements. These values are presented in Table I.

In terms of predicting the stability of the various phases, a very important property to be known is the Gibbs free energy of formation. Along this line, some free energy data have been measured from three-component systems. Piazza and Sinnott (35) and Sowden (43)

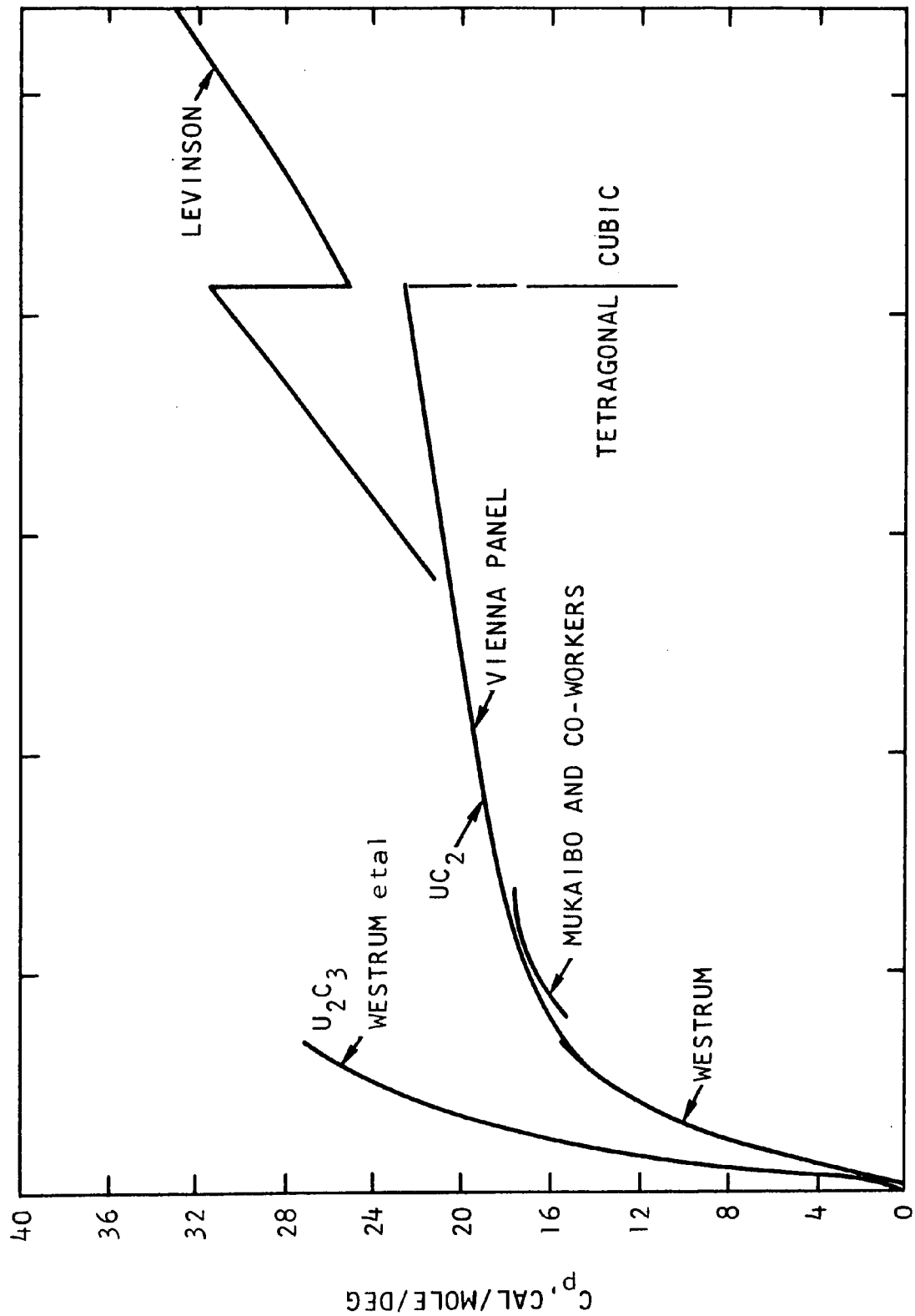


Figure 2. Heat Capacities of UC_2 and U_2C_3

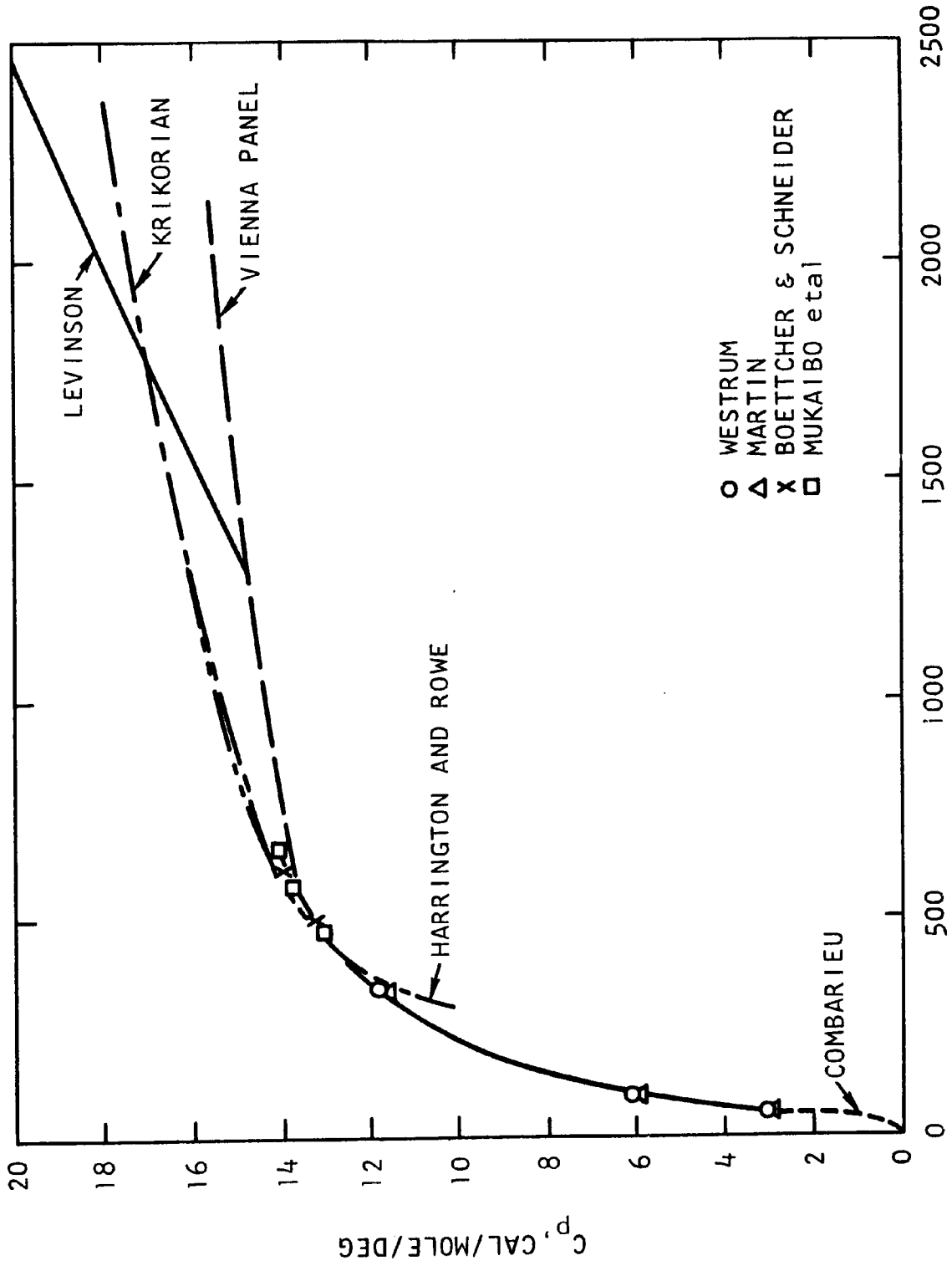


Figure 3. Heat Capacity of UC

TABLE I

HEATS OF FORMATION FOR URANIUM CARBIDES

Carbide	ΔH°_{298}(kcal)	Source
UC	-21.0± 1.0	Farr, Huber, Head, Holley (13)
UC	-20 ±5	Droege, Lemmon, Filbert (11)
UC	-21.7 ± 1	Vienna Panel "Agreed Upon Value" (43)
U_2C_3	-49 ±4	Huber and Holley (20)
U_2C_3	-49 ±4	Vienna Panel "Agreed Upon Value" (43)
UC_2	-21 ± 1.4	Huber, Head and Holley (19)
UC_2	-23 ± 2	Vienna Panel "Agreed Upon Value" (43)

have made equilibrium measurements in the U-C-O system which give the following equations for the free energies of formation of UC_2 and UC:

$\Delta G_f^\circ(UC_2) = -40750 + 8.31T$ (1714 - 1922°K) Piazza & Sinnott

$\Delta G_f^\circ(UC_2) = -35500 + 3.8T$ (1450 - 1770°K) Sowden

$\Delta G_f^\circ(UC) = -43850 + 10.51T$ (1714 - 1922°K) Piazza & Sinnott

with ΔG° in cal/mol and T in °K.

A difficulty with measuring the $\Delta G_f^\circ (UC_2)$ and $\Delta G_f^\circ (UC)$ from equilibrium measurements in the U-C-O system is that the UC or UC_2 will be saturated with oxygen. This may have a considerable effect upon the value of the ΔG_f° obtained according to Henney, Hill and Livey (18). At this time, however, there is no adequate way to account for this problem quantitatively.

Rice, Ragone and Balzhiser (38) reported two values for $\Delta G_f^\circ (UC_2)$ from equilibrium measurements in the U-C-Bi system:

$$\Delta G_f^\circ (UC_2) = -22 \text{ kcal/mol} \qquad T = 1073°K$$

$$\Delta G_f^\circ (UC_2) = -19.5 \text{ kcal/mol} \qquad T = 1273°K$$

Balzhiser and Ragone (5) have recently reported two values of concentration of uranium in bismuth in equilibrium with UC_2 + C. Using the activity coefficient data of Pehlke, et al. (42) for uranium in bismuth, the free energy of formation of UC_2 can be calculated as shown by Eq. 3 in Chapter IV of this treatise.

$$T = 1083°K \qquad x_U = 0.0154 \qquad \Delta G_f^\circ(UC_2) = -23.9 \text{ kcal/mol}$$

$$T = 1273°K \qquad x_U = 0.0185 \qquad \Delta G_f^\circ(UC_2) = -24.6 \text{ kcal/mol}$$

where x_U = the mol fraction of uranium in the bismuth in equilibrium with UC_2 + C.

Robinson and Chiotti (39) have calculated the free energy of formation of UC from EMF measurements in a fused-salt cell. They report

$$\Delta G^{\circ}_{T}\ (UC) = -16915 - 1.90T \qquad (725 - 1025^{\circ}K)$$

Alcock and Grieveson (2) have reported

$$\Delta G^{\circ}_{T}\ (UC) = -25,200 + 3.6T \qquad (1725 - 1825^{\circ}K)$$

from equilibrium measurements of the UC_2-UC-Au ternary system.

Vaporization studies of UC_2 have been carried out by Alcock and Grieveson (2), Eick, Rauh, and Thorn (12), Leitnaker and Witteman (24), Lonsdale and Graves (27), Fujishiro (15), and Alexander, Ward, Ogden and Cunningham (4) by effusion measurements. Recently, Storms (40) and Norman and Winchell (33) have published results of mass-spectrometry effusion investigations of UC_2 vaporization. The results of these investigations are summarized in Figure 4. The vaporization of UC has been measured by Alexander, et al. (4).

From the vaporization studies, the free energy of formation can be computed if the thermodynamics of the vaporization of pure uranium are known. Using the free energy of vaporization of uranium

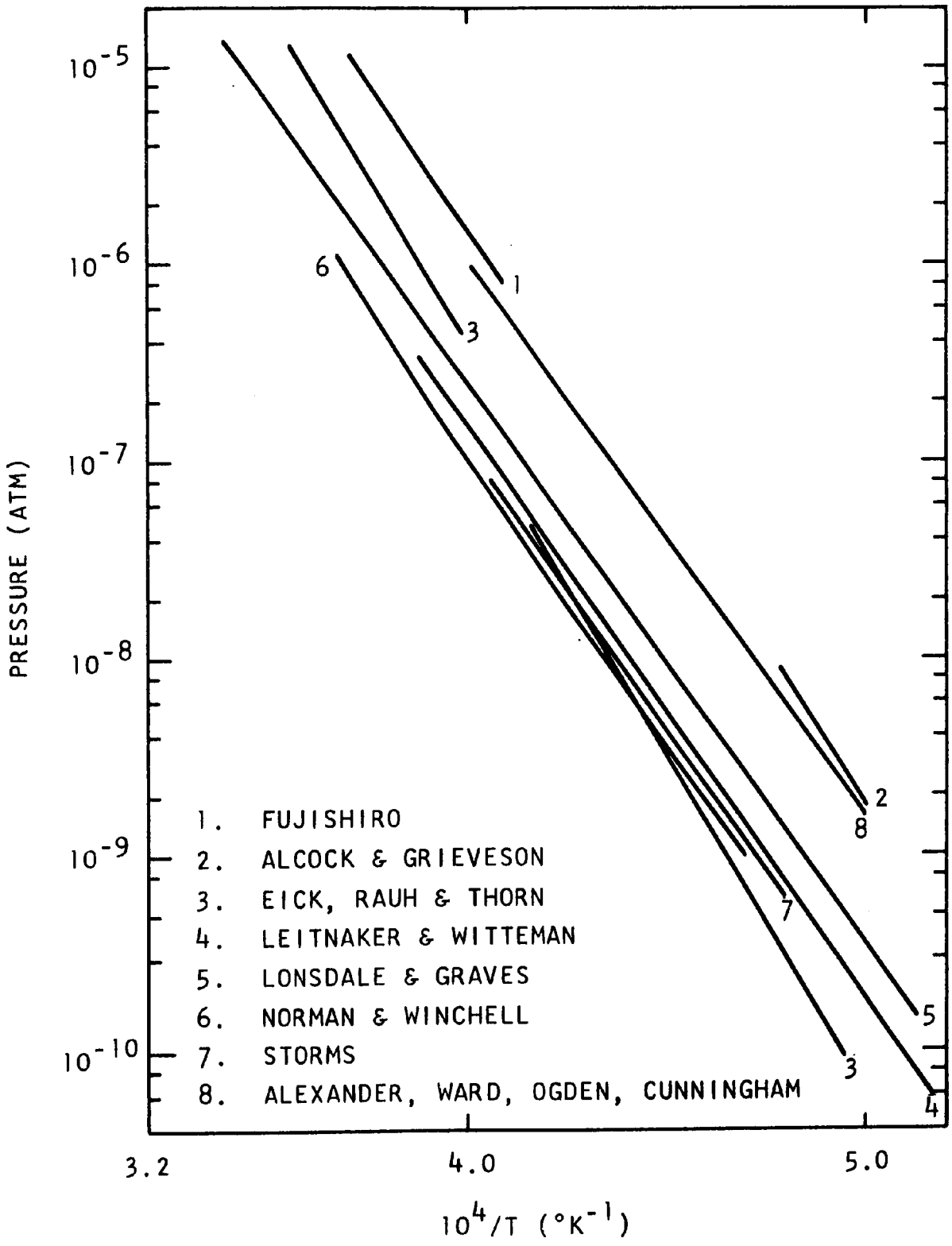


Figure 4. Vaporization Data for UC_2

determined by Rauh and Thorn (37)

$$U_{(\ell)} \rightarrow U_{(g)}$$

$$\Delta G^\circ = 106,800 - 26.1T \qquad \Delta G^\circ \text{ in cal/mol}, \quad T \text{ in } ^\circ K$$

The following equations for $\Delta G_f^\circ (UC_2)$ are presented by Henney, Hill and Livey (17) with T in °K and ΔG° in cal/mol.

$\Delta G_T^\circ (UC_2) = -32,657 + 3.6T$	(2000-2071)°K	Alcock & Grieveson
$\Delta G_T^\circ (UC_2) = -33,240 + 3.0T$	(2448-2731)	Fujishiro
$\Delta G_T^\circ (UC_2) = -23,240 - 4.3T$	(2000-2900)	Lonsdale & Graves
$\Delta G_T^\circ (UC_2) = -26,738 - 3.9T$	(1930-2365)	Leitnaker & Witteman
$\Delta G_T^\circ (UC_2) = -52,240 + 6.1T$	(2060-2460)	Eick, Rauh & Thorn

From the other vaporization investigations, using the pressure of uranium given, and using the $\Delta G^\circ(U_{(\ell)} \rightarrow U_{(g)})$ of Rauh and Thorn, the following equations result:

$\Delta G_T^\circ(UC_2) = -19,470 - 3.0T$	(1900-2660)	Alexander, et al.
$\Delta G_T^\circ(UC_2) = -27,800 - 4.2T$	(2130-2725)	Norman & Winchell
$\Delta G_T^\circ(UC_2) = -22,073 - 6.5T$	(2083-2470)	Storms
$\Delta G_T^\circ(UC) = -19,917 - 0.6T$	(1900-2660)	Alexander, et al.

The ΔG° of formation calculated from vaporization experiments depends very strongly upon the ΔG° of the vaporization of pure uranium. Unfortunately, this is not well known. A recent investigation of the vaporization of uranium by a mass spectrometric technique by Drowart, Pattoret and Smoes (34) gives the free energy of vaporization of uranium

$$\Delta G^\circ = 113,900 - 25.6T \qquad \begin{matrix} T & \text{in } ^\circ K \\ \Delta G^\circ & \text{in cal/mol} \end{matrix}$$

Using this determination of the vaporization of uranium gives values for the $\Delta G_f^\circ(UC_2)$ quite different from those above.

$\Delta G_T^\circ(UC_2) = -28,714 + 5.6T$	(2000-2071)°K	Alcock & Grieveson
$\Delta G_T^\circ(UC_2) = -26,100 + 3.5T$	(2448-2731)	Fujishiro
$\Delta G_T^\circ(UC_2) = -16,100 + 3.8T$	(2000-2900)	Lonsdale & Graves
$\Delta G_T^\circ(UC_2) = -19,575 - 3.35T$	(1930-2365)	Leitnaker & Witteman
$\Delta G_T^\circ(UC_2) = -45,100 + 6.6T$	(2060-2460)	Eick, Rauh & Thorn
$\Delta G_T^\circ(UC_2) = -12,350 - 2.5T$	(1900-2660)	Alexander, et al.
$\Delta G_T^\circ(UC_2) = -14,950 - 6.0T$	(2083-2740)	Storms
$\Delta G_T^\circ(UC_2) = -20,637 - 3.7T$	(2130-2725)	Norman & Winchell
$\Delta G_T^\circ(UC) = -8,306 - 0.1T$	(1900-2660)	Alexander, et al.

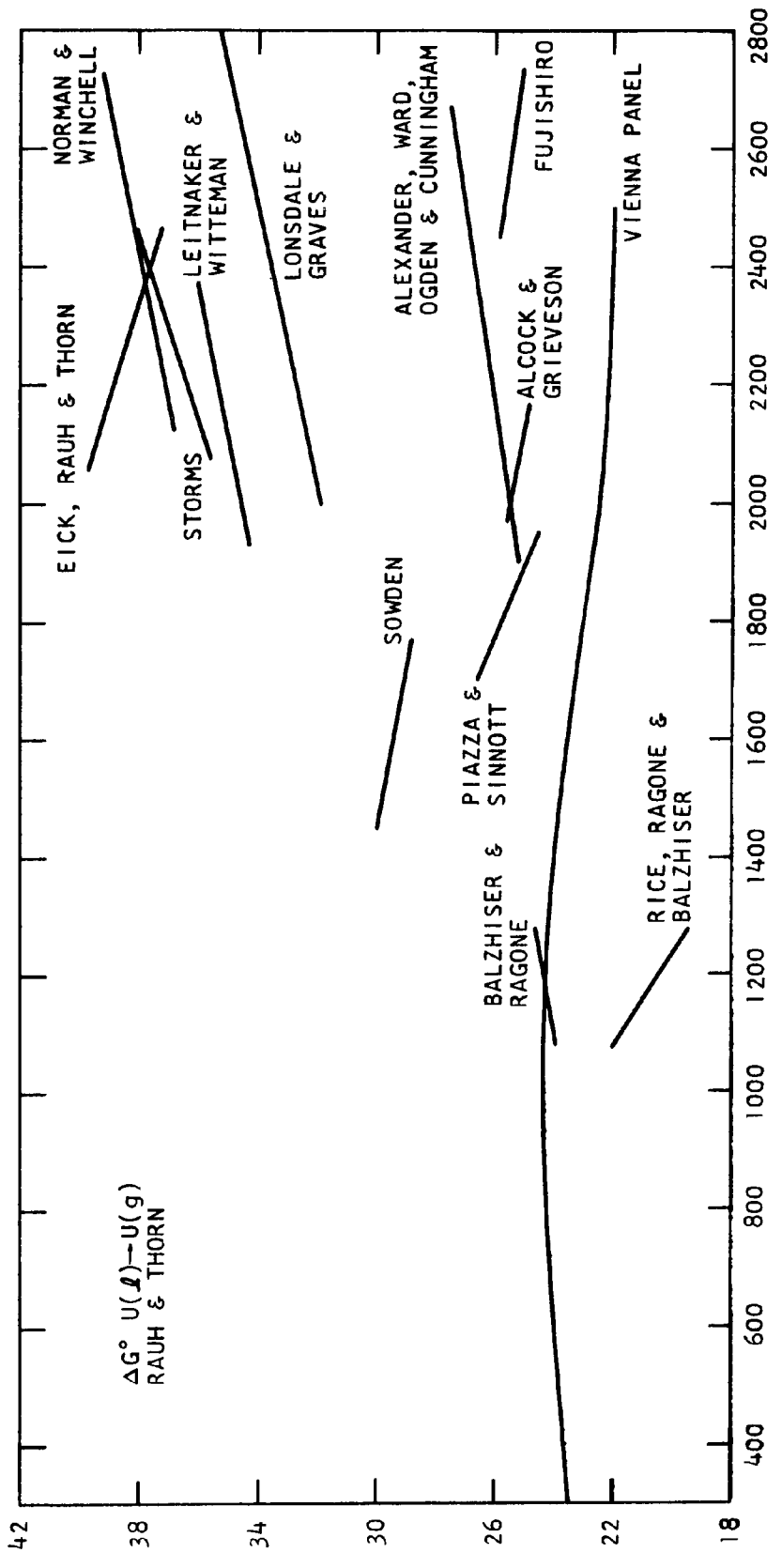


Figure 5. Free Energy of Formation of UC_2 using Rauh & Thorn's Uranium Vaporization Data

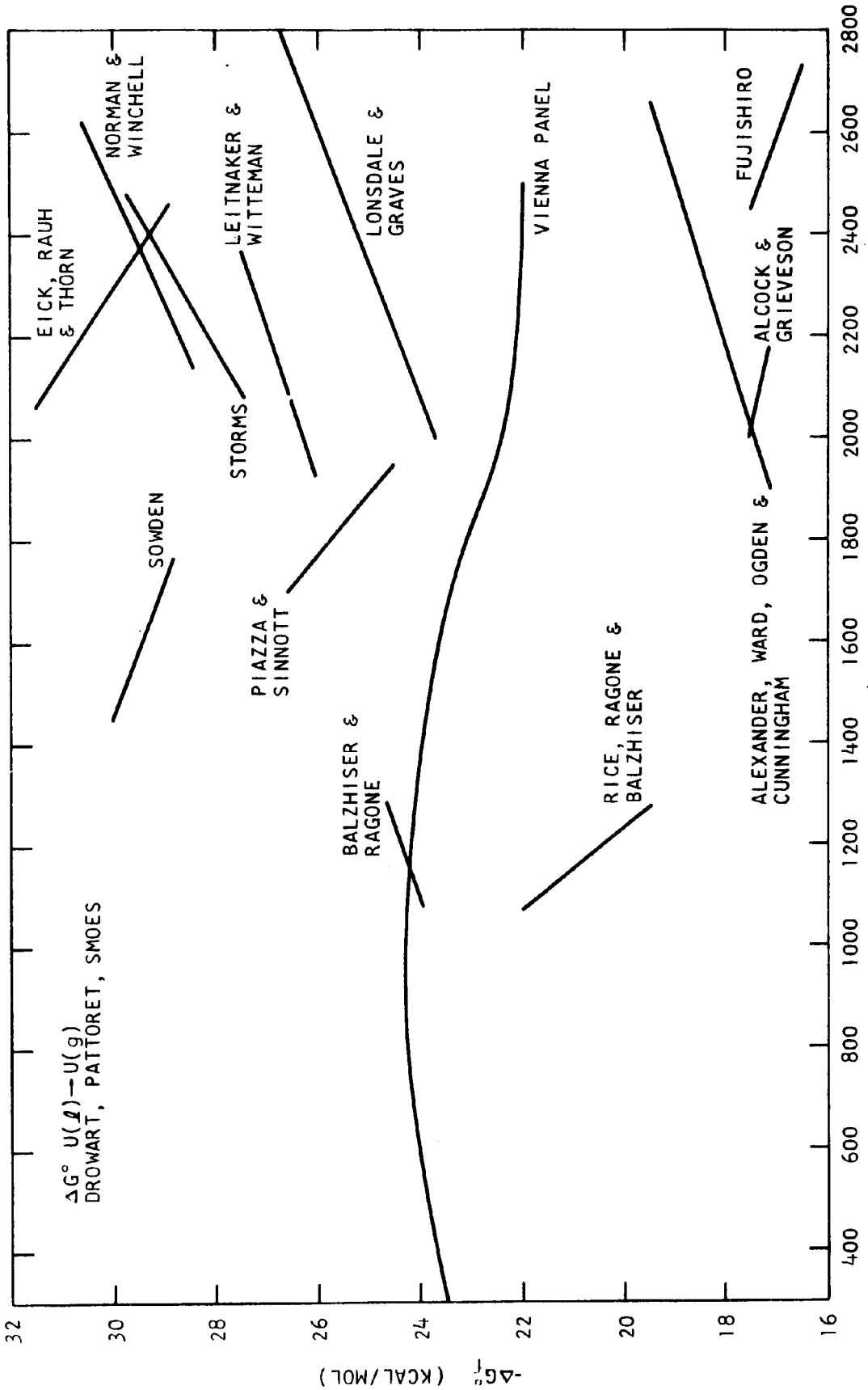


Figure 6. Free Energy of Formation of UC_2 using Drowart, Pattoret and Smoes' Uranium Vaporization Data

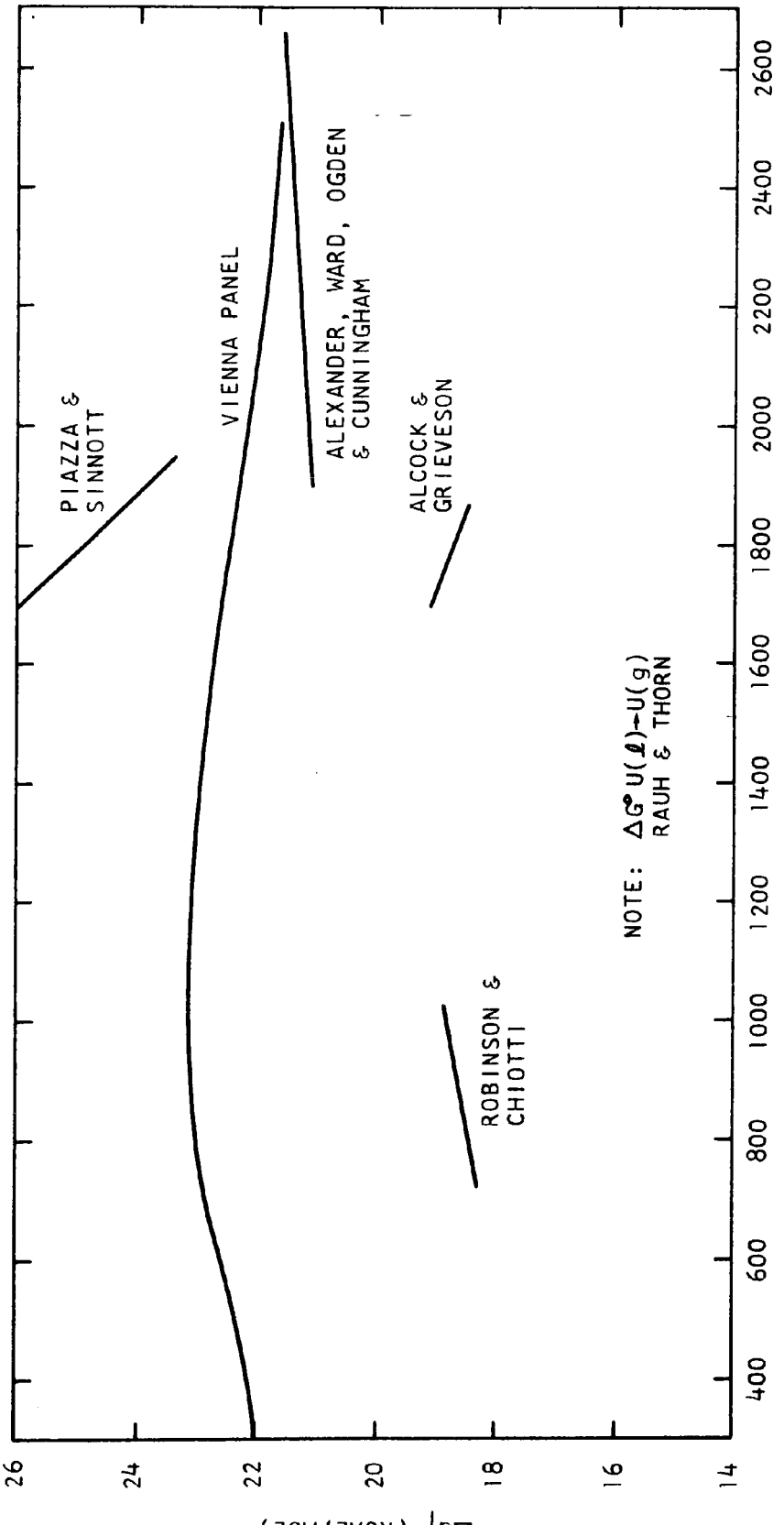


Figure 7. Free Energy of Formation of UC using Rauh & Thorn's Uranium Vaporization Data

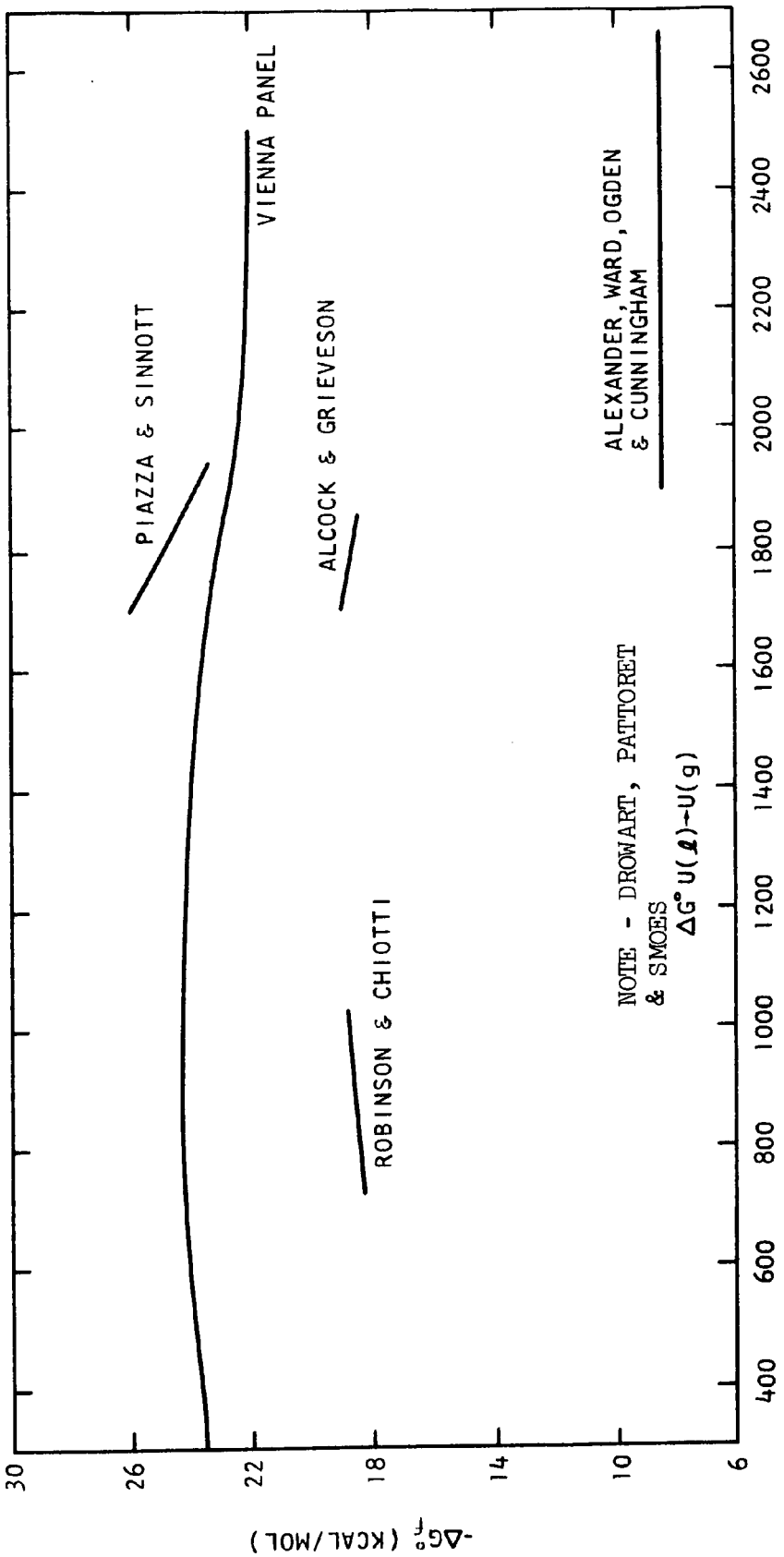


Figure 8. Free Energy of Formation of UC using Drowart, Pattoret and Smoes' Uranium Vaporization Data

These values along with those from the three component systems are summarized in Figures 5, 6, 7 and 8.

As can be seen from Figures 2-8, there is considerable disagreement among the various investigations. The discrepancies among the various vaporization experiments, Figure 4, are discussed by Alcock, Eick, Rauh and Thorn (1). In order to try to reconcile the discrepancies between the various sources of thermodynamic data, a panel was convened in Vienna in October 1962, (43) which made a critical assessment of the then existing data on the uranium-carbon system. The lines on Figures 2-8 marked "Vienna Panel" are the values agreed upon by this panel as being the best estimate with the available data.

The reader is referred also to several other compilations of thermodynamic data for the uranium-carbon system. Rand and Kubaschewski (36), Henney, Hill and Livey (17), and most recently, Storms (41) all have summarized and discussed the data that have been accumulated for the uranium-carbon system.

Alloys

The thermodynamics of uranium alloys are also of interest to this work. In order to investigate the free energies of formation of

UC and UC_2 by the technique used in this work, it was necessary to know the activity of uranium in some liquid metal.

Rice, Ragone and Balzhiser (38) have reported the activity of uranium in bismuth, which was determined using an optical technique to measure the bismuth activities. Pehlke, Tien and Guion (42) have reported the activity of uranium in bismuth from EMF measurements. Their investigation indicates that the uranium obeys Henry's Law. The activity coefficient is given by

$$\log_{10} \gamma_U = -\frac{3740}{T} + 0.44$$

The gold-uranium system has been investigated by Alcock and Grieveson (3). Their work indicates that the uranium activity deviates negatively from Raoult's Law.

The cadmium-uranium system shows a positive deviation from Raoult's Law according to the report of Johnson and Feder (21). Johnson and Feder also reported on the Sn-U, In-U, Tl-U, Ga-U and Pb-U systems.

Chiotti and Klepfer (7) have investigated the thermodynamics of the uranium-zinc system.

CHAPTER III

EXPERIMENTAL PROGRAM

The lack of agreement among the various investigations of the ΔG_f° of UC and UC_2 prompted the work done here. It seemed desirable to make a measurement of the free energies of formation of UC and UC_2 at a temperature somewhat lower than that of the vaporization experiments(1600-2600°C). The method chosen was that of obtaining uranium activities in the two-phase regions UC + UC_2 and UC_2 + C. This was done by equilibrating one of the two-phase mixtures (UC + UC_2 or UC_2 + C) with a liquid metal (bismuth or cadmium) and determining the activity of uranium in the liquid metal. This, of course, would also give the activity of uranium in the two phase mixture, UC + UC_2 or UC_2 + C. Knowing the activity of the uranium in UC_2 + C, one can determine the free energy of formation, ΔG_f°, of UC_2. If the uranium activity is known in UC_2 + C and UC_2, one can determine the ΔG_f° of UC. (See Chapter IV for the details of these calculations.)

Two solvents were used in this study: bismuth and cadmium. The activity of uranium in these metals is known as a function of concentration and temperature for these solvent metals (42, 21). Thus,

for these materials, a measure of the concentration of uranium in the liquid metal in equilibrium with the carbide of interest would give the activity of uranium in the metal and in the carbide.

The materials which were to be in contact with the melt were chosen with care so as not to introduce contaminants into the liquid metal melt. Alumina was tested and gave no evidence of reacting with dilute ($\leq$ 5 wt %) uranium alloys of bismuth or cadmium. For metal parts, it was found that molybdenum, tantalum and tungsten were inert in the dilute uranium alloys of bismuth and cadmium below 1000°C. For the equilibrium studies with UC_2 + C, graphite was an acceptable material for contact with the melt since excess graphite was already present in the carbide.

The experimental technique used was to bring a melt of the solvent metal to equilibrium with the carbide at some temperature and then sample the liquid phase. This necessitated filtering the liquid in order to exclude the carbide.

Equipment

Figure 9 shows a schematic of the equipment. The equipment consisted basically of a vacuum system, an inert gas source, a hydrogen gas source, a reaction chamber, and a furnace.

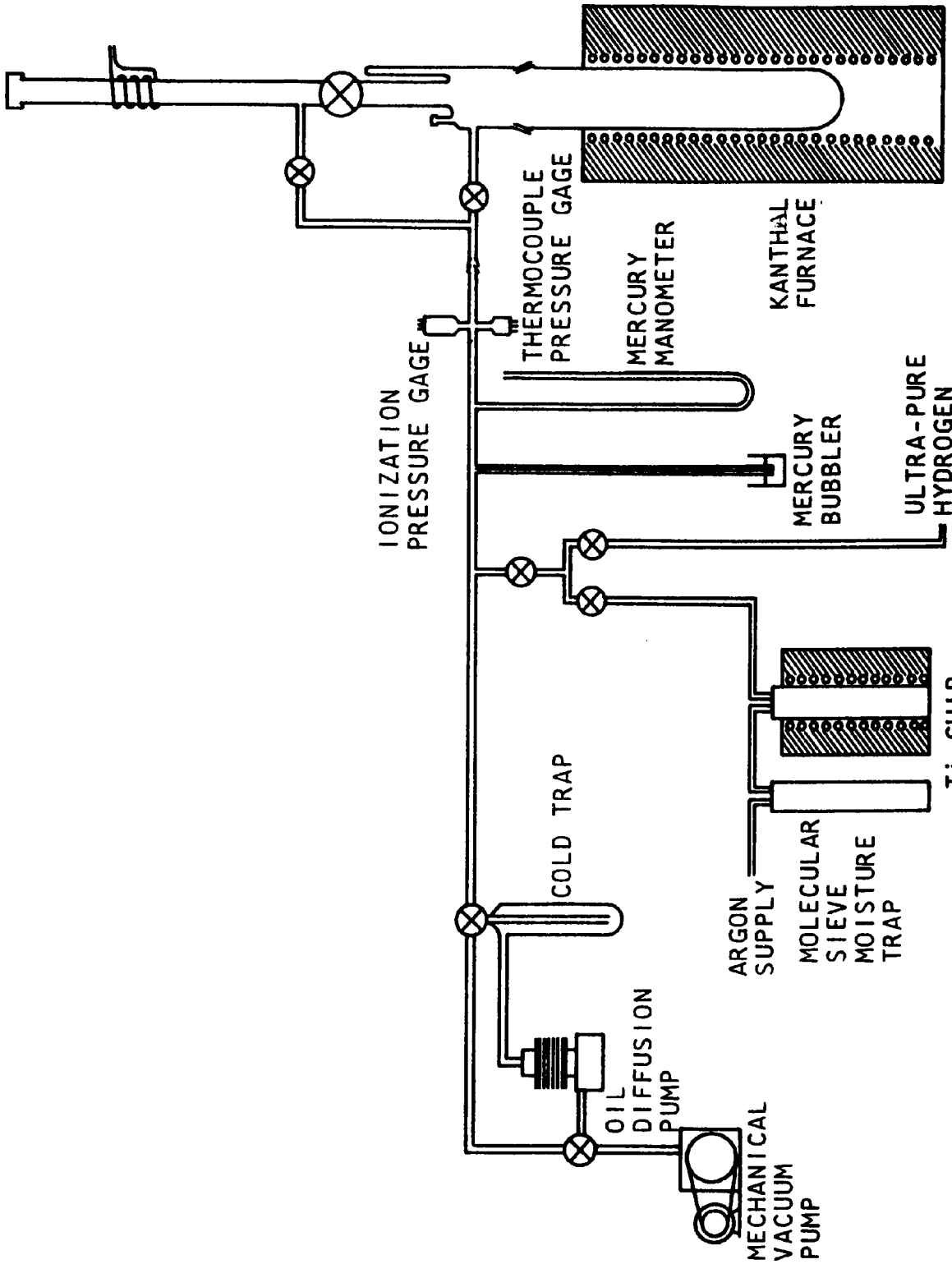


Figure 9. Schematic of Experimental Equipment

The vacuum system was composed of a mechanical pump, a 2 inch-three stage oil diffusion pump, a liquid nitrogen cold trap and three pressure gages. The pressure gages were: (1) a mercury manometer for pressures from 1 atm to 1 torr; (2) a thermocouple vacuum gage for pressures from 0.5 to 10^{-3} torr; (3) an ionization gage for pressures from 10^{-3} to 10^{-6} torr.

The inert gas used was Liquid Carbonics reactor grade argon. In order to remove any water vapor in the argon, it was passed through a molecular sieve bed $2\frac{1}{2}$ inch diameter, 18 inch deep made up of Linde Type 4-A Molecular Sieve. To remove oxygen, the gas was then passed through a titanium chip bed $2\frac{1}{2}$ inch diameter and 18 inch deep maintained at 750-800°C by a 12 inch long, $2\frac{1}{2}$ inch diameter split-wound tube furnace. The hydrogen used was Matheson ultra-pure hydrogen which was not further purified.

The furnace used to maintain temperature in the reaction chamber was a custom made 3 inch tube furnace using a Super-Kanthal heating element. The overall length of the furnace was 22 inch with a 6 inch isothermal region in the center.

The reaction chamber, Figure 10, was made up of a $2\frac{1}{2}$ inch diameter mullite tube closed at one end and joined at the open end to a Pyrex taper-ground joint. This section was joined at the tapered

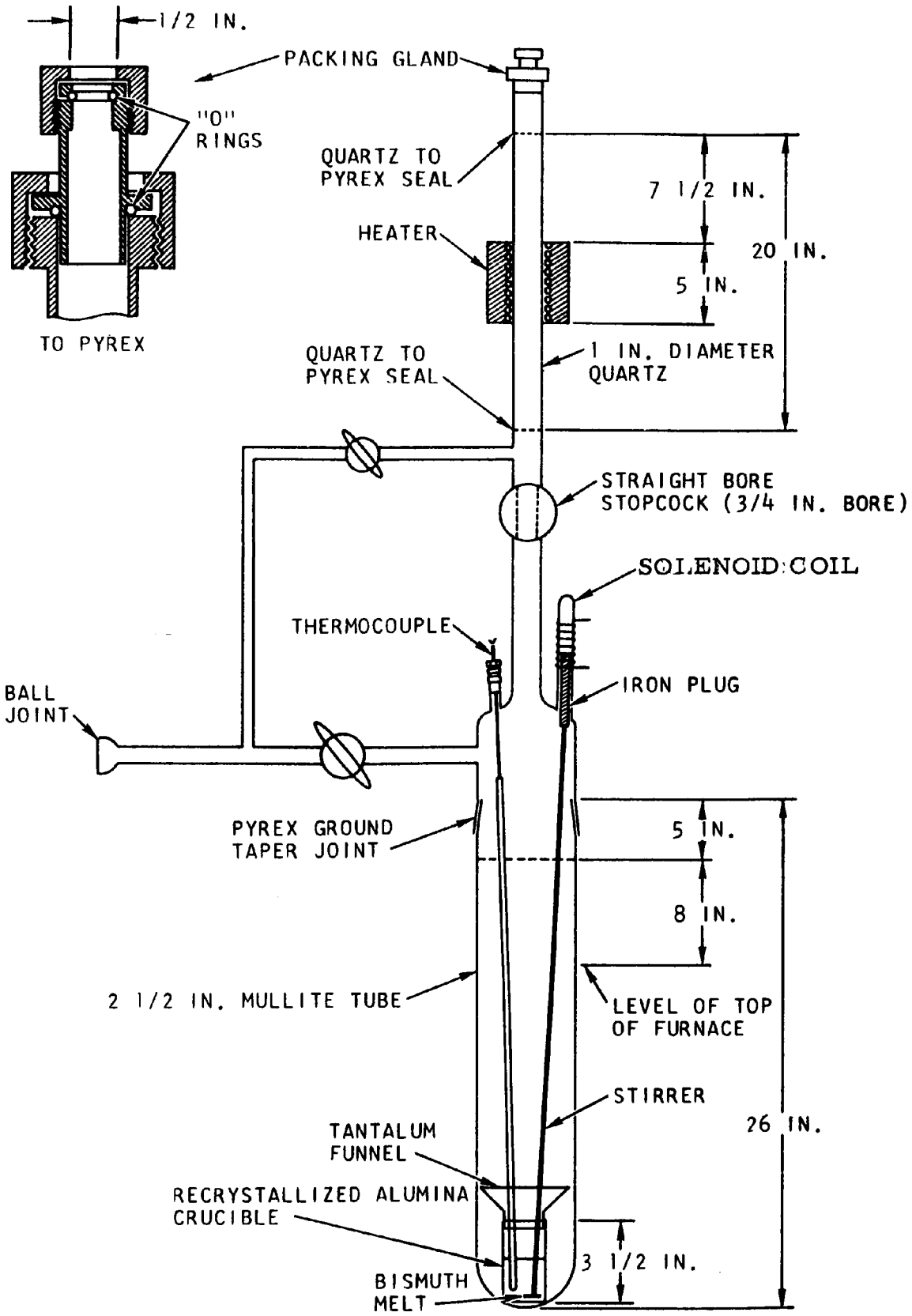


Figure 10. Schematic of Reaction Chamber

joint to a Pyrex upper section which was connected to the vacuum system. Above the straight-bore valve (see Figure 10) there was a 1 inch i.d. quartz section that could be heated to 800°C with a 5 inch long split-wound heater controlled by a Variac. At the top of this section was a $\frac{1}{2}$ inch O-ring seal. The melt of interest was contained in a 1.4 inch diameter recrystallized alumina crucible $3\frac{1}{2}$ inch long. Two runs were made in a tantalum crucible of similar dimensions. At the top of the crucible was a funnel to position the crucible in the center of the mullite tube. The funnel was made of molybdenum or tantalum.

The temperature in the melt was measured by a Chromel-Alumel thermocouple. The thermocouple passed through a 1/16 inch Swagelock fitting fitted with Teflon ferrules. The thermocouple was sheathed with 1/16 inch Inconel tubing which was sheathed in either tantalum or molybdenum. The same thermocouple was used to control the temperature as was used to measure it. The output of the thermocouple was fed into a Model 402 Wheelco temperature controller which actuated the relay controlling the power to the furnace. The power level to the furnace was controlled by a Variac. This control arrangement gave temperature control about the set point of ± 3°C or better.

The melt was stirred continuously by a tantalum or a tungsten coated molybdenum stirrer. The stirrer is shown in Figure 11. The

stirrer was operated by magnetic coupling through the glass in the manner of a solenoid, and thus did not require an opening in the system. The power to the coil was controlled by a transistorized power supply (see Appendix B), that delivered direct current in a saw-tooth wave. The frequency could be varied by changing the motor on the motor-driven potentiometer. Two motors were used giving frequencies of 15 cycles per minute and of 8 cycles per minute. The length of travel of the stirrer could be varied from 0 to 1 inch.

Samplers

The materials used for the samplers were selected so as neither to contaminate the melt nor to disturb the equilibrium between the carbide and the solvent metal. For the equilibrium studies with UC_2 + C, graphite was an acceptable material as noted above. These samplers were made from Nuclear Grade Type AGOT Graphite obtained from Carbon Products Division of Union Carbide. The filters were made of Grade 60 or Grade 45 porous carbon obtained from Carbon Products Division of Union Carbide. The filters were 1/8-1/16 inch thick with a diameter just larger than the diameter of the sampler at the shoulder (see Figure 12). The filter disc was pressed into place giving a very tight fit in order to prevent leakage around the filter. No differences were noted depending upon which grade of porous carbon

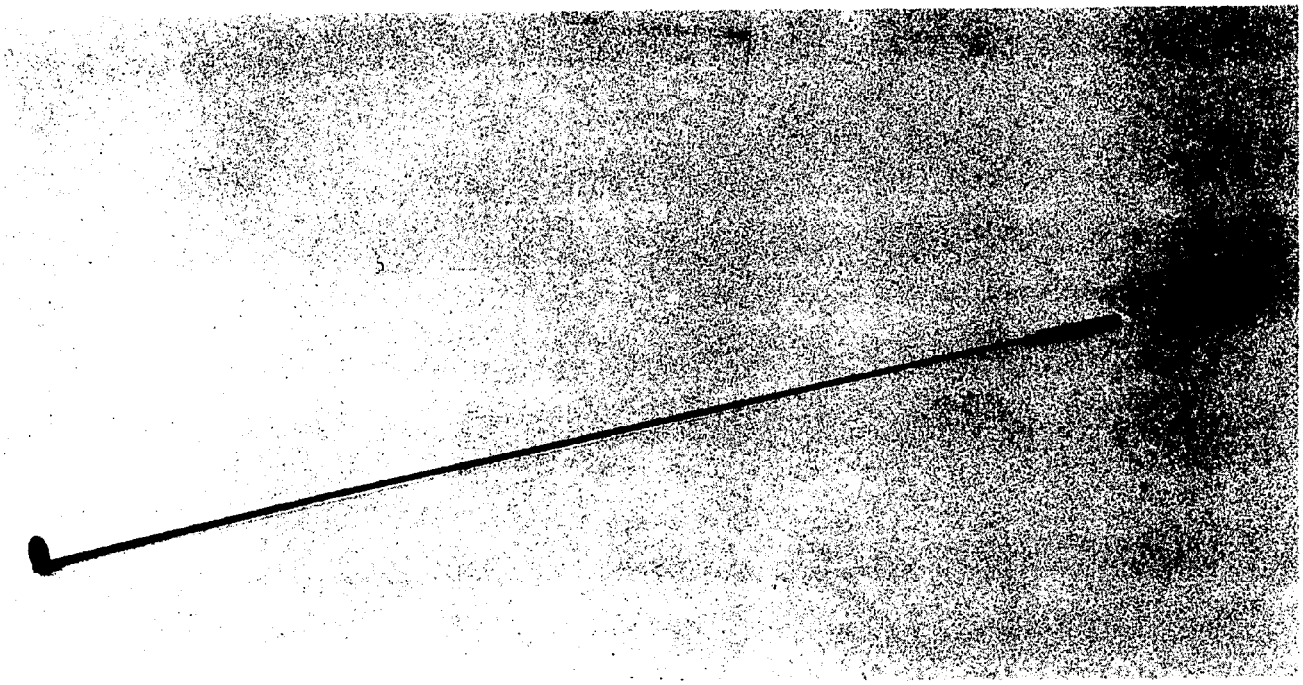
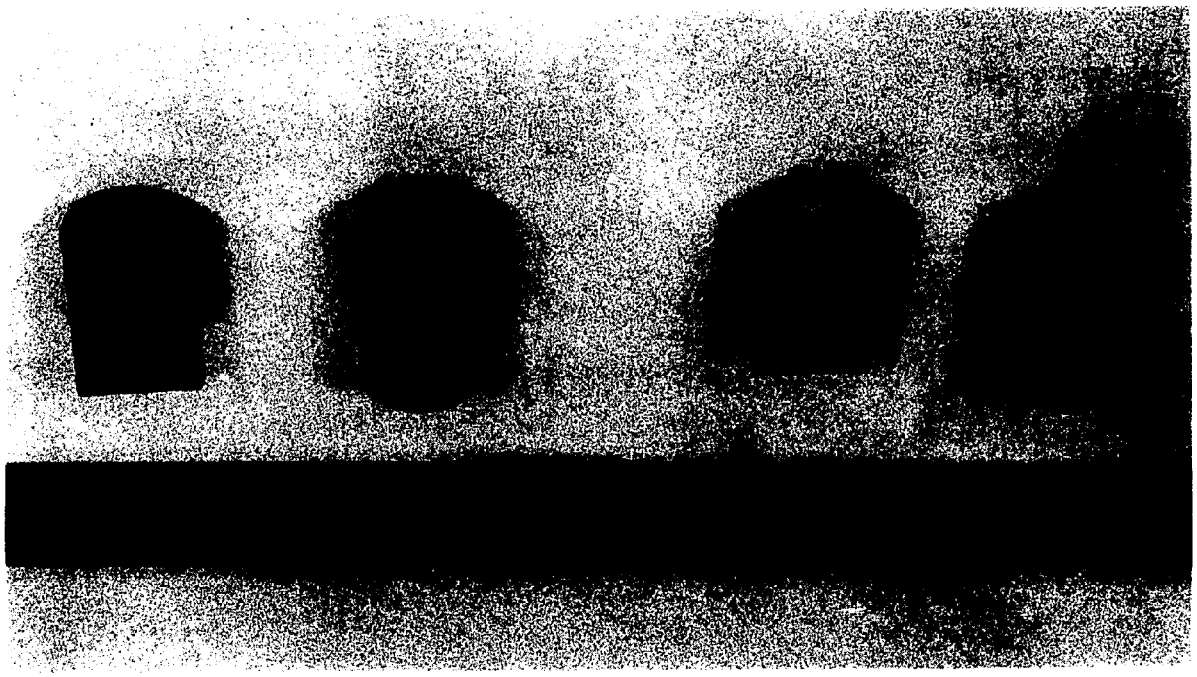


Figure 11. Stirrer and Coil



Tungsten-Coated Graphite Graphite

Figure 12. Samplers

was used. The properties of this material are summarized in Table II.

TABLE II

PROPERTIES OF POROUS CARBON

Grade	Porosity (%)	Pore Diameter (Micron)	Smallest Particle Retained (Micron)
60	48	33	1.85
45	48	60	3.40

The samplers were outgassed at 1850°C for 1 hour and were kept in a vacuum desiccator until used. The desiccator was always filled with argon before opening.

The samplers to be used for the UC + UC_2 equilibrium studies presented somewhat of a problem. Several types of samplers were considered. A sampler made of Vycor with a Vycor filter was tried, but it apparently reacted with the uranium in the melt. See Appendix E, Run Bi-19, Sample Number 17. Samplers of molybdenum, tantalum or tungsten were considered, but the cost of the material and the machining made them impractical. The samplers used for this work were identical to those used for the UC_2 + C work except that after

outgassing they were coated with tungsten. The filters were made by hot-pressing small tungsten spheres (420μ) into 1/8-1/16 inch thick discs of the proper diameter (just larger than the diameter of the sampler at the shoulder). See Appendix A for the details of making and testing the tungsten filters. The tungsten filters filtered out all particles larger than 5μ diameter.

The samplers were coated with tungsten by reacting WF_6 with H_2 at the surface of the graphite sampler. The reaction proceeds well at ~1000°F.

$$WF_{6(g)} + 3H_2 \rightarrow W_{(s)} + 6HF \quad .$$

An impervious coating of from 0.008-0.010 inch thick was applied to both the inside and outside of the sampler. See Appendix A for the details of the coating procedure.

Considerable difficulty was experienced in getting the bismuth-uranium alloy to filter through the porous carbon filters. Only about 50-60% of the sampling attempts produced filtered samples. It is believed that this lack of consistency is due to the nonuniformity of porous carbon. The porosity of the material is quite uniform, but the permeability must be nonuniform. With the pressed tungsten filters, on the other hand, filtering was not a problem. No difficulty was experienced in filtering with the tungsten filters.

Materials

Bismuth

The bismuth used was obtained from United Mineral & Chemical Corporation and was 99.999% pure. The bismuth was melted and filtered prior to use in order to remove the oxide layer that was present on the "as-received" material. The filter apparatus is shown in Figure 13. The filter apparatus was loaded with approximately 800 grams of bismuth, evacuated to $< 10^{-3}$ torr and heated to 300°C, which is above the melting point of bismuth, 271°C. At this point the lower section was sealed off and the upper section was pressurized to 700 torr with argon. The filtered material was cooled under vacuum $< 10^{-3}$ torr. In some cases, a small amount of uranium (approximately 0.5 wt %) was added to the bismuth to be filtered. In these cases, the temperature was raised to 500°C and held there for 3 hours to allow the uranium to dissolve before filtering. A quartz filter apparatus was used in these cases.

Cadmium

The cadmium used was 99.999% pure, obtained from United Mineral & Chemical Corporation. The cadmium was filtered at 350°C in a manner similar to that described above.



Figure 13. Pyrex Filtering Apparatus

$UC_2 + C$

This material was obtained from the Fuel Operations Division of General Atomic. It was made by reacting UO_2 with excess carbon to form uranium dicarbide with excess carbon. The material as received contained 650 ppm oxygen. It was felt that it would be desirable to reduce the oxygen content if possible. The carbide was heated in a vacuum furnace to 1750°C for 5 hours at vacuum $< 10^{-4}$ torr. Table III summarizes the properties of the material.

TABLE III

PROPERTIES $UC_2 + C$ CARBIDE
(4094 DC)

	As Received	As Used
Total Carbon (wt %)	13.4	14.1
Free Carbon (wt %)	5.43	5.92
Uranium (wt %)	86.1	85.1
Oxygen (ppm)	650	91
Nitrogen (ppm)	<10	<10
Particle size (μ)	208-295	208-295

No phases other than UC_2 and C were detected by x-ray diffraction, and no phases other than UC_2 and C were detected from photomicrographs of the material. See Appendix C for a further discussion of the x-ray analysis and metallography.

After each run with this carbide, the residue of the run was checked metallographically to insure that UC_2 and C were still the only phases present in the carbide. In no case were other phases detected.

$UC + UC_2$

Two types of this material were used. One type was obtained from the Fuel Operations Division of General Atomic. This material (5000 DC) was made by reacting UO_2 with carbon. The other material (AM-11, AM-12) was made by melting the elemental materials together. Approximately 23.5 grams of previously cleaned uranium and 1.5 grams of carbon were arc melted in an argon atmosphere using a tungsten electrode and a copper hearth. Prior to melting the carbides, a 20 gram piece of uranium was melted to help remove any oxygen from the argon in the arc-melting chamber. The uranium was cleaned in nitric acid prior to melting. A summary of the properties of these carbides is given in Table IV.

TABLE IV

PROPERTIES OF UC + UC_2 CARBIDE

	5000 DC	AM-11	AM-12
Total Carbon (wt %)	5.80	6.3	6.8
Free Carbon (ppm)	< 10	<10	<10
Uranium (wt %)	94.0	94.1	93.0
Oxygen (ppm)	99	125	173
Nitrogen (ppm)	<10	<10	<10

These carbides were examined by x-ray diffraction. No phases other than UC and UC_2 were detected in any of the carbides. Photomicrographs of the material indicated that these were the only phases present. See Appendix C.

The materials were stored in a vacuum desiccator which was always filled with argon before opening. The arc melted UC + UC_2 carbide was in the form of 25 gram buttons. It was not broken up until immediately prior to its addition to the melt.

After each run the carbide in the residue of the run was checked metallographically to determine the phases present. In no case were phases other than UC and UC_2 detected.

Flux

The flux used to promote wetting of the carbide by the bismuth was made up of 50% KCl and 50% NaCl, which were melted together from analytical reagent grade NaCl and KCl obtained from Mallinckrodt Company.

Procedure

The crucible, funnel, stirrer and thermocouple were placed in the reaction chamber and outgassed overnight at 1000°C in a vacuum $< 5 \times 10^{-5}$ torr. The system was cooled under vacuum and then filled with argon.

$(UC_2 + C)$ + Bismuth

A charge of approximately 50 grams of carbide was placed in the alumina crucible in the reaction chamber. A 380-400 gram piece of refiltered bismuth was suspended in the reaction chamber above the hot zone. Attached to the bismuth using tantalum wire were 1-2 grams of flux, and enough uranium to give the desired initial concentration. The suspension of the bismuth, flux, and uranium was accomplished by passing the sample rod through the O-ring seal at the top of the upper section of the reaction chamber, through the straight-bore stopcock with the bismuth attached to the bottom of the tube using

tantalum wire. See Figure 14. The sample rod was a long (5 feet) tube of 304 stainless steel closed at the bottom with a 304 stainless steel plug. Threaded into the stainless steel plug was a 6 inch piece of tantalum rod. See Figure 15.

With the bismuth, flux and uranium in place (Figure 14), and with the carbide in the crucible, the lower section of the reaction chamber was attached to the upper section using de Khotinsky sealing wax on the ground taper joint. The system was then evacuated to $< 10^{-4}$ torr and heated to the first temperature of interest, 677-892°C. After the temperature had been reached, the vacuum system was sealed off and H_2 was let into the reaction chamber until the pressure reached 350 torr. The H_2 was left in the reaction chamber for 5 minutes and the system was then evacuated to $< 10^{-3}$ torr. The vacuum system was sealed off once again and H_2 was again let into the system until a pressure of 350 torr was reached. The H_2 was left in the system for 10 minutes and then pumped out. The third H_2 cycle was left in the system for 15 minutes before evacuating to $< 10^{-3}$ torr. Hydrogen was then let into the system until a pressure of 3 torr was reached. At this point, the system was filled to one atmosphere with argon, and the bismuth was lowered into the funnel at the top of the crucible. After the bismuth had melted ($\sim$5-10 minutes), the long

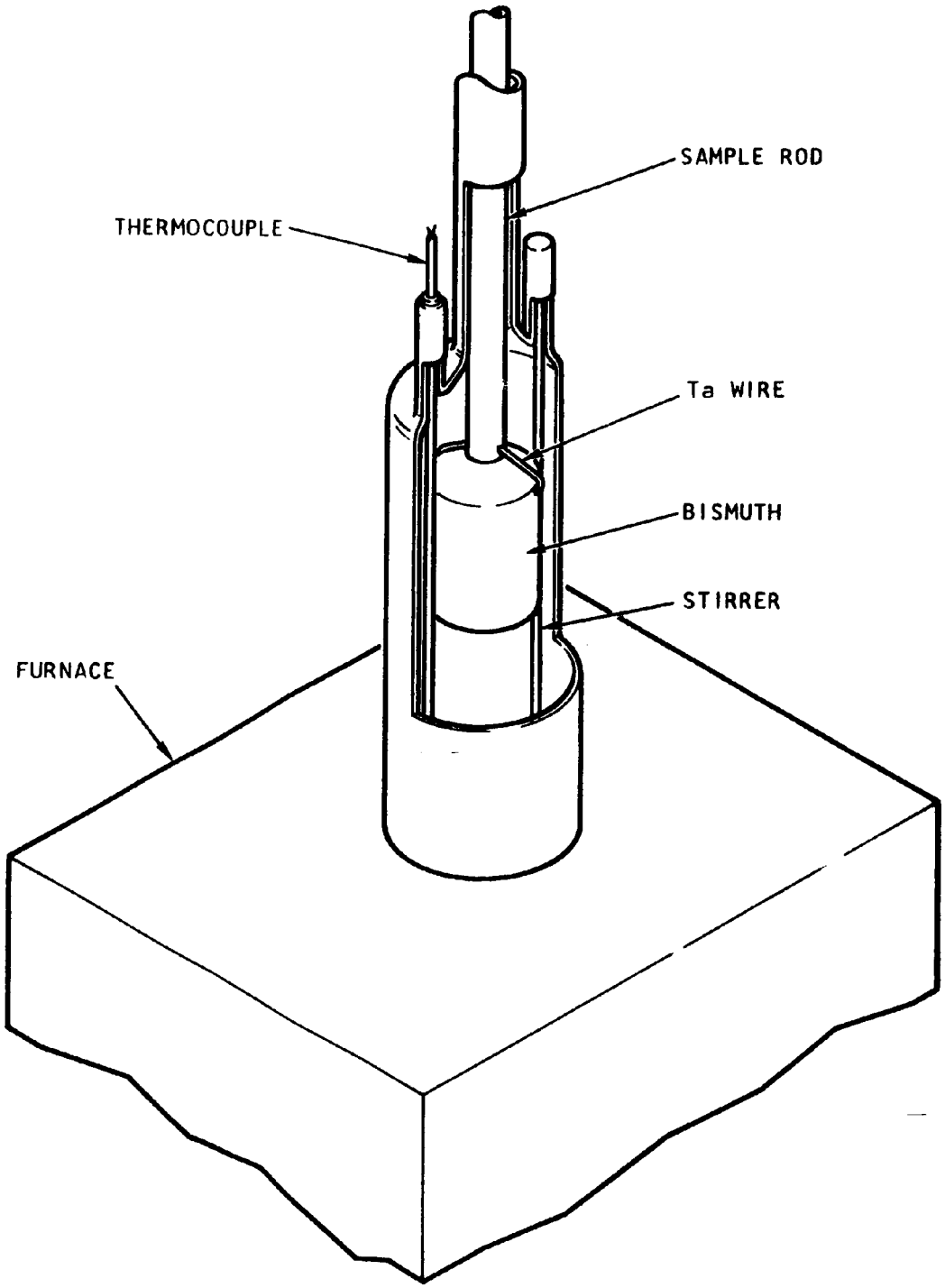


Figure 14. Cutaway of Equilibrium Chamber Showing Bismuth Position at Start of Run

tube was pulled up out of the reaction chamber and above the straight-bore stopcock. The stopcock was closed and the long tube was removed through the O-ring seal. The stirrer was started immediately after the bismuth had melted.

The hydrogen treatment described above was used to remove any surface contamination that might have been formed on the carbide. After this hydrogen treatment was initiated, very good wetting of the carbide by the bismuth was experienced.

In the experiments employing the hydrogen treatment, molybdenum was used for the funnel and thermocouple sheath, since tantalum reacts with hydrogen at these temperatures. The stirrer used in these runs was of tungsten-coated molybdenum.

The melt was allowed to equilibrate from 30-60 hours before sampling was begun. Samples were taken at intervals of approximately 24 hours. After two or three samples had been taken at one temperature, the temperature was changed (usually about 50°C). The melt was allowed to equilibrate at the new temperature for 24-48 hours and then a sample of the liquid was taken, etc. This procedure was continued until the melt was exhausted, the plan for a given run was completed, or equipment difficulties forced the termination of the run.

$(UC_2 + C)$ + Cadmium

Two experiments with cadmium were made even though the estimated equilibrium concentration was $\sim 10^{-9}$ mol fraction (21). Because of the high vapor pressure of cadmium, it was necessary to devise a lid for the crucible. The lid used is shown in Figure 17. The lid was constructed of two molybdenum discs 0.03 inch thick and a piece of 0.001 inch thick tungsten. The tungsten was cut in an "X" design to allow the sampler and sample rod to pass through the lid into the melt and then to close when the rod and sampler were removed.

The experimental procedure was the same for the cadmium experiments as with the bismuth experiments.

$UC + UC_2$

The procedure described for the $UC_2 + C$ work was used during the first 6 runs of the $UC + UC_2$ work (Run Bi-21 - Run Bi-26). It was noted during Run Bi-24 that all of the carbide seemed to have settled to the bottom of the crucible and was presenting very little surface to the melt, thus impeding the approach to equilibrium. It was felt that carbide should be added during the run to present new carbide surface to the melt as the run progressed. This was accomplished by the use of the tube shown in Figure 16. The open end of the tube was plugged with a bismuth disc, and the carbide that was

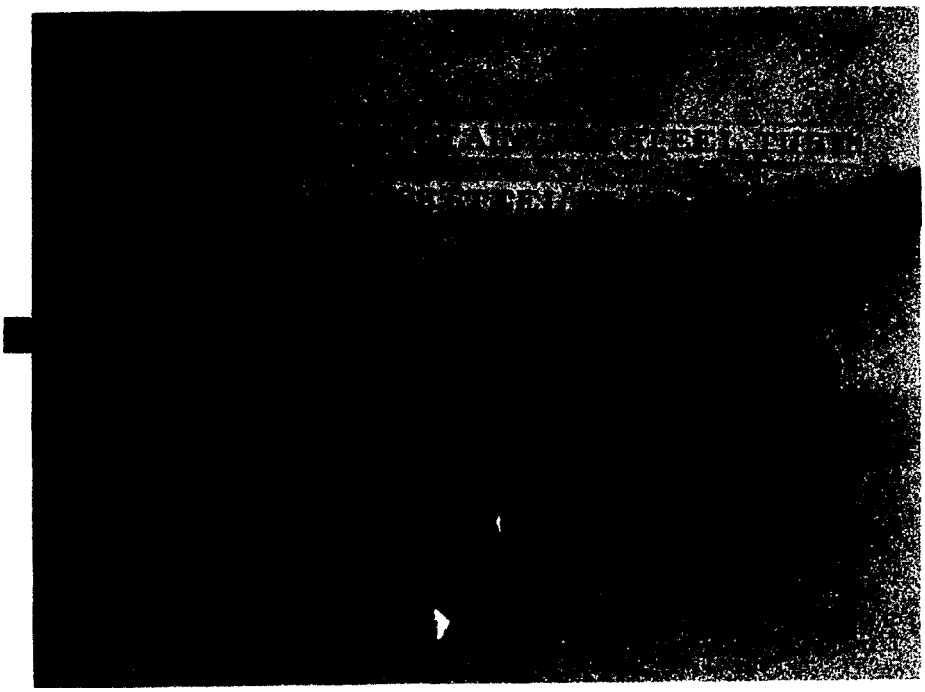


Figure 15. Sample Rod

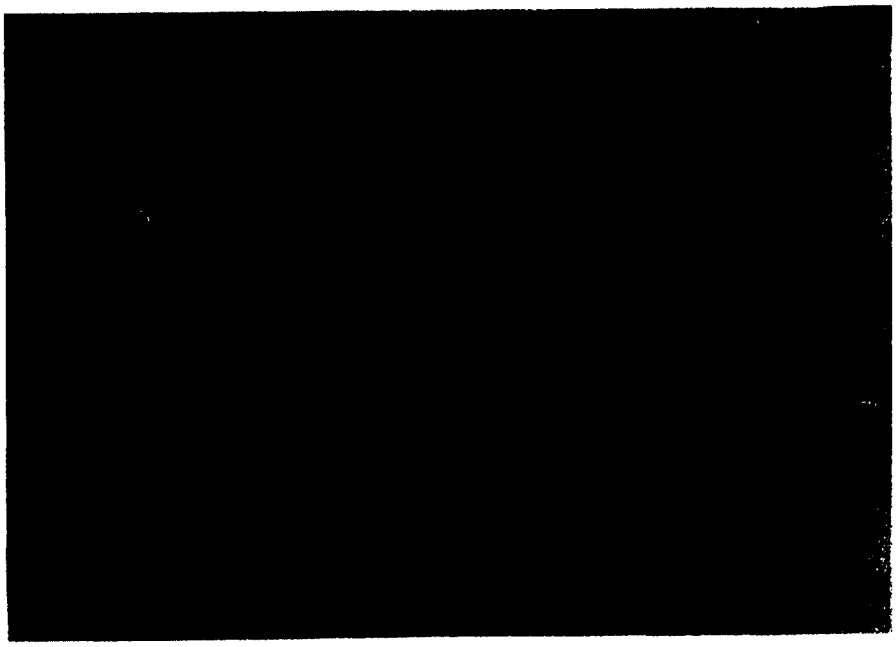


Figure 16. Carbide Addition Tube

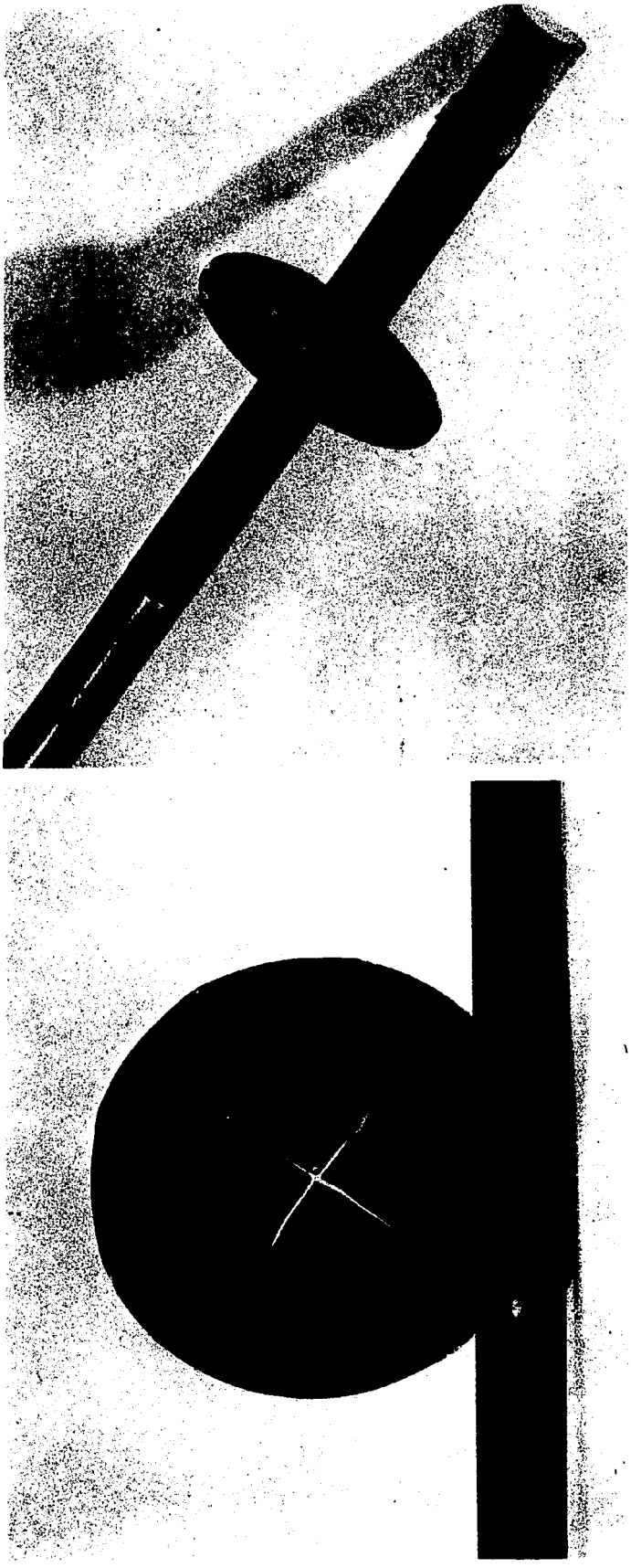


Figure 17. Crucible Lid for Cadmium Experiments

to be added was poured into the tube above the disc. The tube was then attached to the end of the sample rod and placed in the upper section of the reaction chamber. This chamber was evacuated to $<10^{-3}$ torr for 15 minutes and then filled to 1 atm with argon. The straight-bore stopcock was opened and the tube was lowered into the melt. The bismuth plug would melt and the carbide would fall from the tube into the melt. The sample rod and addition tube were then removed from the system.

Beginning with Run Bi-27, the procedure was changed to some extent. The hydrogen treatment was discontinued, and the run was started without carbide. After outgassing as described above, the crucible was loaded with 380-400 grams of bismuth, and an amount of uranium sufficient to give the desired initial concentration. The lower section of the reaction chamber was then attached as before, and the reaction chamber evacuated. When the pressure had been reduced to $< 10^{-4}$ torr, the temperature was increased to 450°C. At that point, the stirrer was started and the system was filled with argon until the pressure reached 1 atmosphere. The temperature was then raised to the temperature of interest, 670-900°C. After the melt had been at temperature for three hours, a sample was taken to establish the initial concentration. Immediately after the sample was removed

from the system, a charge of carbide was added as described above. The melt was allowed to equilibrate for 24 hours and a sample was then taken. The melt was sampled every 25-50 hours, with periodic additions of carbide. By adding the carbide under the surface of the melt, good wetting of the carbide by the bismuth-uranium melt was experienced.

During some of the runs, it was desirable to raise the concentration of uranium in the liquid. Uranium was added to the melt in the same manner as was carbide as described above.

In the runs that did not use the hydrogen treatment, tantalum was used for the funnel, the thermocouple sheath, and the stirrer.

It should be noted that in all the runs after Run Bi-27, the runs were isothermal.

Sampling

A sampler was fitted with a filter (Figure 11) and the sampler was attached to the end of the sample rod (Figure 15). In the studies of $UC_2 + C$, a graphite sampler and carbon filter were used, and in the $UC + UC_2$ studies a tungsten coated sampler and a tungsten filter were used. The sampler was attached to the sample rod with tantalum wire.

The sampler was placed in the upper section of the reaction chamber with the sampler centered in the section that could be heated (see Figure 10). The upper section was then evacuated to $< 10^{-3}$ torr and heated to 650-700°C for 20 minutes. The upper section was then filled to 1 atmosphere pressure with argon, and the straight-bore stopcock opened. The sampler was lowered until it was $\frac{1}{2}$ to $\frac{3}{4}$ inch above the surface of the liquid in the crucible.

The sampler was left in this position for a minimum of 15 minutes in order to allow it to reach the same temperature as the melt.

The entire reaction chamber was then evacuated to about 10^{-3} torr. The sampler was lowered beneath the surface of the melt and the system was repressurized to 1 atmosphere with argon. The sampler was left under the melt for 15-30 minutes in the case of the porous carbon filters, and for 3-5 minutes in the case of the tungsten filters. The sampler was then removed from the system.

The sample was removed from the sampler by breaking the sampler open and removing all the material below the filter. This material was then analyzed for uranium content; see Appendix D.

The tungsten filters were cleaned in concentrated nitric acid and used again.

CHAPTER IV

RESULTS

As was mentioned above, it was considered desirable to measure the Gibbs free energies of formation of UC_2 and UC at temperatures lower than those of the vaporization experiments (2, 4, 12, 15, 27, 33, 40, 45). The method used was to equilibrate $UC_2 + C$ with bismuth or cadmium to determine the ΔG_f° of UC_2, and to equilibrate $UC + UC_2$ with bismuth to determine the ΔG_f° of UC. The details are given below.

$UC_2 + C$

When a mixture of solid $UC_2 + C$ is brought to equilibrium with bismuth or cadmium, the reaction that occurs is:

$$UC_2 \rightleftarrows \underline{U} + 2C \tag{1}$$

The standard free energy for this reaction may be written:

$$\Delta G^\circ = -RT \ln \frac{a_U a_C^2}{a_{UC_2}} \tag{2}$$

This is, of course, the negative of the free energy of formation of UC_2

$$\Delta G_f^\circ(UC_2) = -RT \ln \frac{a_{UC_2}}{a_U a_C^2} \tag{3}$$

In the two-phase region UC_2 + C (Figure 1), UC_2 and C are in equilibrium with each other. These two materials are present in their pure state, and thus their thermodynamic activities in this region are unity. In order to determine the activity of uranium in this region, the two-phase mixture, UC_2 + C, was equilibrated with a liquid metal, bismuth or cadmium, that would not dissolve UC_2 or C, nor would dissolve in them. At equilibrium, then, the activity of uranium in the liquid metal is equal to the activity of uranium in the two-phase region. Bismuth and cadmium were selected as the solvent metals, since they show no solubility for UC, UC_2, or C within the limits of our detection. Neither solvent could be detected by metallographic techniques as dissolving in the UC_2 + C or the UC + UC_2 phases. The activity of uranium in the bismuth or cadmium was determined by sampling the liquid in equilibrium with UC_2 + C mixture and determining the concentration of uranium.

Bismuth

The activity of uranium in bismuth as a function of concentration has been measured by Pehlke, Tien and Guion (42). Then, knowing the activity of uranium, the $\Delta G_f^\circ(UC_2)$ can be evaluated using Eq. 3.

The activity coefficient of uranium in bismuth is given by Pehlke, et al. as

$$\log_{10} \gamma_U = - \frac{3740}{T} + 0.44 \qquad (4)$$

with T in °K.

Figure 18 shows the concentration data for the uranium-bismuth alloy in equilibrium with UC_2 + C. The arrows beside the data points indicate the direction of change in concentration between that sample and the previous sample. This arrow should also indicate the direction of approach toward an equilibrium concentration at any given temperature. The points without accompanying arrows are points that did not show any significant change in concentration between that sample and the previous sample.

The line in Figure 18 passes through the data such that all the data which indicate approach toward equilibrium from a supersaturated condition (arrow pointing down) are above the line and all the data which are approaching equilibrium from a subsaturated condition are below the line. The concentration at $10^{-3}/T = 0.94$, (T = 1065°K), is the best point in terms of having data both above and below the line. At the highest temperature, $10^{-3}/T \approx 0.86$ ($T \approx 1160$°K), all the concentrations are increasing, so the line must pass through or above the highest concentration, which it does. At the lowest temperature with a

reasonable amount of data, $10^{-3}/T \approx 0.985$ ($T \approx 1015°K$), the opposite is true.

From the concentrations represented by the line in Figure 18, the activities of uranium in the bismuth melt and the two-phase mixture (UC_2 + C) can be calculated using the activity coefficient data of Pehlke, et al. (42). The activities derived are shown in Figure 19. From the activities, the free energies of formation of UC_2 can be computed from Eq. 3. The free energy data are shown in Figure 20, along with the $\Delta G_f^\circ(UC_2)$ of other investigations. As can be seen, the agreement between the data of this investigation and the line agreed upon by the Vienna Panel (43) is quite good. These data are summarized in Table V. The uncertainties associated with the $\Delta G_f^\circ(UC_2)$ are calculated and discussed in Chapter V of this paper.

Cadmium

The same arguments given for (UC_2 + C) + Bi can be applied to (UC_2 + C) + Cd. Two cadmium runs were tried. The excess free energy data for uranium in cadmium, $\bar{G}_U^{xs}$, given by Johnson and Feder (21) can be used to give the activity coefficient of uranium in cadmium. Using the "Vienna Panel line" of Figure 20 for the $\Delta G_f^\circ(UC_2)$, an estimate of the expected concentration of uranium in cadmium in

TABLE V

$(UC_2 + C) + Bi$ EQUILIBRIUM DATA

T(°K)	x_U(mol fraction)	$a_U(UC_2\text{-}C)^{\dagger}$	U+2C UC_2 $\Delta G_f^{\circ}(UC_2)^{*}$ (kcal/mol)
1015	1.13×10^{-2}	6.43×10^{-6}	-24.11 ± 0.42
1065	1.35×10^{-2}	1.14×10^{-5}	-24.08 ± 0.44
1115	1.57×10^{-2}	1.91×10^{-5}	-24.07 ± 0.46
1160	1.81×10^{-2}	2.98×10^{-5}	-24.03 ± 0.48

†Standard State - pure, solid uranium.

*Standard State - solid, pure uranium and solid, pure carbon.

equilibrium with $UC_2 + C$ can be made. The estimated concentration at 723°K is $x_U = 5 \times 10^{-10}$ mol fraction uranium in the cadmium melt. No uranium was detected in the samples taken. The limit of detection by x-ray fluorescence of uranium in cadmium is approximately 100 parts per million. See Appendix D.

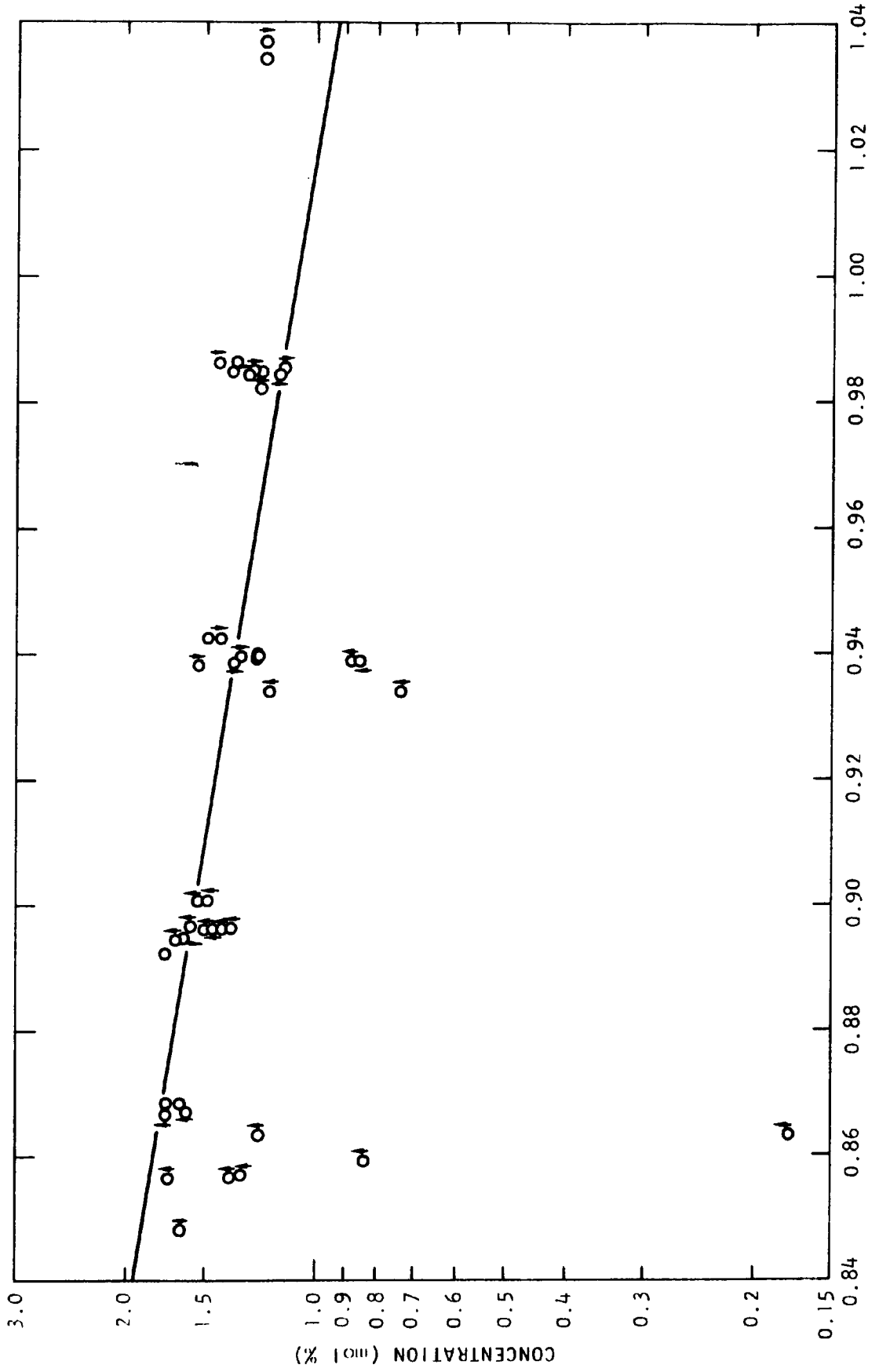


Figure 18. Concentration of Uranium in Bismuth in Equilibrium with UC_2 + C

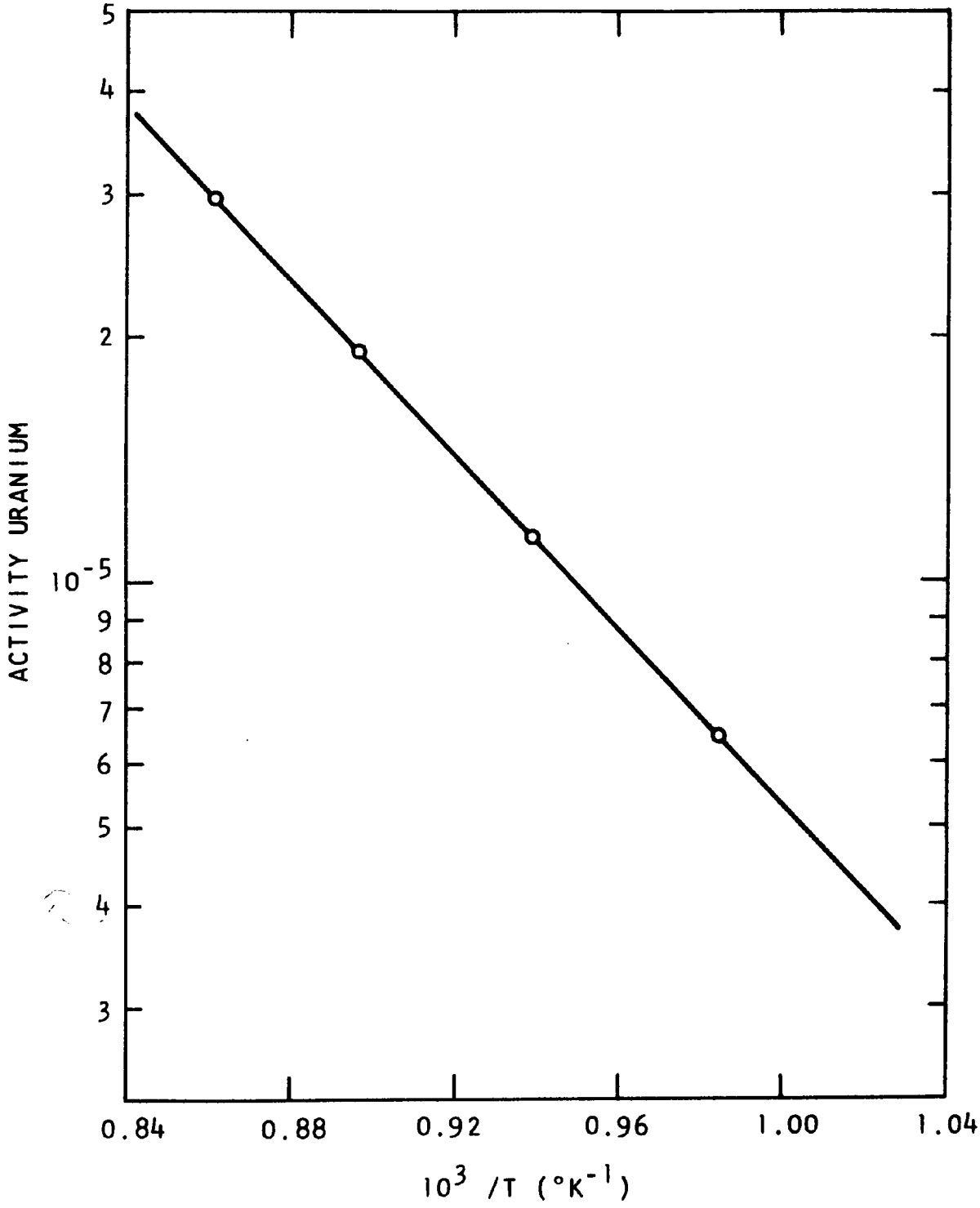


Figure 19. Activity of Uranium in the Two-Phase Region UC_2+C

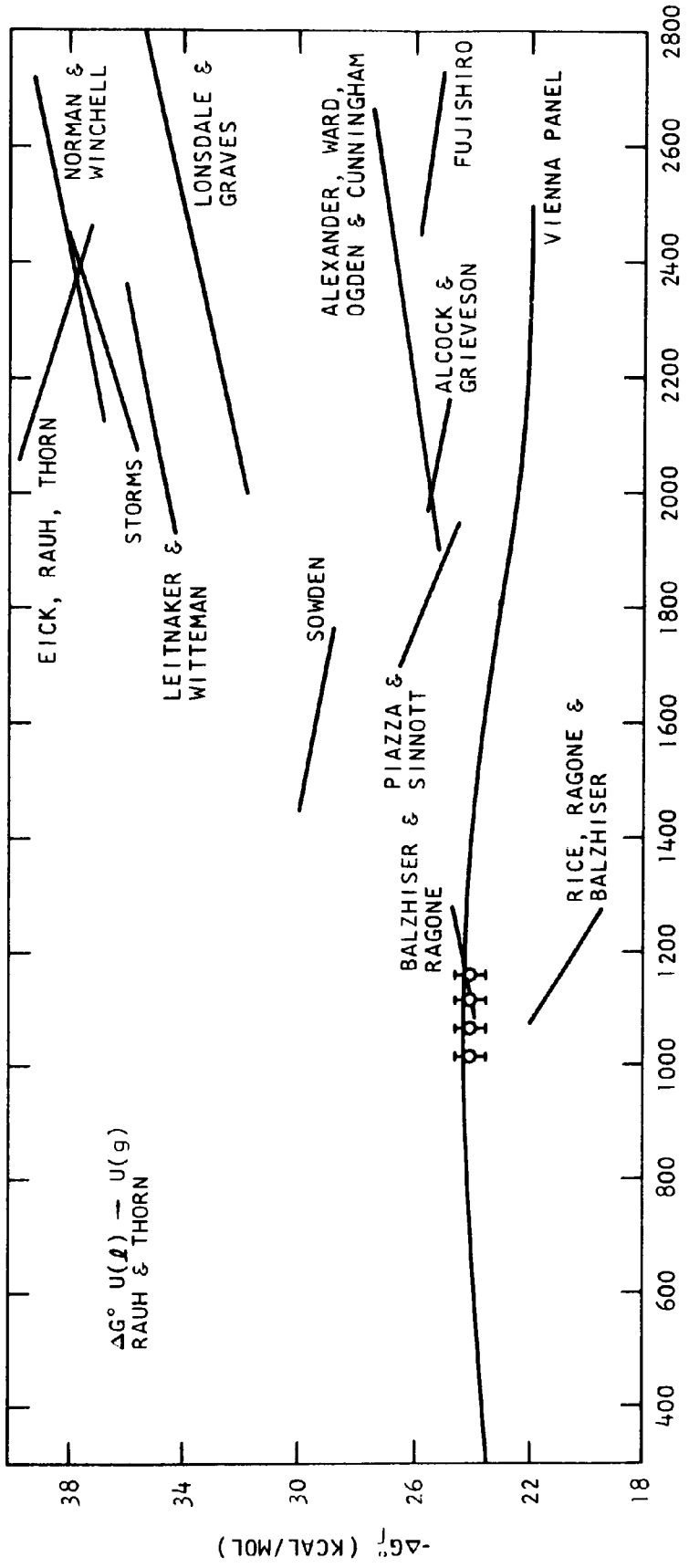


Figure 20. Free Energy of Formation of UC_2

$UC + UC_2$

For the studies involving $UC + UC_2$, the reaction taking place is:

$$2\ UC \rightarrow UC_2 + \underline{U} \tag{5}$$

The standard free energy change for this reaction is given by:

$$\Delta G^\circ = -RT \ln \frac{a_{UC_2} a_U}{a^2_{UC}} \tag{6}$$

The free energy change for Eq. 5 may also be written in terms of the standard free energy of formation, ΔG_f°, of the reactants and products.

$$\Delta G^\circ = \Delta G_f^\circ(UC_2) + \Delta G_f^\circ(U) - 2\Delta G_f^\circ(UC) \tag{7}$$

but,

$$\Delta G_f^\circ(U) \equiv 0$$

and combining Eq. 6 with Eq. 7,

$$\Delta G_f^\circ(UC) = \tfrac{1}{2}\Delta G_f^\circ(UC_2) + \tfrac{1}{2}RT \ln \frac{a_{UC_2} a_U}{a^2_{UC}} \tag{8}$$

In the two-phase region $UC + UC_2$ (Figure 1), UC_2 and UC are present as pure phases, and thus the activities of UC and of UC_2 are unity.

Then, as before, if the activity of uranium can be measured and if the $\Delta G_f^\circ(UC_2)$ is known, the ΔG_f° of UC can be calculated from Eq. 8.

Figures 21 and 22 show the concentration of uranium in the bismuth melt in contact with UC + UC_2 as a function of time. Run Bi-26, Figure 21, was made at 1165°K. The initial scatter in Figure 21 is attributed to the fact that the stirrer was not functioning. At ~70 hours, oxidation of the melt probably occurred. Uranium was added to the melt at 94 hours to increase the concentration above the equilibrium value. The concentration then dropped back to 1.86 mol % uranium.

Run Bi-32, Figure 22, was made at 1115°K. The initial concentration was below the equilibrium concentration. The concentration increased to 1.70 mol % uranium. At 435 hours, uranium was added to drive the concentration above the equilibrium value. (Note that the time scale in Figure 22 is broken at 420 hours.) The concentration then decreased toward the equilibrium value. The run was terminated at 740 hours.

In both of these experiments, the equilibrium concentration was approached from above and below.

Once again, using the activity coefficient data of Pehlke, et al., Eq. 4, the activities of uranium in the two-phase region

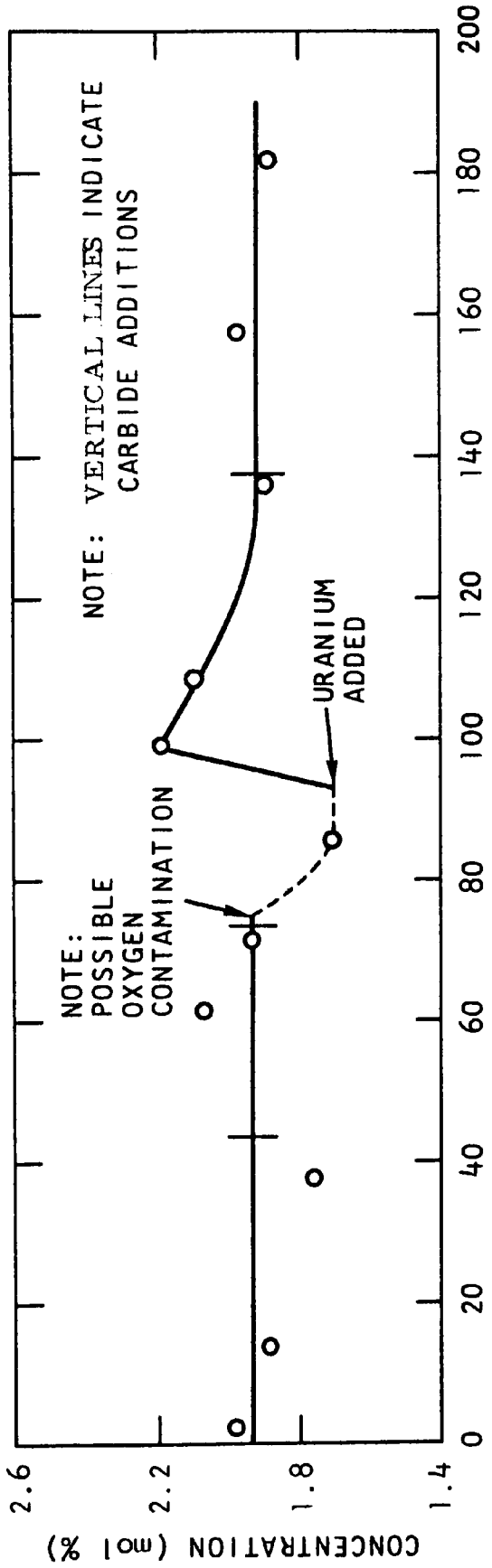


Figure 21. Concentration of Uranium in Bismuth for Run Bi-26

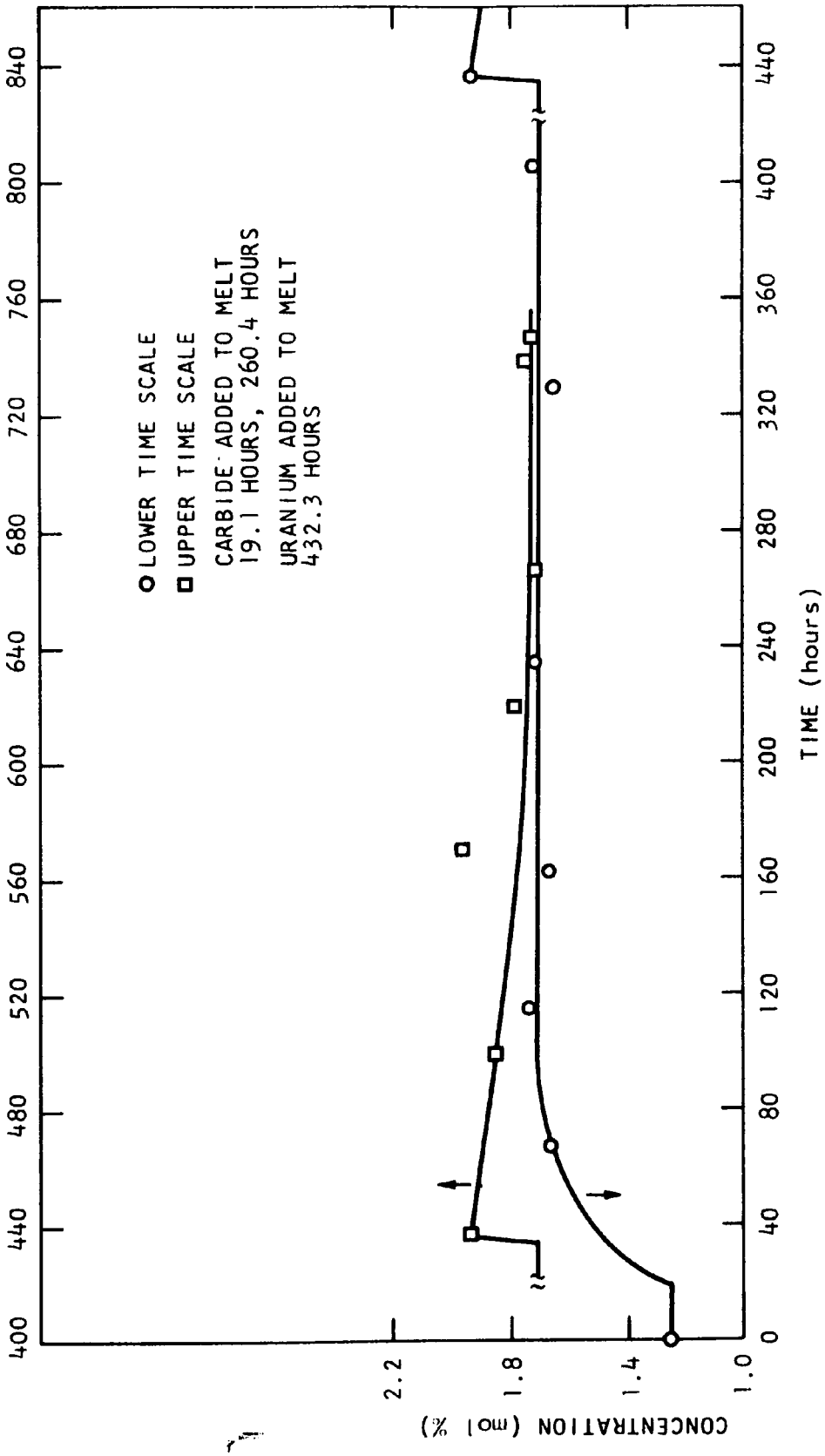


Figure 22. Concentration of Uranium in Bismuth for Run Bi-32

$UC + UC_2$ can be calculated. These are plotted in Figure 23, with the $\Delta G_f^\circ(UC)$ as calculated from Eq. 8, shown in Figure 24. The $\Delta G_f^\circ(UC)$ can also be written in terms of the elemental reactants,

$$U + C \rightarrow UC \tag{9}$$

$$\Delta G_f^\circ(UC) = -RT \ln \frac{a_{UC}}{a_U \, a_C} \tag{10}$$

In the two-phase region $UC + UC_2$, the activity of UC = 1. The activity of uranium in $UC + UC_2$ has been determined, Figure 23. Then, using the $\Delta G_f^\circ(UC)$ in Figure 24, the activity of carbon can be computed using Eq. 10.

Table VI summarizes the $UC + UC_2$ data. The uncertainties associated with the $\Delta G_f^\circ(UC)$ are calculated and discussed in Chapter V.

TABLE VI

$(UC + UC_2)$ + Bi EQUILIBRIUM DATA

T(°K)	X(mol fraction)	$a_u(UC+UC_2)^{\dagger}$	$a_C(UC+UC_2)^{\ddagger}$	$\Delta G_f^\circ(UC_2)^*$	$\Delta G_f^\circ(UC)^*$
1165	0.01926	3.269×10^{-5}	0.974	-24.03	-23.97 ± 0.36
1115	0.01720	2.094×10^{-5}	0.955	-24.07	-23.97 ± 0.33

†Standard State - pure solid uranium.

‡Standard State - pure solid carbon.

*Standard State - pure solid uranium and pure solid carbon.

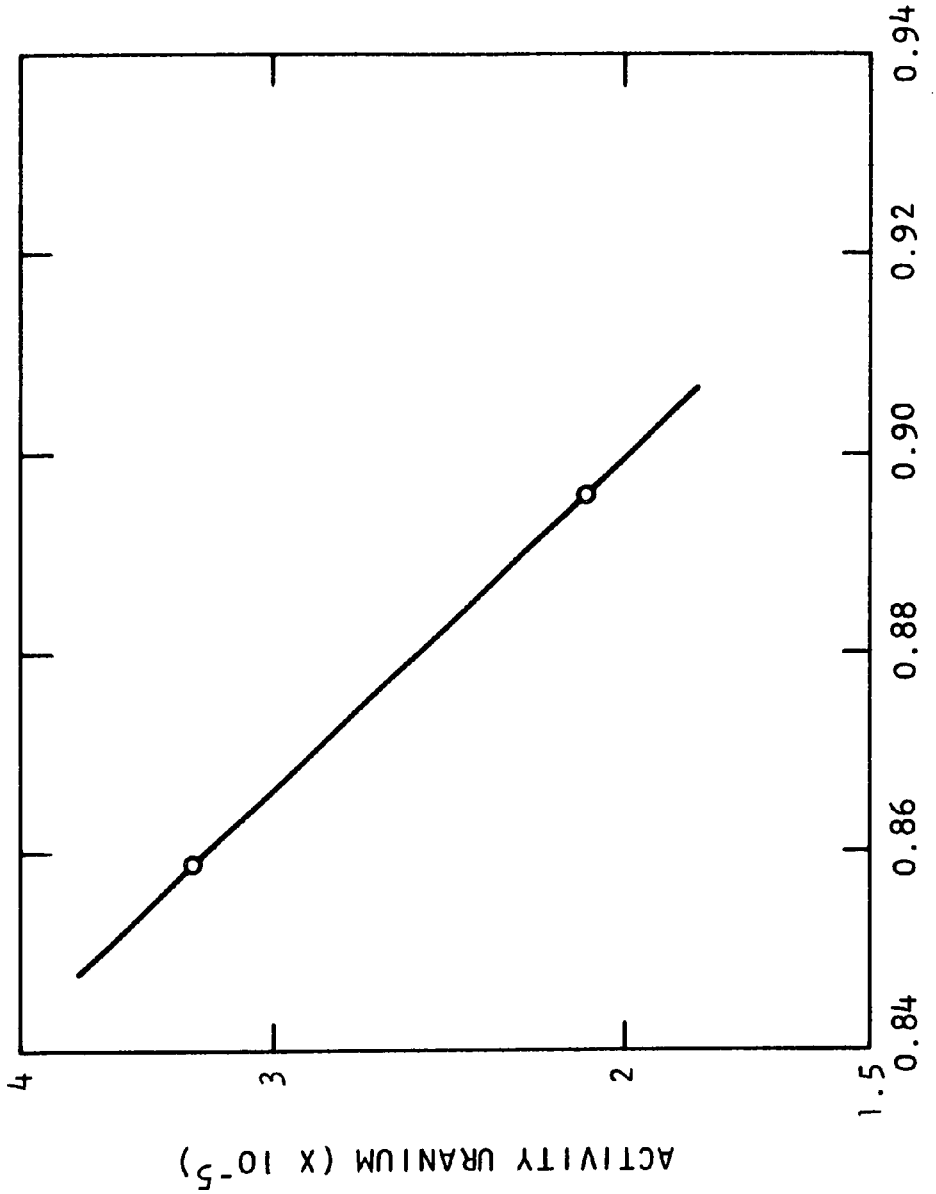


Figure 23. Activity of Uranium in the Two-Phase Region UC + UC_2

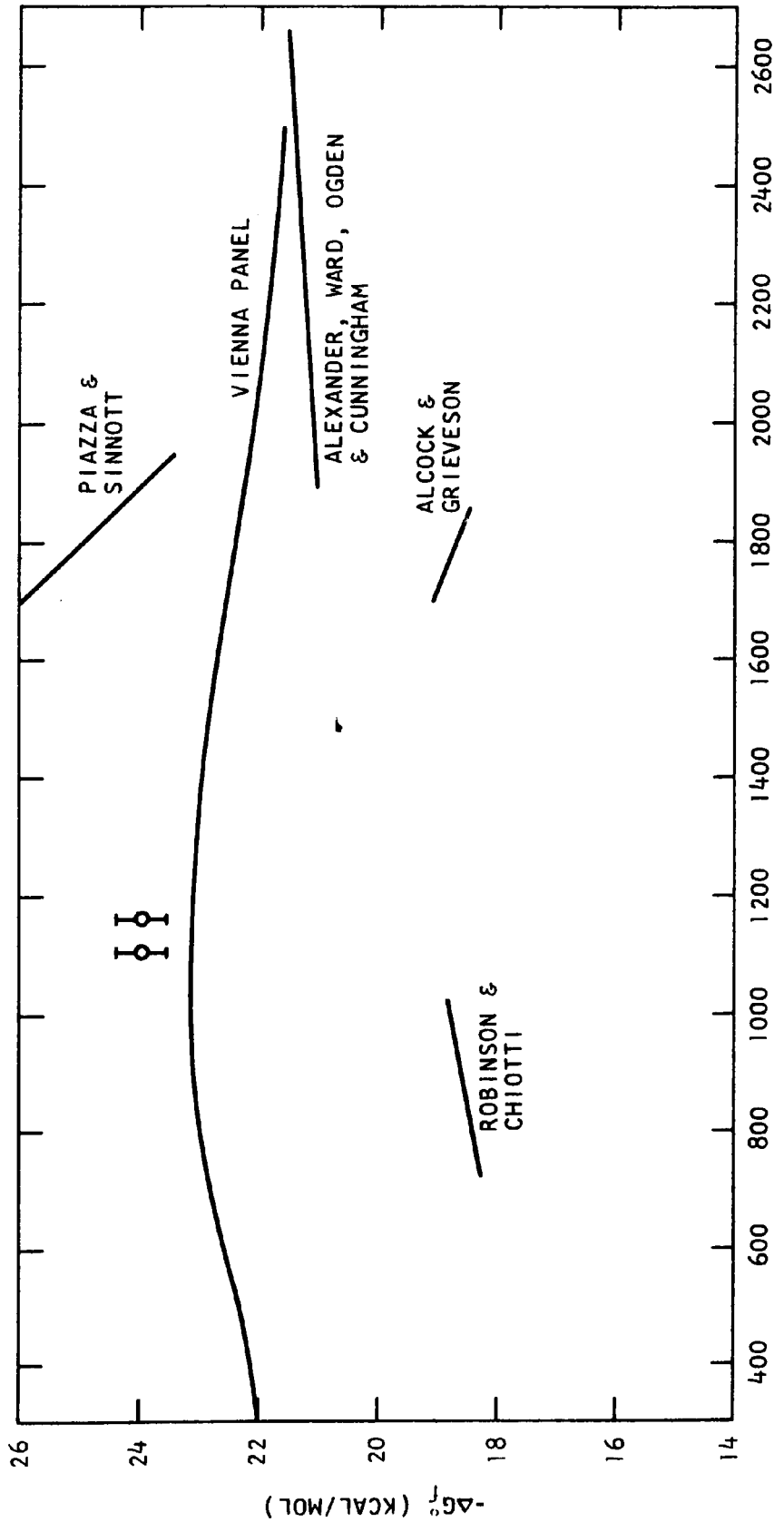


Figure 24. Free Energy of Formation of UC

CHAPTER V

DISCUSSION OF RESULTS

In both of the equilibrium studies, $UC_2 + C$ or $UC + UC_2$ with bismuth, the equilibrium concentrations were approached from supersaturated, as well as subsaturated solutions. This is quite important in any equilibrium study and removes the doubt that what appears to be an equilibrium value might be only a reflection of very slow kinetics.

The values of activities and of free energies of formation derived from the concentration data are dependent upon the validity of the activity coefficient data used. The good agreement between the $\Delta G_f^\circ(UC_2)$ of this study with that determined from thermal data by the Vienna Panel (Figure 20) increases confidence both in the concentration data of this study and in the activity coefficient data of Pehlke, et al. (42), in the uranium-bismuth system.

The agreement between the $\Delta G_f^\circ(UC)$ from this study and that agreed upon by the Vienna Panel is not as good as with the $\Delta G_f^\circ(UC_2)$, but the difference is only of the order of one kilocalorie per mol.

As was noted, the agreement between this work and the Vienna Panel line for $\Delta G_f^\circ(UC_2)$ gives confidence in the activity coefficient data of Pehlke, et al. However, an interesting comparison between

the thermodynamic stabilities of UC and UC_2 can be made from the concentration data even if the activity coefficient is not well known. The difference between $\Delta G_f^\circ(UC_2)$ and $\Delta G_f^\circ(UC)$ is independent of the activity coefficient in cases where the activity coefficient is independent of concentration. Eq. 3 can be written:

$$\Delta G_f^\circ(UC_2) = RT \ln a_U(UC_2 + C) \qquad (11)$$

since $a_{UC_2} = a_C = 1$ in the $UC_2 + C$ region. Eq. 8 can be written,

$$\Delta G_f^\circ(UC) = \tfrac{1}{2}\left[\Delta G_f^\circ(UC_2) + RT \ln a_U(UC + UC_2)\right] \qquad (12)$$

since $a_{UC} = a_{UC_2} = 1$ in the $UC + UC_2$ region. Subtracting Eq. 11 from Eq. 12, and substituting Eq. 11 for $\Delta G_f^\circ(UC_2)$ in Eq. 12 gives

$$\Delta G_f^\circ(UC)-\Delta G_f^\circ(UC_2) = \tfrac{1}{2}\left[RT \ln a_U(UC_2+C) + RT \ln a_U(UC+UC_2)\right] - RT \ln a_U(UC_2+C)$$

or,

$$\Delta G_f^\circ(UC) - \Delta G_f^\circ(UC_2) = \frac{RT}{2}\left[\ln a_U(UC+UC_2) - \ln a_U(UC_2+C)\right]$$

or,

$$\Delta G_f^\circ(UC) - \Delta G_f^\circ(UC_2) = \frac{RT}{2} \ln \frac{a_U(UC+UC_2)}{a_U(UC_2+C)} \qquad (13)$$

But,

$a_U = \gamma_U x_U$

x_U = concentration mol fraction

γ_U = activity coefficient

Substituting into Eq. 11 gives

$$\Delta G_f^\circ(UC) - \Delta G_f^\circ(UC_2) = \frac{RT}{2} \ln \frac{x_U(UC+UC_2)}{x_U(UC_2+C)} \qquad (14)$$

which is independent of the activity coefficient, γ_U. Eq. 14 can be evaluated at T = 1115°K and T = 1165°K, the two temperatures at which both concentrations are known. As can be seen from Table VII, the thermodynamic stabilities of these two materials, UC and UC_2, are very nearly the same.

TABLE VII

COMPARISON OF $\Delta G_f^\circ(UC)$ WITH $\Delta G_f^\circ(UC_2)$

T(°K)	$x_U(UC+UC_2)$ (Table VI)	$x_U(UC_2+C)$ (Fig. 18)	$\Delta G_f^\circ(UC)-\Delta G_f^\circ(UC_2)$ kcal/mol
1165	0.0193	0.0182	0.07 ± 0.06
1115	0.0172	0.0157	0.1 ± 0.02

Some comments about possible errors in the data seem in order. In order to eliminate the possibility of some consistent error

due to the type of crucible used to contain the melt, two types of crucibles were used, recrystallized alumina and tantalum. No differences in the results were noted. In addition, the samples taken from the melt were periodically checked for contamination from the materials in contact with the melt (see Figure 10). The samples were checked for Al, Mo, Ta, and W. None of these materials were ever detected in any of the samples checked.

Each of the thermocouples used in the experiments was calibrated by the Standards Laboratory of Convair Division of General Dynamics Corporation. None of the thermocouples were off by more than 2°K in the temperature range of interest. Since the error in the thermocouple reading was very small, $\leq$ 2°K out of 1000°K ($\leq$ 0.2%), no corrections for the calibration were made. As was mentioned above, the controller used maintained the temperature at ± 3°K about the set point. Thus, the maximum error in temperature is probably no greater than ± 5°K which is at most 0.5% of the temperature.

Another source of error was in the chemical analysis of the sample for uranium. A description of the technique is given in Appendix D. From time to time, dummy samples of known uranium content were made up and sent to chemistry for analysis. The average error in the amount of uranium reported was 0.782% of the reported

value. The error at the 95% confidence limit, taking into account the limited number of check analyses, 13, was 2.16% of the reported value.

In order to establish the repeatability of measuring a given uranium concentration in the melt by the technique employed, a melt having no carbide in it was sampled four times, as rapidly as possible. Since there was no carbide in the melt, the concentration of uranium in the liquid should have remained constant except for the vaporization of the bismuth. The vaporization of bismuth from a U-Bi alloy blanketed by one atmosphere of argon is quite slow. Melts of from 375-400 grams from which 50-60 grams of bismuth were removed by sampling still had from 150-200 grams of bismuth left after 400 hours at temperature. The concentration of the melt being sampled may be considered to have been constant over the 5 hour period of the sampling. The samples ranged from 0.0252 to 0.0257 mol fraction uranium with the average being 0.0254. Using these four samples, the error in the reported value was ±2.6% at the 95% confidence limit taking into account the limited number of samples. This is only slightly greater than the error in chemical analysis. Thus, the confidence in the technique of sampling appears to be justified.

In order to determine the error in concentration under the actual conditions of data taking, the data of Run Bi-32 were analyzed.

For the seven points taken after reaching equilibrium, an average value of $x_U = 0.01720$ with a standard deviation of $\sigma = 2.34 \times 10^{-4}$ was determined.

In the calculation of $\Delta G_f^\circ(UC_2)$ from Eq. 3,

$$\Delta G_f^\circ(UC_2) = -RT \ln \frac{a_{UC_2}}{a_U a_C^2}$$

or,

$$\Delta G_f^\circ(UC_2) = 2.303\ RT\ [\log_{10} x_U + \log_{10} \gamma_U] \qquad (15)$$

There are three sources of error: 1) the error in temperature; 2) the error in the concentration, x_U; 3) the error in the activity coefficient, γ_U. From Volk (46), the variance of $\Delta G_f^\circ(UC_2)$ is given by

$$\sigma^2[\Delta G_f^\circ(UC_2)] = \left[\frac{\partial \Delta G}{\partial T}\right]^2 \sigma^2(T) + \left[\frac{\partial \Delta G}{\partial x_U}\right]^2 \sigma^2(x_U) + \left[\frac{\partial \Delta G}{\partial \gamma}\right]^2 \sigma^2(\gamma_U) \qquad (16)$$

If the uncertainty in T is taken to be $\pm 5°$ at the 95% confidence limits (see preceding remarks on the temperature measurements), then $\sigma(T) = 2.5$ and $\sigma^2(T) = 6.25$. The variance of x_U is discussed above. For the variance of γ_U, $\sigma^2(\gamma_U)$, the equation given by Pehlke, et al. is

$$\log_{10} \gamma_U = -\frac{3740}{T} + 0.44$$

σ (slope) = 170 $\quad\quad$ σ^2 (slope) = 2.89×10^{-4}

σ (intercept) = 0.09 $\quad\quad$ σ^2 (intercept) = 8.1×10^{-3}

It can be shown that σ^2 (intercept) is an upper bound for $\sigma^2(\log \gamma_U)$, Volk (46), page 237. In the absence of the complete set of statistics for the $\log_{10}\gamma_U$ equation, $\sigma^2(\log_{10}\gamma_U) = 8.1 \times 10^{-3}$ will be used. Then, since $\sigma^2(\log_{10}\gamma_U)$ is known but $\sigma^2(\gamma_U)$ is not, it is more convenient to evaluate the following equation rather than Eq. 16.

$$\sigma^2[\Delta G_f^\circ(UC_2)] = \left[\frac{\partial \Delta G}{\partial T}\right]^2 \sigma^2(T) + \left[\frac{\partial \Delta G}{\partial x_U}\right]^2 \sigma^2(x) + \left[\frac{\partial \Delta G}{\partial \log_{10}\gamma_U}\right]^2 \sigma^2(\log_{10}\gamma_U) \qquad (17)$$

Differentiating Eq. 15 and substituting into Eq. 17 gives

$$\sigma^2[\Delta G_f^\circ(UC_2)] = (2.303R)^2\left[(\log_{10}\bar{\gamma}_U + \log_{10}\bar{x}_U)^2\,\sigma^2(T) + (\bar{T})^2\,\sigma^2(\log_{10}\bar{\gamma}_U) + (\bar{T})^2\,\frac{\sigma^2(x_U)}{\bar{x}_U^2}\right] \qquad (18)$$

Evaluating Eq. 18 gives the error limits $\sigma[\Delta G_f^\circ(UC_2)]$ which are shown in Table V and Figure 20.

Similarly, for $\Delta G_f^\circ(UC)$, taking Eq. 8,

$$\Delta G_f^\circ(UC) = \tfrac{1}{2}\,\Delta G_f^\circ(UC_2) + RT \ln \frac{a_{UC_2}\, a_U}{a_{UC}}$$

or,

$$\Delta G_f^\circ(UC) = \frac{\Delta G_f^\circ(UC_2)}{2} + \frac{2.303\,RT}{2}\left[\log_{10} x_U + \log_{10} \gamma_U\right] \qquad (19)$$

as before

$$\sigma^2[\Delta G_f^\circ(UC)] = \left[\frac{\partial \Delta G_f^\circ(UC)}{\partial \Delta G_f^\circ(UC_2)}\right]^2 \sigma^2[\Delta G_f^\circ(UC_2)] + \left[\frac{\partial \Delta G_f^\circ(UC)}{\partial T}\right]^2 \sigma^2(T)$$
$$+ \left[\frac{\partial \Delta G^\circ(UC)}{\partial x_U}\right]^2 \sigma^2(x_U) + \left[\frac{\partial \Delta G^\circ(UC)}{\partial \log_{10}\gamma_U}\right]^2 \sigma^2(\log_{10}\gamma_U) \qquad (20)$$

Differentiating Eq. 19 and substituting into Eq. 20 gives

$$\sigma^2[\Delta G_f^\circ(UC)] = \frac{\sigma^2[\Delta G_f^\circ(UC_2)]}{4} + \left[\frac{2.303\,R}{2}\left(\log_{10} x_U + \log_{10}\gamma_U\right)\right]^2 \sigma^2(T)$$
$$+ \left[\frac{2.303\,R\bar{T}}{2}\right]^2 \left[\sigma^2(\log_{10}\gamma_U) + \frac{\sigma^2(x_U)}{\bar{x}_U^2}\right] \qquad (21)$$

Using, as before, $\sigma^2(\log_{10}\gamma_U) = 8.1 \times 10^{-3}$ and $\sigma^2(T) = 6.25$, and then values for $\sigma^2[\Delta G_f^\circ(UC_2)]$ computed above, Eq. 21 can be evaluated for

$T = 1165°K$ where $\sigma^2(x_U)/\bar{x}_U^2 = 2.08 \times 10^{-3}$ for the equilibrium data of Run Bi-26 (Figure 21), and for $T = 1115°K$ where $\sigma^2(x_U)/\bar{x}_U^2 = 1.845 \times 10^{-4}$ for the equilibrium data of Run Bi-32 (Figure 22). The uncertainties computed, $\sigma[\Delta G_f^\circ(UC)]$, are shown in Table VI and Figure 24.

The major source of error in all of these calculations is the error in the activity coefficient data. This error is due, for the most part, in having to extrapolate the data beyond the range in which it was taken. Even with this handicap, the uncertainty in the free energy values is quite small. It is smaller than 0.5 kilocalorie per mol in every case.

CHAPTER VI

SUMMARY

Because of the lack of agreement among the various investigations of the free energies of formation of UC and UC_2, the present study was undertaken. In order to determine the ΔG_f° of UC and UC_2, the activities of uranium were investigated in the two two-phase regions UC_2+C and $UC + UC_2$ in the temperature range 1015-1165°K.

The activity of uranium in the two-phase region, UC_2+C or $UC+UC_2$, was determined by measuring the concentration of uranium in a liquid bismuth bath in equilibrium with the solid carbide. The concentration of uranium along with the activity coefficient data of Pehlke, Tien and Guion (42) gave the activity of uranium in the liquid phase which was, of course, equal to the activity of uranium in the two phase mixture.

In order to measure the concentration of uranium in the liquid bismuth, a sample of the liquid which excluded the solid carbide phase had to be taken at the temperature of interest. This was accomplished by filtering the liquid phase through a porous carbon filter into a graphite cup for the $UC_2 + C$ equilibrations. For the $UC + UC_2$ equilibrium studies, the liquid was filtered with a tungsten filter into a tungsten-coated graphite cup. The tungsten filter was made by hot-pressing 420μ diameter tungsten spheres into filter discs.

The activities determined by this technique are summarized in Table VIII.

TABLE VIII

URANIUM ACTIVITIES

Temperature (°K)	Uranium Activity* $UC + UC_2$	Uranium Activity* $UC_2 + C$
1165	3.27×10^{-5}	3.1×10^{-5}
1115	2.09×10^{-5}	1.91×10^{-5}
1065		1.14×10^{-5}
1015		6.43×10^{-5}

*Standard State - pure, solid uranium.

Cadmium - (UC_2 + C) equilibrations were sampled, but no uranium was detected in the samples. The concentrations estimated from the thermodynamics of uranium-cadmium alloys reported by Johnson and Feder (21) were of the order of 10^{-9} mol fraction uranium in the cadmium.

From the activity of uranium in the $UC_2 + C$ two-phase region, the free energy of formation of UC_2 can be computed.

$$\Delta G_f^\circ(UC_2) = -RT \ln \frac{a_{UC_2}}{a_U \, a_C^2} \qquad (22)$$

In the two phase region $UC_2 + C$, $a_{UC_2} = a_C = 1$. The values of the $\Delta G_f^\circ(UC_2)$ are summarized in Table IX.

TABLE IX

FREE ENERGY OF FORMATION OF URANIUM DICARBIDE

Temperature (°K)	$\Delta G_f^\circ(UC_2)^*$ (kcal/mol)
1160	-24.03 ± 0.48
1115	-24.07 ± 0.46
1065	-24.08 ± 0.44
1015	-24.11 ± 0.42

*Standard State - pure, solid uranium and pure, solid carbon.

The free energy of formation of UC can be computed from the activity of uranium in the UC + UC_2 two-phase region, when the $\Delta G_f^\circ(UC_2)$ is known.

$$\Delta G_f^\circ(UC) = \tfrac{1}{2}\Delta G_f^\circ(UC_2) + \tfrac{1}{2}\ RT\ \ln \frac{a_U\ a_{UC_2}}{a_{UC}^2} \qquad (23)$$

TABLE X

FREE ENERGY OF FORMATION OF URANIUM MONOCARBIDE

Temperature (°K)	$\Delta G_f^\circ(UC)^*$ (kcal/mol)
1165	-23.97 ± 0.36
1115	-23.97 ± 0.33

*Standard State - pure, solid uranium and pure, solid carbon.

The free energy of formation of uranium dicarbide obtained from this study agrees very well with the "agreed upon values" of the Vienna Panel (IAEA, 1962) (43). This agreement increases confidence in the results of this investigation, the method of this investigation, and in the activity coefficient data of Pehlke, et al. (42).

The free energy of formation of UC determined in this investigation agrees within one kilocalorie per mol with that of the Vienna Panel.

APPENDICES

APPENDIX A

TUNGSTEN FILTERS AND SAMPLERS

Filters

The tungsten filter discs used in the ($UC + UC_2$) + Bi experiments were made by hot-pressing tungsten spheres (420μ diameter) into discs about 1/16 to 1/8 inch thick. The hot-pressing was done in a vacuum hot-press using dies made of UT-2S graphite obtained from United Carbon Products Company; see Figure A-1. Filters with 70-80% theoretical density were produced by pressing at ~1800°C, 7000 psi for 3-5 minutes while maintaining a vacuum ~5-10 x 10^{-3} torr.

The filters were checked for particle retention using a slurry of water and aluminum oxide powder, 0.3μ - 25μ particle size. A sample of the slurry was filtered using a tungsten filter, and the filtrate was collected and examined with a microscope to determine the size of any particles found. Care was taken not to allow a "filter-cake" to build up on the filter. Eight filters from six separate pressings were each tested five times for particle retention. In no case were particles larger than 5μ in diameter found in the filtrate.

Samplers

The graphite samplers after being outgassed were coated with tungsten by reacting tungsten hexafluoride with hydrogen at the surface of the sampler.

$$WF_{6(g)} + 3H_2 \rightarrow W_{(s)} + 6\,HF$$

The samplers were coated four at a time first on the outside, and then on the inside. In order to get a uniform coating on the inside of the samplers, the gas mixture (H_2 + WF_6) was jetted through 0.002 inch capillary tubing down into the samplers. See Figure A-3.

A schematic of the equipment used is shown in Figure A-2. The samplers were placed in the Vycor chamber as shown in Figure A-3, and evacuated to $\sim 10^{-3}$ torr. The samplers were then heated to 1000°F by induction heating. At this point, the vacuum pump was isolated from the system and hydrogen was started flowing through the system at the rate of 900 cc/min (standard conditions). The hydrogen was removed from the system by the air pump which kept the chamber pressure at about 1 psia throughout the coating process. After 1-2 minutes of hydrogen flow, WF_6 was let into the chamber at 500 cc/min (SC). A coating time of 15 minutes gave a coating of 0.008-0.010 inch thick.

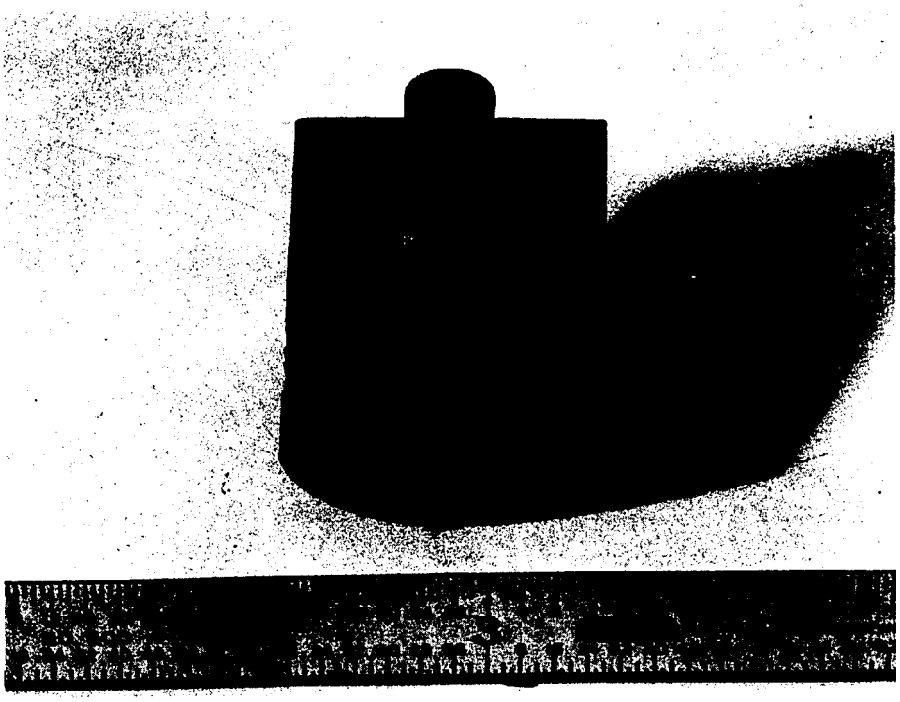


Figure A-1. Graphite Die and Tungsten Filters

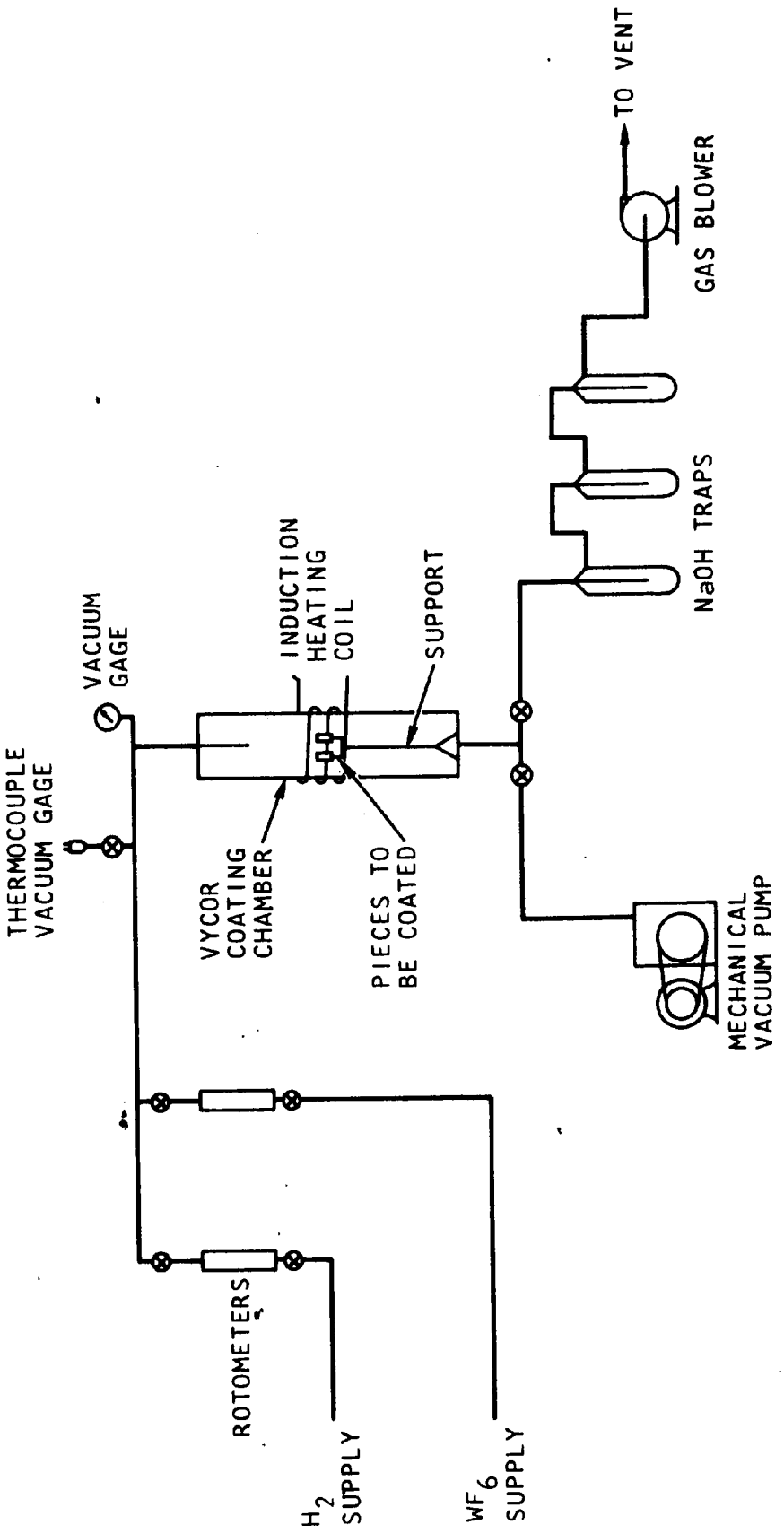
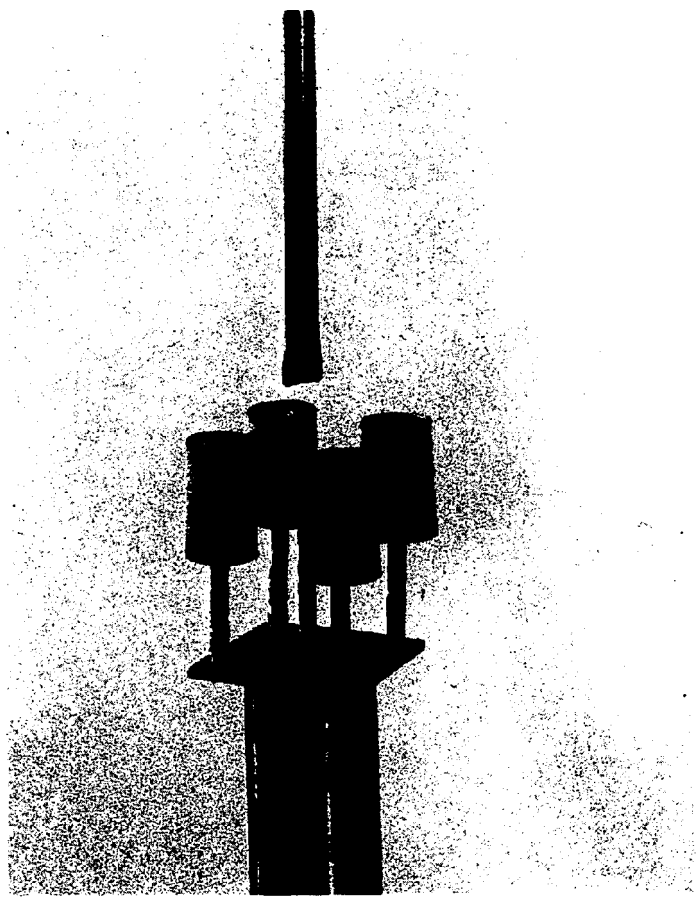
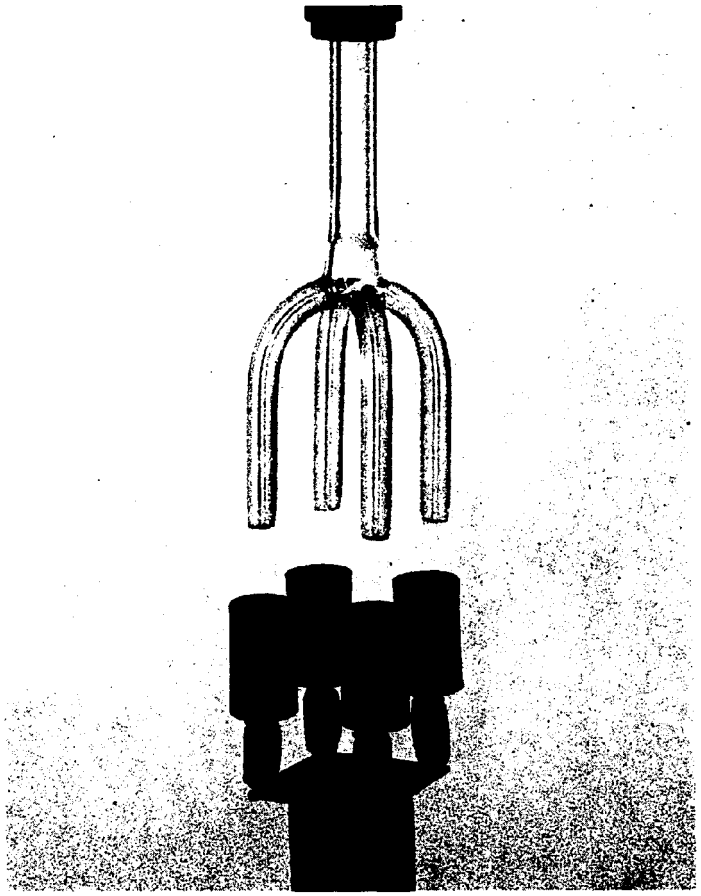


Figure A-2. Schematic of Tungsten Coating Apparatus



Outside Arrangement



Inside Arrangement

Figure A-3. Coating Arrangement for Samplers

APPENDIX B

STIRRER

Several factors were considered during the design of a stirrer for the system. It was felt that a propeller type stirrer would not be practical because of the strong possibility that it would become entangled with the thermocouple which was also in the melt. A disc on the end of a rod which was to be lifted and lowered was chosen.

It was felt that a mechanical coupling through a packing gland was to be avoided if possible. Any misalignment in a mechanical coupling through glass would have been a constant source of trouble. Thus, a magnetic drive was chosen.

The stirrer, then, is basically a solenoid with the iron plug attached to the stirrer. However, a simple on-off type solenoid would lift the stirrer quite rapidly, and then drop it. This was considered undesirable. Dropping the stirrer through even a short distance might very well break the alumina crucible containing the melt. Also, lifting the stirrer too rapidly might cause some of the melt to splash out of the crucible. So, the power to the solenoid coil was programmed in a saw-tooth wave. This was accomplished by controlling the power through the transistorized power supply shown in Figure B-1 with a

motor-driven, center-tapped, 500Ω potentiometer. The frequency of the stirring action was controlled by the speed of the motor. Two motors were used, one giving 8 cycles per minute, and one giving 15 cycles per minute.

A picture of the stirrer is shown in Figure 11.

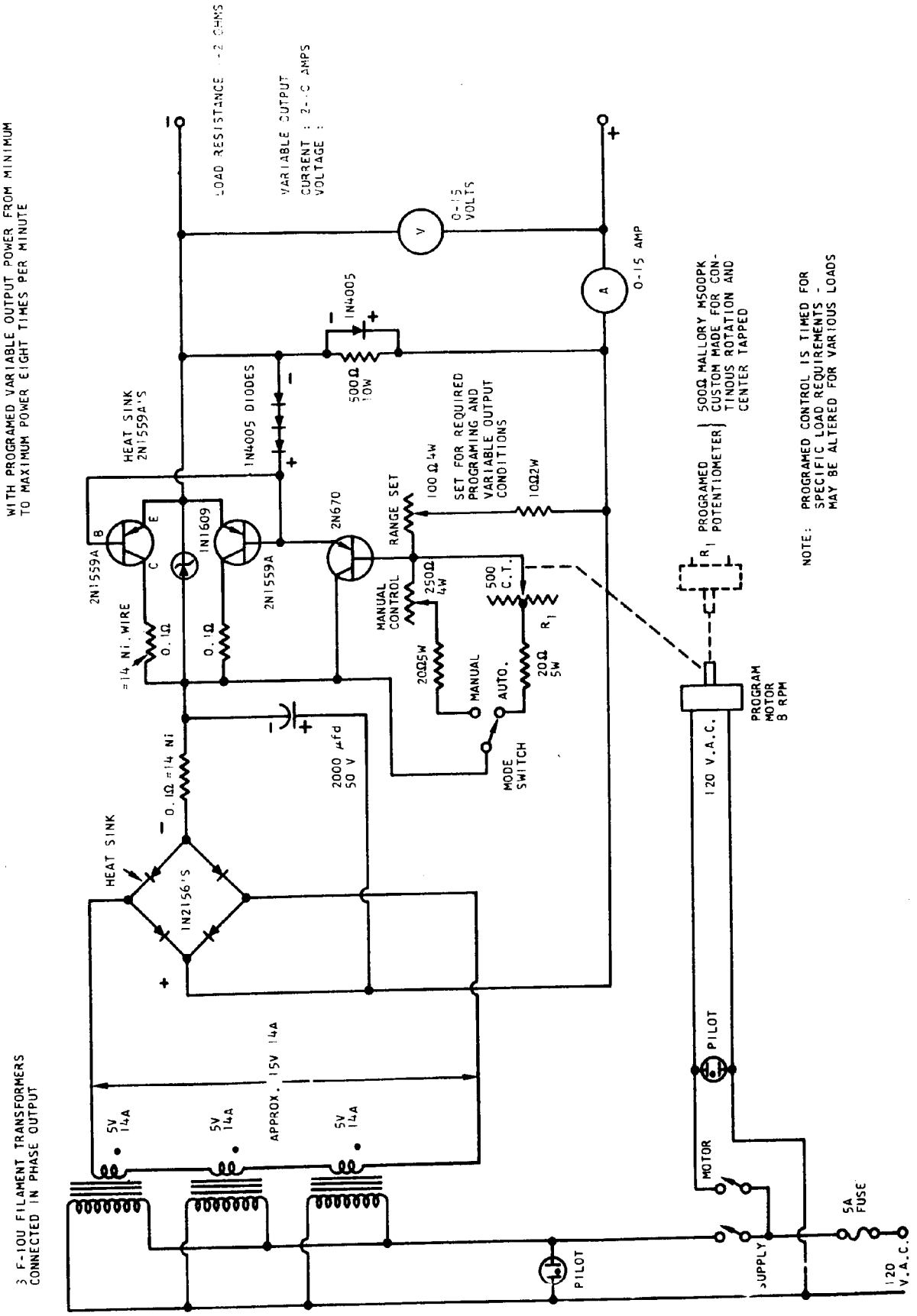


Figure B-1. Schematic of Solenoid Power Supply

APPENDIX C

CHARACTERIZATION OF CARBIDES

The carbides used for the equilibrium studies were checked by x-ray diffraction and by metallographic techniques, in addition to chemical analysis to insure that they were composed only of the phases desired: UC_2 and C, or UC and UC_2.

Metallography

The particles of the various carbides were mounted in resin, polished, and etched with an etch composed of equal parts of nitric acid, acetic acid, and water. The particles were then compared with the photomicrographs of material of various C/U ratios prepared by C.G. Hoffman of Los Alamos Scientific Laboratories, Figure C-1. Figure C-1 is printed by permission of Mr. C.G. Hoffman.

UC_2 + C

Photomicrographs of 4094 DC, the carbide used for the UC_2 + C studies, are shown in Figure C-2. They show only UC_2 with excess carbon.

The residue of each run was examined to insure that the carbide was still composed of only UC_2 and C. In no case were other phases detected.

UC + UC_2

Photomicrographs of 5000 DC, AM-11, AM-12 are shown in Figures C-3, C-4, C-5 respectively. No phases other than UC and UC_2 could be detected.

The residue of each run was examined, as before, for the phases present. As an example, photomicrographs of the carbide in the residue of Run Bi-32 are shown in Figure C-6. No phases other than UC and UC_2 were ever detected in the carbide.

X-Ray Diffraction

All of the carbides were checked for the phases present by x-ray diffraction techniques using a diffractometer with a powder sample.

TABLE C-I

Carbide	Phases Present	
4094 DC	UC_2, C	(All peaks accounted for)
5000 DC	UC, UC_2	(All peaks accounted for)
AM-11	UC, UC_2	(All peaks accounted for)
AM-12	UC, UC_2	(All peaks accounted for)

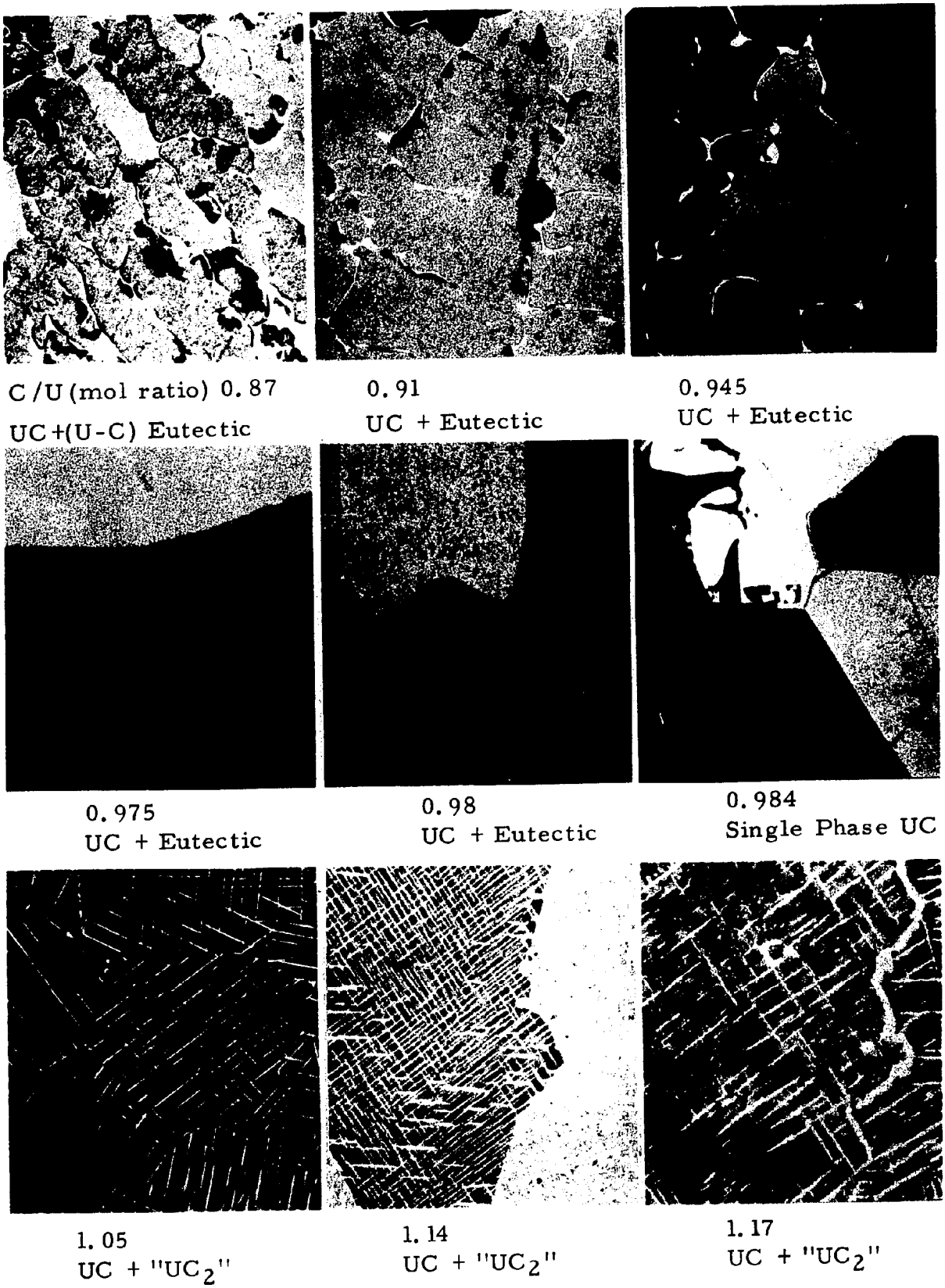


Figure C-1a. Microstructures in the Uranium Carbon System (250X). Printed with the permission of Mr. C.G. Hoffman

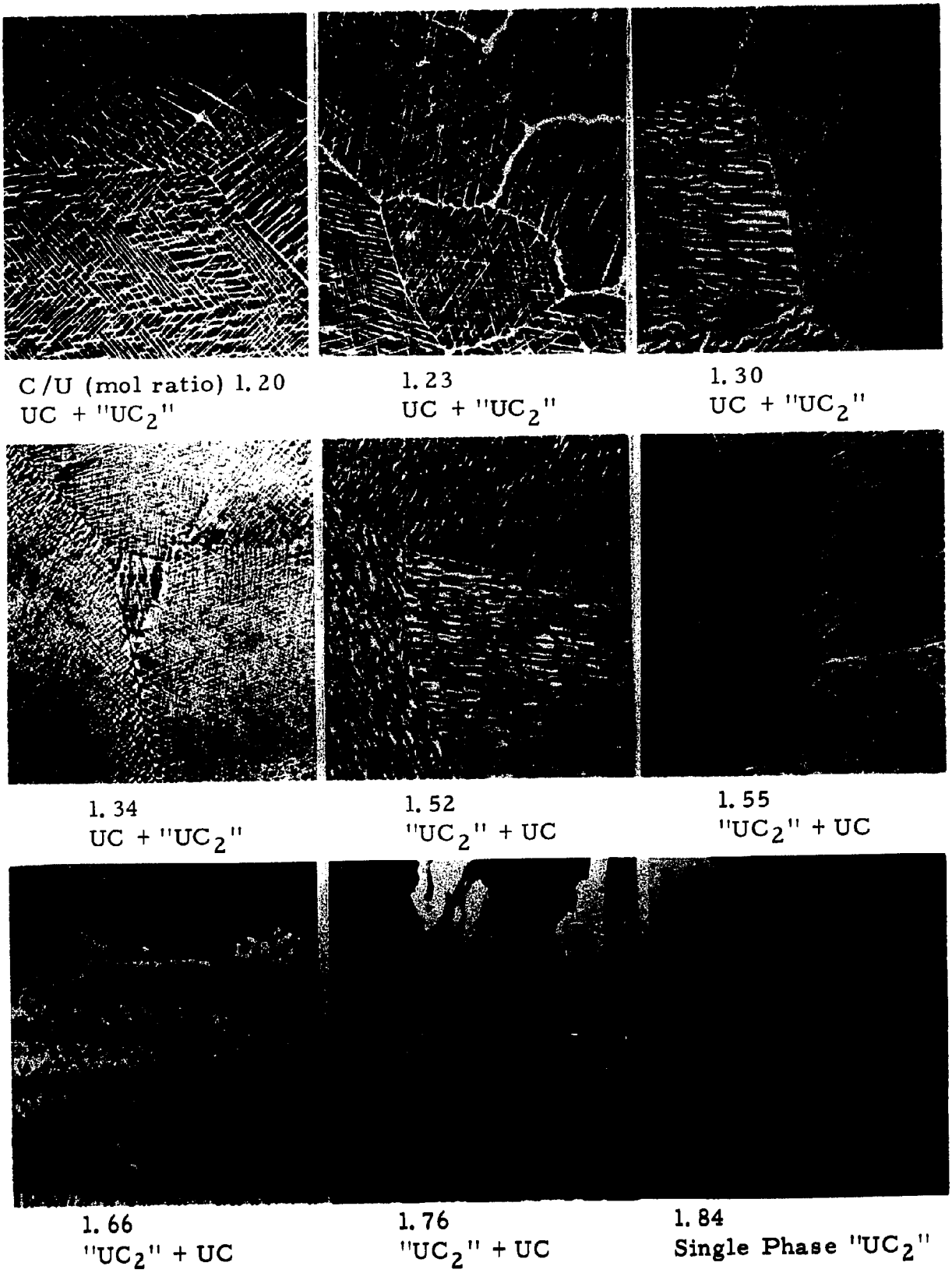


Figure C-1b. Microstructures in the Uranium Carbon System (250X). Printed with the permission of Mr. C.G. Hoffman.

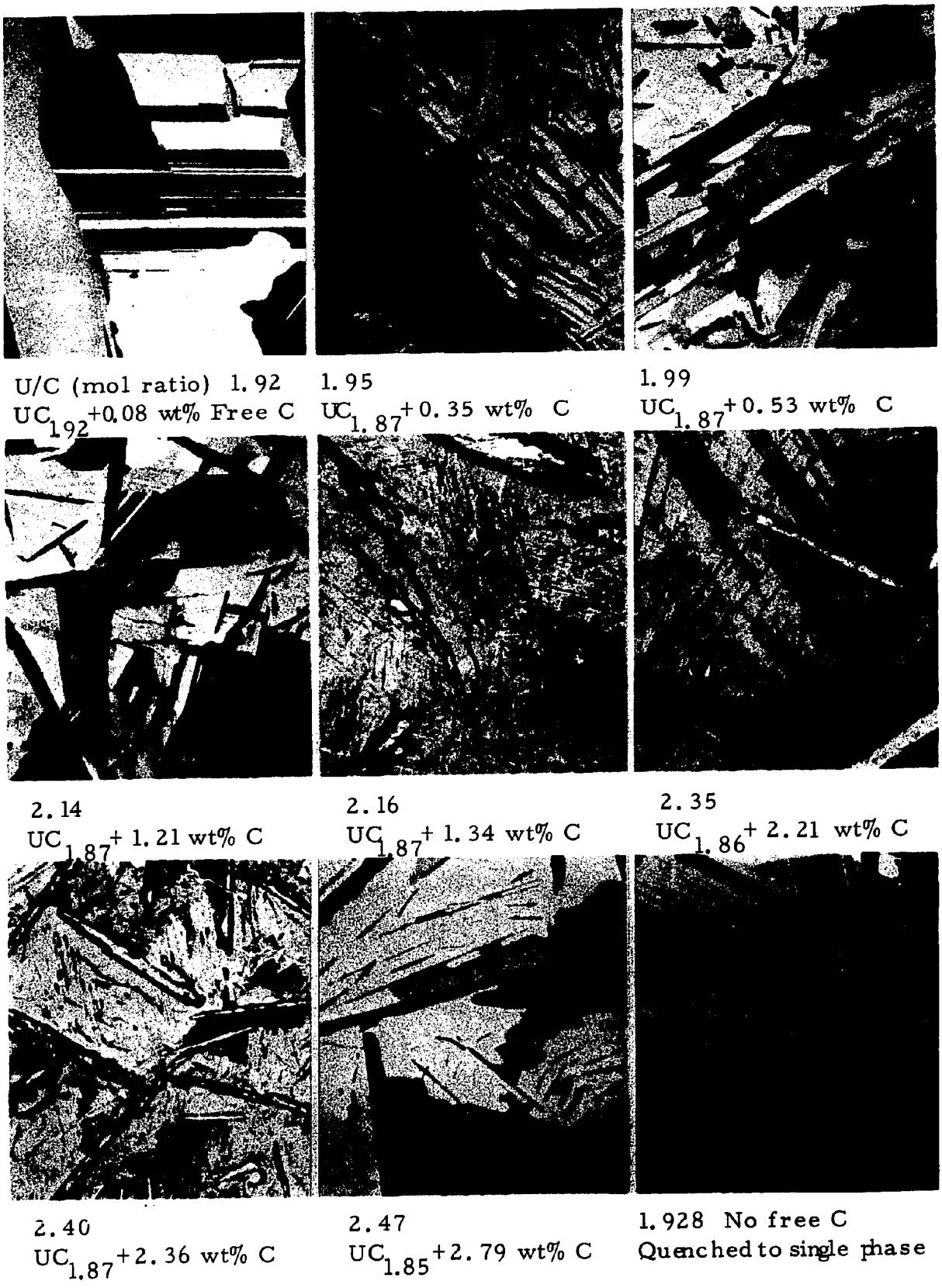
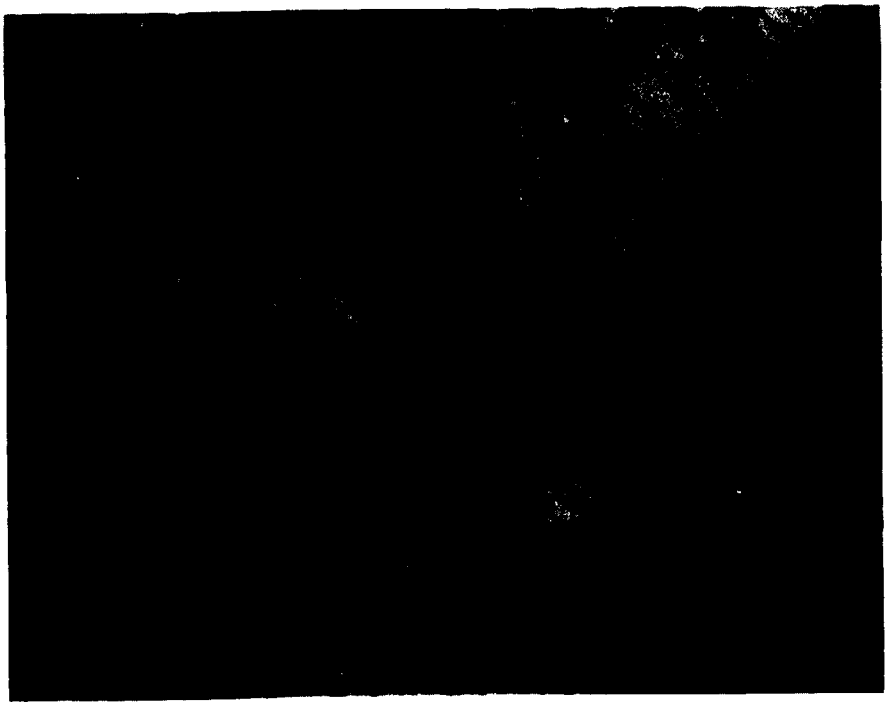


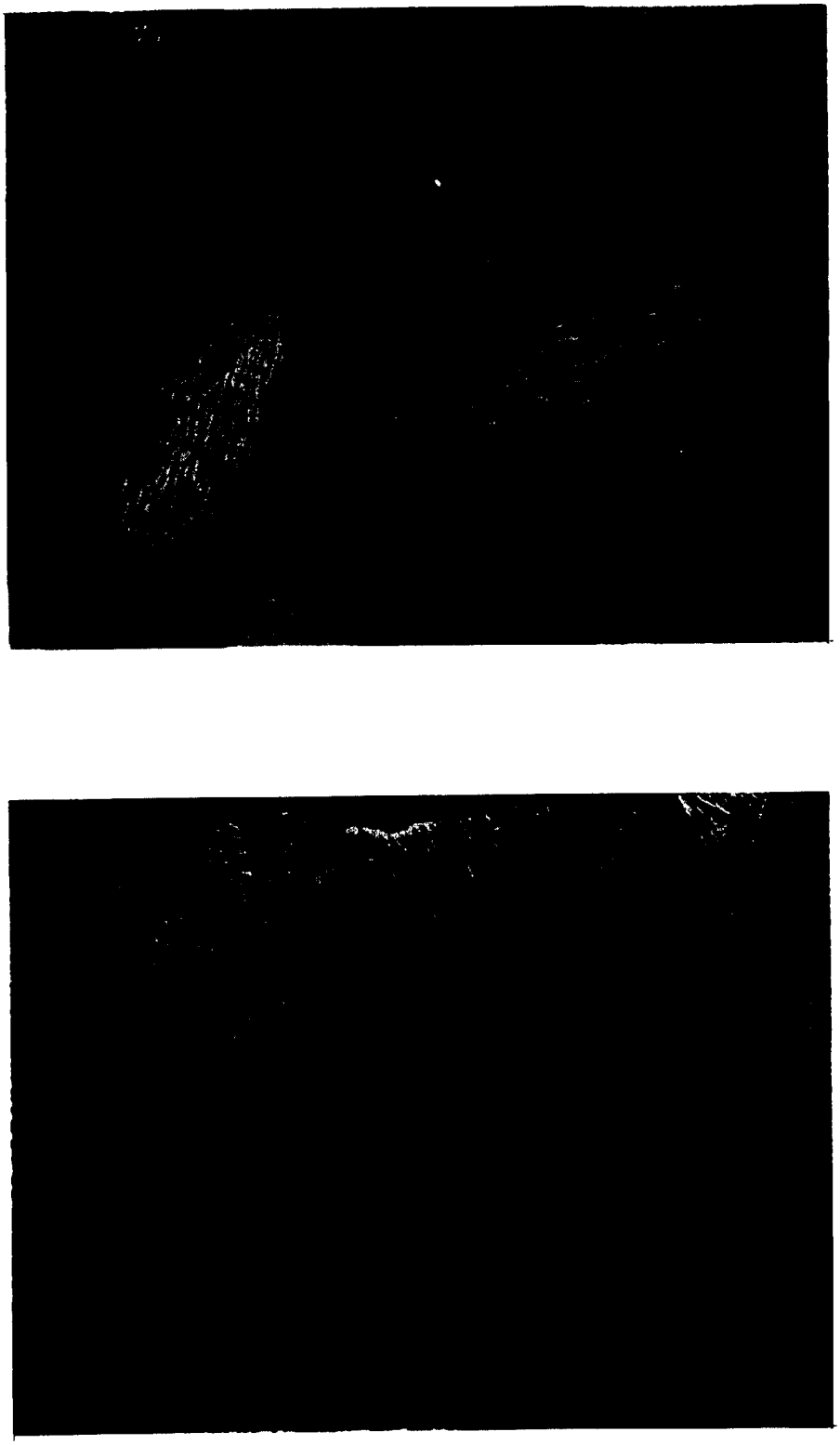
Figure C-1c. Microstructures in the Uranium Carbon System (250X). Printed with the permission of Mr. C.G. Hoffman.





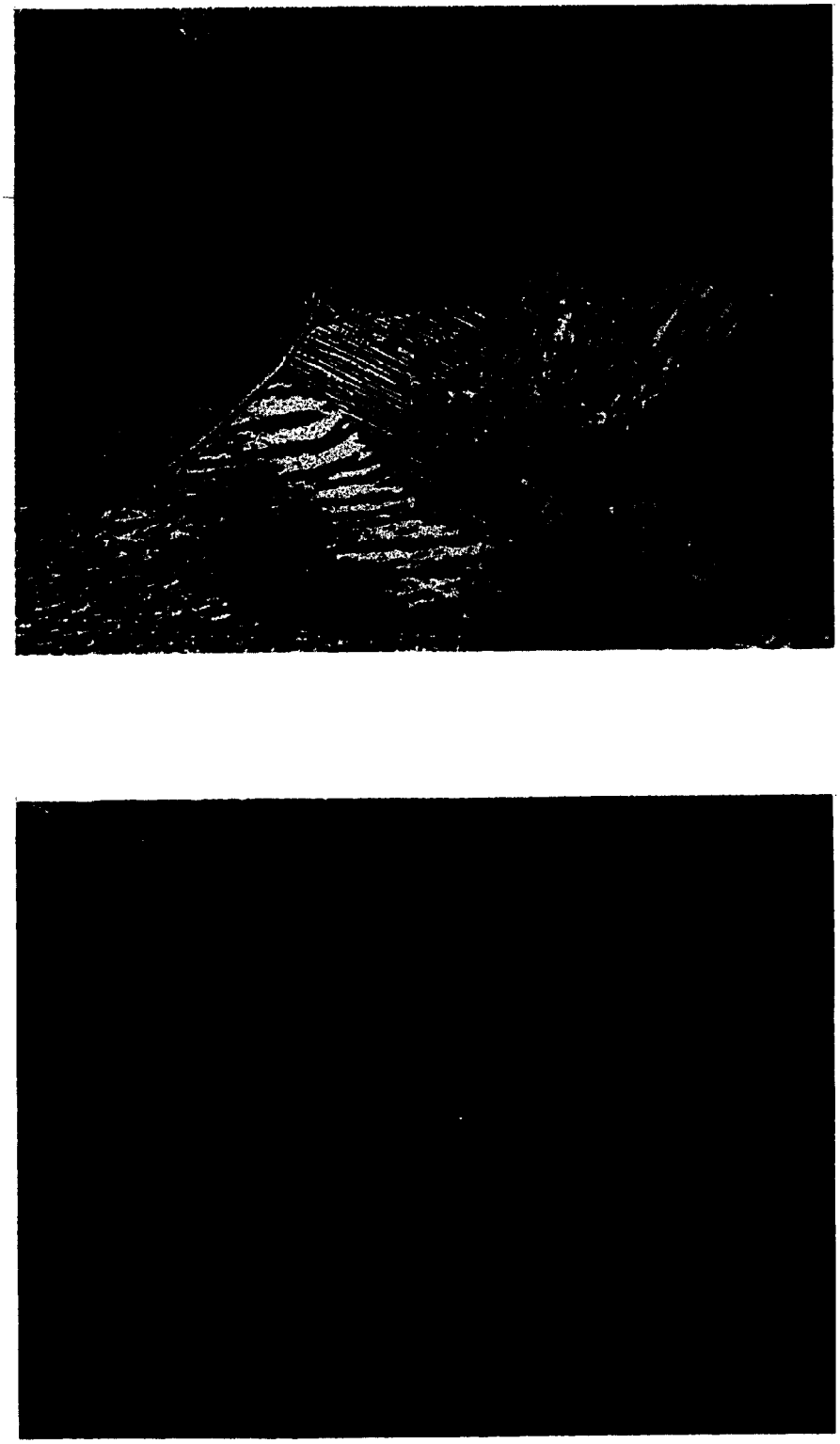
4049 DC
(500x)

Figure C-2. Microstructure of UC_2+C (4094 DC)



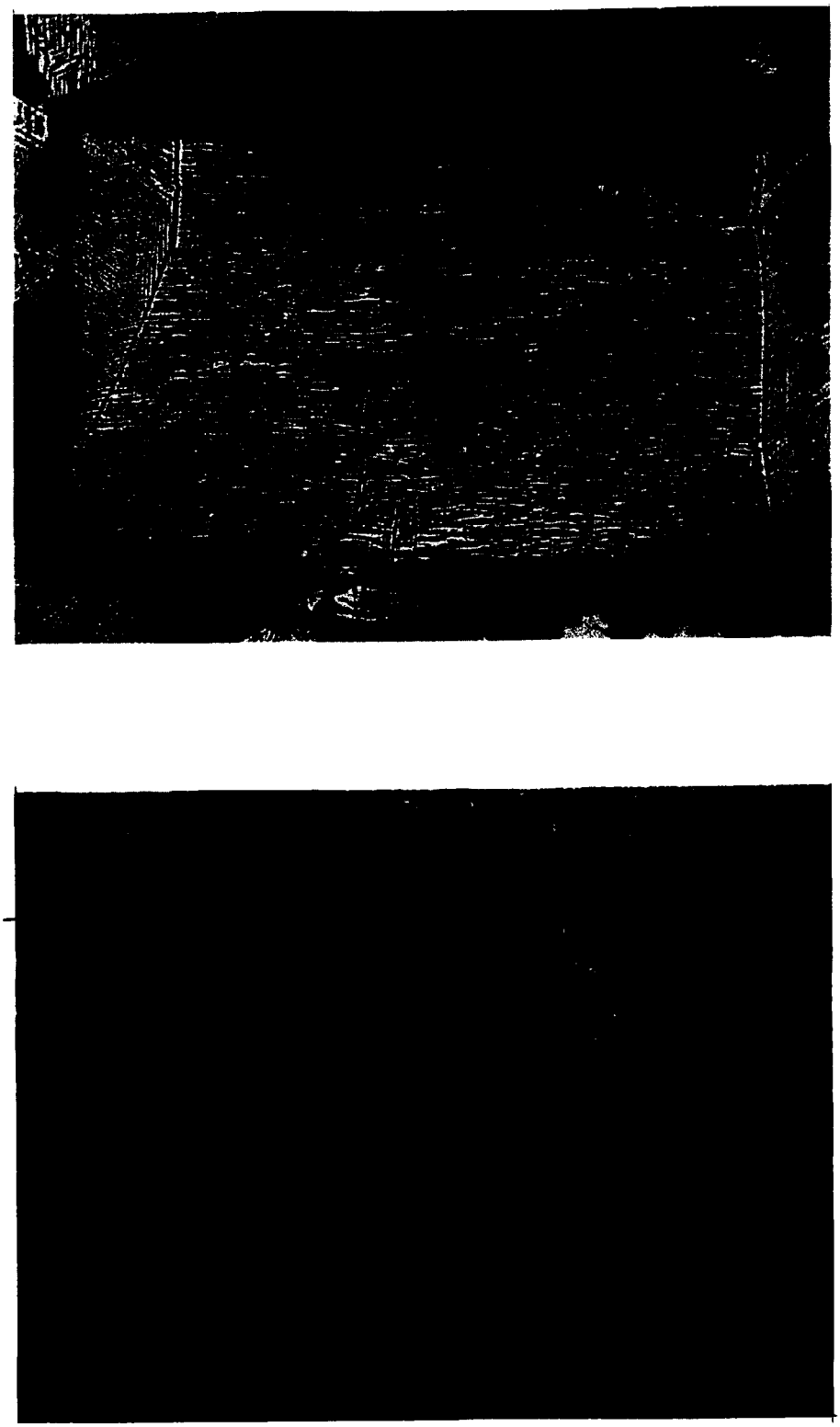
(500x) 5000 DC (250x)

Figure C-3. Microstructure of UC+UC_2 (5000 DC)



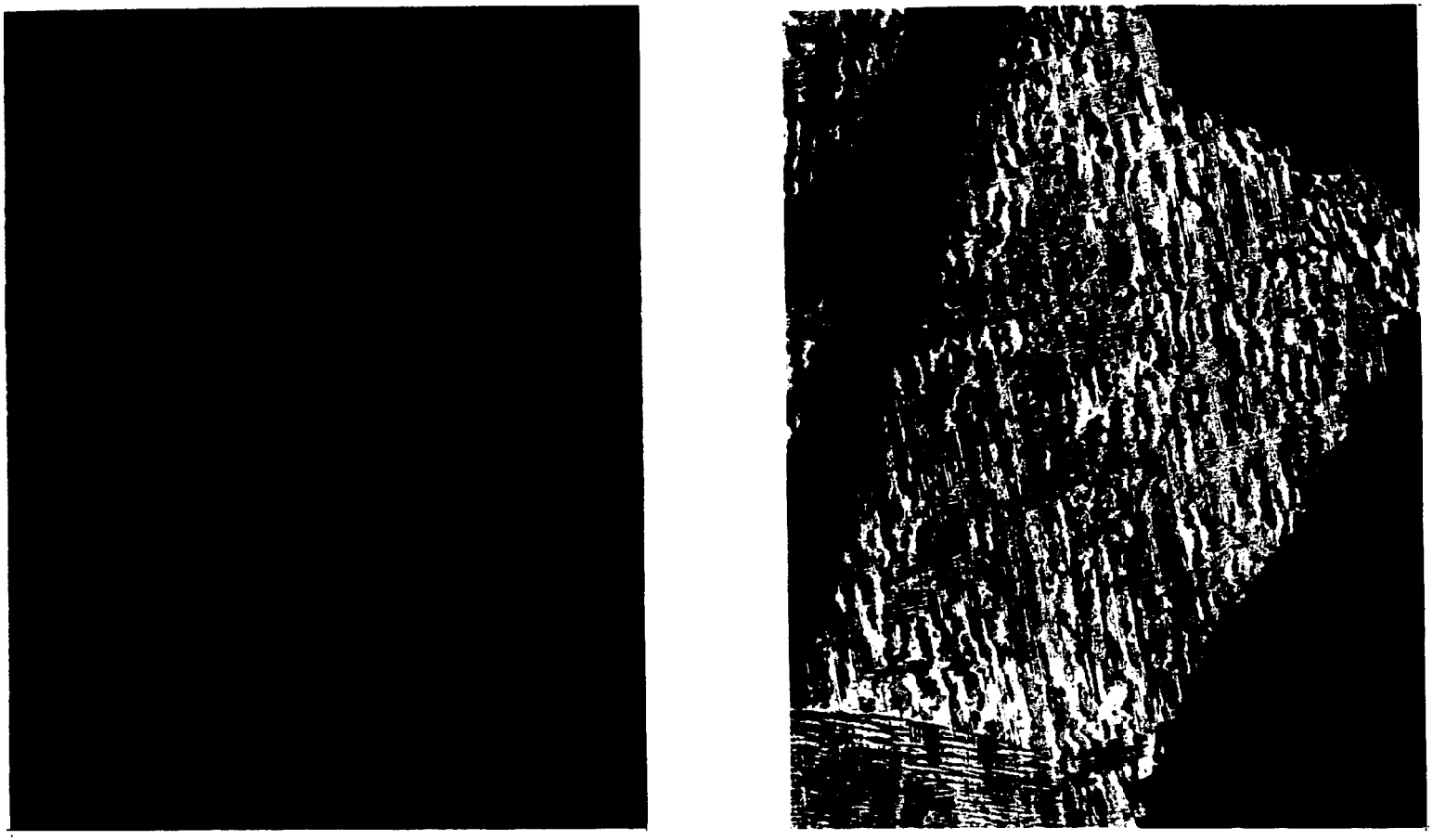
AM-11
(250x)

Figure C-4. Microstructure of Arc-Melted UC+UC_2 (AM-11)



AM-12
(250x)

Figure C-5. Microstructure of Arc-Melted UC+UC_2 (AM-12)



Residue Bi-32
(250x)

Figure C-6. Microstructure of Carbide in Residue of Bi-32

APPENDIX D*

CHEMICAL ANALYSIS

An X-Ray Spectrochemical Technique for Analyzing Low Uranium Concentrations in a Bismuth Matrix

Gordon W. Rankin

General Atomic/Division of General Dynamics Corporation
John Jay Hopkins Laboratory for Pure and Applied Sciences
San Diego, California

SUMMARY: An x-ray spectrochemical procedure for the analysis of low uranium concentrations in the presence of bismuth, using strontium as an internal standard, is described. The limit of detection is 0.1% and the accuracy is ±2% at the 2-3% level. The bismuth sample weight may vary up to 25% of the optimum 1.0 gram per 100 mls of solution with no serious change in accuracy. Average analysis time is 30 minutes.

*This appendix is printed with the permission of Mr. Rankin and is to be published as part of a report at a later time.

INTRODUCTION

Continued investigation of the uranium monocarbide and the uranium dicarbide compounds at General Atomic created a need for a rapid and quantitative method for analyzing bismuth melts for low uranium concentrations. The uranium concentration, it was thought at the time, varied from 1% to 3% by weight. In addition, it was necessary that any single analysis be completed in as little as 30 minutes from time of submittal.

Several approaches to this problem were available, most of them involving a separation of uranium and bismuth. All of these required more time per analysis than was available or were impractical to use. The more direct approach of determining uranium in the presence of bismuth by an x-ray spectrochemical technique was also considered. Ultimately, with the resolution of certain inherent problems, this latter procedure was developed.

The final x-ray procedure is an aqueous solution technique using strontium as an internal standard. The Kα line of strontium at 0.87660 Å and the Lα line of uranium at 0.91053 Å are used as analytical lines and their respective intensities are great enough to predict an accuracy of ±2%, or better, and a lower limit of detection of 0.1% uranium. These are obtainable, on an experimental basis, as indicated in the text.

STANDARD PREPARATION

Reagent grade uranyl nitrate, nitric acid, strontium nitrate, and bismuth metal are used for standard preparation.

A master solution of about 10 mg/ml of uranium is prepared by dissolving an appropriate quantity of uranyl nitrate in a predetermined volume. This is then standardized and the standard solutions are prepared by pipetting volumes containing 1, 5, 10, 20, 50 mg quantities of uranium into 100 ml volumetric flasks. To this is added 12.0 mg of strontium and 1.0 gram of bismuth (in solution). The standard is then diluted to volume with 5% by volume nitric acid.

The strontium master solution is prepared by dissolving strontium nitrate in water (~300 mg/ml). Successive dilutions produce other solutions of more usable concentrations. For instance, a 1/10 dilution is used in this procedure.

A 100 mg/ml bismuth solution is prepared by dissolving bismuth metal in nitric acid.

SAMPLE PREPARATION

The uranium-bismuth melt is dissolved in nitric acid and the sample solution is diluted to an appropriate calibrated volume.

Our samples are normally received in solution forms, the solid having been dissolved by the principal investigator. A volume of sample solution corresponding to 1 gram of bismuth is then transferred to a 100 ml volumetric flask, the strontium concentration is adjusted to 0.120 mg/ml and the acid concentration is adjusted to 5% by volume at full dilution.

These solutions are then compared to the standard solutions under the instrumental conditions as described herein.

INSTRUMENTAL CONDITIONS AND READOUT

The instrumentation used in the laboratory is an unmodified Norelco (Philips Electronics Company) full wave rectified 60 kv x-ray emission spectrograph. The source of excitation is a Philips Electronics Model FA-60 tungsten target x-ray tube operated at 50 kv - 40 ma. A 0.005" blade type entrance collimator, flat lithium fluoride crystal, and a sodium iodide-thallium activated scintillation detector are used to respectively collimate, diffract, and detect the characteristic radiation.

The intensities of the analytical lines are determined on a fixed count basis (i.e., the time required to record a specified number of counts is recorded). The count rates for both the strontium Kα

and the uranium Lα lines are recorded on each sample solution. These lines lie at 25.15°2θ and 26.14°2θ on our lithium fluoride crystal.

RESULTS AND DISCUSSION

In initiating this investigation, even though uranium is determined in many other matrices in the laboratory, some questions arose concerning the practicality of the method proposed (i.e., what would be the uranium Lα line to background ratio in the presence of large quantities of bismuth, since the bismuth $L\beta_1$ could conceivably swamp the uranium line; how would the close proximity of the bismuth L_{III} absorption edge affect the uranium Lα intensity; how much change in matrix characteristics would the strontium internal standard normalize without introducing significant error?). The answers to these questions seemed to be the determining factors so far as the applicability of the procedure was concerned.

A study of the L spectrum of bismuth in a bismuth-uranium melt indicated adequate resolution to enable one to resolve the uranium Lα from the bismuth $L\beta_1$. No problem was anticipated with the bismuth $L\beta_9$, $L\beta_{10}$, and $L\beta_5$ lines and even though line to background ratio for the uranium Lα was discouraging, 1.3 for a uranium concentration of 2% by weight, the counting statistics still predicted an accuracy better than ±2% and 0.1% as a limit of detection. Seemingly

then the effect of the bismuth L_{III} absorption edge did not decrease the uranium $L\alpha$ intensity so much as to seriously hamper the possibilities of a ±2% accuracy.

The applicability of strontium as an internal standard is illustrated in Table D-I. The sample weight values were allowed to vary 15-25% of the optimum weight of 1.0 gram and analyzed using standards based on the 1.0 gram weight. The precision of the resulting numbers is within the ±2% accuracy limits. It might be worth noting that the theoretical consideration that analysis of the system without an internal standard would produce numbers which were inversely proportional to the bismuth content was verified experimentally, making a direct comparison procedure impractical.

Table D-II is a tabulation of the analyzed results on several standards which were submitted periodically as control samples and effectively indicates the routine accuracy of the procedure. Several other standards were analyzed, but the resulting data only serves to substantiate the trend observed in Table D-II. Sample 32-6 represents the widest spread observed between analyzed and prepared data and was included for this reason.

A representative calibration curve, prepared by plotting the ratio of strontium line intensity to uranium line intensity against concentration for each standard, is represented in Figure D-1. The curve is smooth, continuous and reproducible.

TABLE D-I

EFFECT OF THE CHANGE IN SAMPLE WEIGHT
WHEN USING STRONTIUM AS AN INTERNAL STANDARD

	I		II		III	
Sample Wt.	0.7722g	0.9266g	1.0451g	0.7835g	0.9684g	1.2105g
% Uranium	3.79	3.76	3.57	3.56	3.99	3.93

TABLE D-II

REPRODUCIBILITY AND ACCURACY OF THE DETERMINATION OF URANIUM. COMPARISON OF X-RAY ANALYSIS DATA TO KNOWN VALUES

	Uranium Concentrations (mg)	
Samples	X-Ray Analysis	Known Values (added)
26-17	51.7, 51.1	51.9
26-18	54.9, 55.1	55.2
31-11	52.9	53.3
31-12	48.9	49.0
32-5	55.7, 55.7	55.2
32-6	62.0, 62.3	61.1

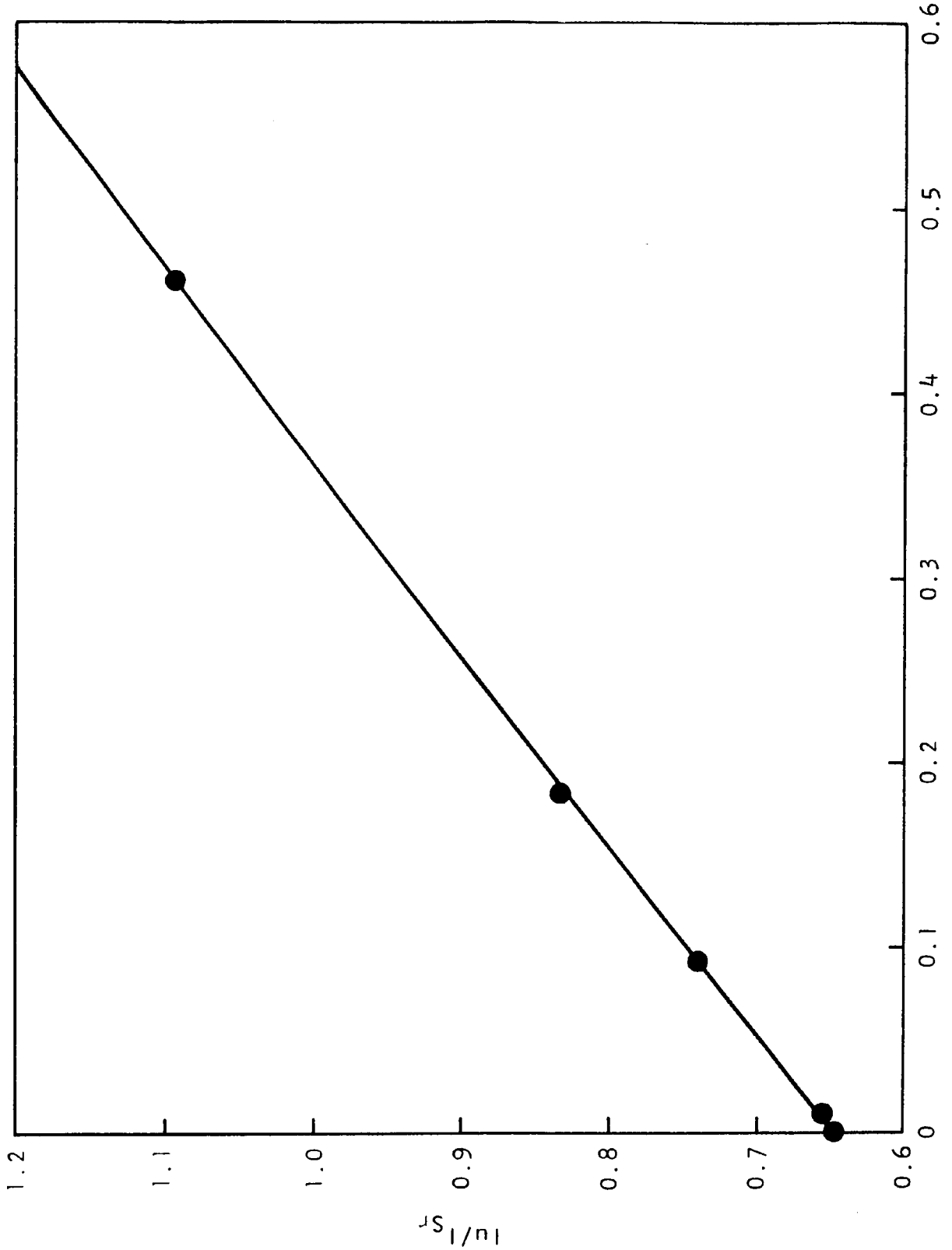


Figure D-1. Representative Calibration Curve

APPENDIX E

DATA

Run Bi-14

Melt - Bismuth

Carbide - UC_2 + C (4094 DC)

Sample Number	Temperature (°K)	Concentration (Wt % U)
1	1066	No Sample
2	1066	No Sample
3	1065	0.99, 0.91
4	1065	0.99
5	1116	No Sample
6	1118	No Sample

Run Bi-16

Melt - Bismuth

Carbide - UC_2 + C (4094 DC)

Sample Number	Temperature (°K)	Concentration (Wt % U)
1	1070	0.83, 0.84
2	1071	No Sample
3	1069	No Sample
4	1068	No Sample
5	1070	1.4, 1.3
6	1116	1.7, 1.6
7	1116	1.5, 1.6
8	1179	1.9, 1.8
9	1168	1.5, 1.6

Note: Power turned off accidentally ~120 hours; back up to temperature 1180°K at 140 hours.

Run Bi-18

Melt - Bismuth

Carbide - UC_2 + C (4094 DC)

Sample Number	Temperature (°K)	Concentration (Wt % U)
1	1164	0.95
2	1118	1.9
3	1115	No Sample
4	1116	No Sample
5	1116	No Sample
6	1115	No Sample
7	1018	1.4
8	1116	1.6
9	1064	1.5
10*	1064	1.2

*Sample probably low in uranium due to oxidation because of leak in reaction chamber.

Run Bi-19

Melt - Bismuth

Carbide - UC_2 + C (4094 DC)

Sample Number	Temperature (°K)	Concentration (Wt % U)	Lapsed Time (hours)
1	1158	0.18, 0.22	24
2	1158	1.4, 1.4	44
3	1110	1.7, 1.7	67.8
4	1107	1.7, 1.8	92.6
5	1061	1.7, 1.7	118.1
6	1061	1.6, 1.6	138.3
7	1016	1.4, 1.5	195.4
8	1015	1.4, 1.4	213.2
9	1065	1.4, 1.4	237.1
10	1065	1.4, 1.4	256.6
11	1116	1.67, 1.73	283.3
12	1115	1.81, 1.76	306.3
13	1014	1.62, 1.62	330.2
14	1015	1.54, 1.57	353.4
15	1153	1.79, 1.86	378.0
16	1152	1.87, 1.85	381.5
17*	1150	0.79, 0.83	383.9
18	1154	1.94, 2.00	404.0
19	1152	1.94, 1.98	405.4
20	1153	No Sample	426.0

*Used Vycor sampler - appears to have reacted with the sample.

Note: Power shut off (relay failure) at ~142 hours - back up to temperature (1015°K) at 163 hours.

Power shut off at 1935 hours to replace relay - back at temperature (1015°K) 195 hours.

Run Bi-20

Melt - Bismuth

Carbide - UC_2 + C (4094 DC)

Sample Number	Temperature (°K)	Concentration (Wt % U)	Lapsed Time (hours)
1	1167	1.5, 1.52	69.1
2	1168	1.93, 1.96	93.5
3	1121	1.96, 1.98	114.6
4	1117	1.84, 1.86	141.4
5	1066	1.75, 1.75	160.6
6	1066	No Sample	185.9
7	1065	1.53, 1.54	233.7
8	1014	1.52, 1.54	263.0
9	1015	1.41, 1.43	286.0
10	964	1.34, 1.39	310.6
11	967	1.37, 1.40	333.6
12	1016	1.30, 1.31	380.4
13	1015	1.27, 1.31	405.3
14	1065	No Sample	429.4
15	1065	1.26, 1.28	432.7
16	1065	1.27, 1.30	450.3
17	1110	No Sample	473.3
18	1114	No Sample	
19	1113	No Sample	
20	1114	No Sample	521.3

Run Cd-2

Melt - Cadmium

Carbide - UC_2 + C (4094 DC)

Sample Number	Temperature (°K)	Concentration (Wt % U)	Lapsed Time (hours)
1	750	<100 ppm	53.4
2	751	<100 ppm	75.1
3	803	<100 ppm	102.5
4	803	<100 ppm	122.1
5	849	No Sample	148.3

Run Bi-26

Melt - Bismuth

Carbide - $UC + UC_2$ (5000 DC)

Sample Number	Temperature (°K)	Concentration (Wt % U)	Lapsed Time (hours)
1	1162	2.23, 2.27	2.3
2	1165	2.11, 2.17	13.6
3	1166	1.98, 2.01	36.4
4	1163	2.36, 2.36	61.5
5	1164	2.19, 2.21	71.8
6*	1165	1.92, 1.95	85.6
7**	1163	2.47, 2.50	99.1
8	1163	2.34, 2.43	108.9
9	1165	2.19, 2.13	136.1
10	1165	2.27, 2.23	157.5
11	1164	2.14, 2.15	181.6
12	1015	2.19, 2.26	205.5
13	1014	2.08, 2.05	229.7
14	1013	2.02, 2.03	254.0
15	1013	1.94, 1.95	277.3
16	1160	1.80, 1.78	303.5

*This point probably low due to oxidation melt which occurred at 73.2 hours.

**This point is high because uranium was added at 96.4 hours to drive the concentration above the equilibrium value.

Note: Stirrer was not working during first 85 hours of run. Carbide was added at 43.7, 73.2, 137.2, 214.6, and 255.7 hours.

Run Bi-27

Melt - Bismuth

Carbide - UC + UC_2 (5000 DC)

Sample Number	Temperature (°K)	Concentration (Wt % U)	Lapsed Time (hours)
1*	1114	2.76, 2.72	4.7
2*	1116	2.77, 2.80	24.4
3*	1116	2.76, 2.73	46.7
4*	1115	2.88, 2.92	70.5
5*	1115	2.88, 2.86	94.3
6*	1116	2.85, 2.84	95.5
7*	1115	2.93, 2.91	96.8
8*	1115	2.88, 2.92	99.2
9	1115	2.52, 2.56	142.7
10	1118	2.39, 2.43	166.9
11	1117	2.17, 2.13	193.6
12	1116	2.59, 2.63	214.0
13	1116	1.93, 1.94	237.7
14	1117	1.96, 1.96	261.3
15	1117	1.73, 1.73	285.1
16	1118	1.57, 1.56	309.5
17	1118	1.57, 1.56	333.8
18**	1119	1.13, 1.13	358.6

*No carbide in melt.

**Probably no good due to oxidation of melt because of an open valve.

Note: Carbide added 122 hours and then after each subsequent sample.

Run Bi-32

Melt - Bismuth

Carbide - AM-12

Sample Number	Temperature (°K)	Concentration (Wt % U)	Lapsed Time (hours)
1*	1115	1.42, 1.42	0
2	1116	1.88, 1.89	67.5
3	1117	1.97, 1.97	114.7
4	1117	1.90, 1.90	163.0
7	1117	1.95, 1.95	234.4
8**	1115	1.88, 1.88	329.5
9	1116	1.95, 1.97	405.6
10	1114	2.19, 2.20	436.2
11	1115	2.10, 2.10	498.3
12***	1115	2.22, 2.24	570.4
13	1116	2.02, 2.03	619.0
14	1115	1.95, 1.95	666.7
15	1115	1.99	738.4
16	1115	1.95, 1.96	746.7

*No carbide in the melt.

**Sample analysis in doubt because of loss of some of the sample.

***Sample probably no good because of poorly seated filter.

Note: Carbide added at 19.1 and 260.4 hours.
Uranium added at 432.3 hours.

BIBLIOGRAPHY

1. Alcock, C.B., H.A. Eick, E.G. Rauh and R.J. Thorn, "A Comparison of the Calculated and Observed Vaporization Behavior of the Uranium Dicarbide Phase", International Symposium on Compounds of Interest in Nuclear Reactor Technology, Colorado, August 3-5, 1964.

2. Alcock, C.B. and P. Grieveson, "Study of Uranium Borides and Carbides by Means of the Knudsen Effusion Technique", Symposium on the Thermodynamics of Nuclear Materials, International Atomic Energy Agency, Vienna, May 21-25, 1962 .

3. Alcock, C.B. and P. Grieveson, "A Thermodynamic Study of the Compounds of Uranium with Silicon, Germanium, Tin, and Lead", J. Inst. Metals 90, 304-310 (1962).

4. Alexander, C.A., J.J. Ward, J.S. Ogden and G.W. Cunningham, "Thermodynamics for Compatibility Studies of Metal Clad Uranium Carbide", Symposium on Carbides in Nuclear Energy, Harwell, November 5-7, 1963.

5. Balzhiser, R.E. and D.V. Ragone, "Decomposition of Uranium Dicarbide in Bismuth", Symposium on Liquid Metal Corrosion and Phenomena, Washington, D.C., 1965.

6. Boettcher, A. and G. Schneider, Proceedings of the Second United Nations International Conference on the Peaceful Uses of Atomic Energy, Geneva, 1958.

7. Chiotti, P., H.H. Klepfer and K.J. Gill, "Uranium-Zinc System", J. of Metals, 51-55 (1957).

8. Combarieu, A. de, P. Costa and J.C. Michel, Compt. Rend. 256, 5518-21 (1963).

9. Cunningham, G.W., J.J. Ward and C.A. Alexander, "Thermodynamics for Compatability Studies of Metal-Clad Uranium Carbide", Report No. BMI-1601, 1962.

10. Darken, L.S. and R.W. Gurry, "Physical Chemistry of Metals", McGraw-Hill Book Company, Inc., New York, 1953.

11. Droege, J. W., A. W. Lemmon and R. B. Filbert, Report No. BMI-1313, 1959.

12. Eick, H. A., E. G. Rauh and R. J. Thorn, "Vaporization Studies of the Uranium Dicarbide Phase", Symposium on the Thermodynamics of Nuclear Materials, International Atomic Energy Agency, Vienna, May 21-25, 1962.

13. Farr, J. D., E. J. Huber, E. L. Head and C. E. Holley, J. Chem. Phys. 63, 1455 (1959).

14. Farr, J. D., W. G. Witteman, P. L. Stone and E. F. Westrum, Jr., "Uranium Dicarbide and Diuranium Tricarbide: Preparation and Chemical Thermodynamic Properties from 5 to 350°K", Third Symposium on Thermophysical Properties, Purdue University, March 22-26, 1965.

15. Fujishiro, S. J., J. Atomic Energy Soc. Japan 3, 913 (1961).

16. Harrington, L. C. and G. H. Rowe, "The Enthalpy and Heat Capacity of Uranium Monocarbide to 1200°C", Report No. PWAC-426, 1964.

17. Henney, J., N. A. Hill and D. T. Livey, "A Review of Data in the Light of Recent Phase Equilibrium Studies", Report No. AERE-R 4175, 1962.

18. Henney, J., D. T. Livey, N. A. Hill, "Some Effects of Oxygen and Nitrogen as Impurities on Equilibria in the Uranium Carbon System", Report No. AERE-R 4176, 1963.

19. Huber, E. J., Jr., E. L. Head and C. E. Holley, Jr., "The Heat of Formation of Uranium Dicarbide", J. Phys. Chem. 67, 1730-1 (1963).

20. Huber, E. J., Jr. and C. E. Holley, Jr., "The Thermodynamic Properties of the Actinide Carbides Including New Measurements of the Heats of Formation of some Thorium, Uranium, and Plutonium Carbides", Symposium on the Thermodynamics of Nuclear Materials, International Atomic Energy Agency, Vienna, May 21-25, 1962.

21. Johnson, I. and H. M. Feder, "Thermodynamics of the Binary Systems of Uranium with Zn, Cd, Ga, In, Tl, Sn and Pb", Symposium on Thermodynamics of Nuclear Materials, International Atomic Energy Agency, Vienna, May 21-25, 1962.

22. Katz, J. J. and E. Rabinowitch, "The Chemistry of Uranium", McGraw-Hill Publishing Company, Inc., New York, 1951.

23. Lebeau, P., Compt. Rend. 152, 955 (1911).

24. Leitnaker, J. M. and W. G. Witteman, "The Dissociation Pressure of Uranium Dicarbide", J. Chem. Phys. 36, 1443-52 (1962).

25. Levinson, L. S., "High Temperature Heat Content of Uranium Carbides", Symposium on Carbides in Nuclear Energy, Harwell, November 5-7, 1963.

26. Lewis, G. N. and M. Randall, Revision by K. S. Pitzer and L. Brewer, "Thermodynamics", McGraw-Hill Book Company, Inc., New York, 1961.

27. Lonsdale, H. K. and J. N. Graves, "Vaporization of the Dicarbides of Uranium, Thorium and Protactinium", Report No. GA-3015, 1962.

28. Mallett, M. W., A. F. Gerds and H. R. Nelson, "The Uranium-Carbon System", J. Electrochem. Soc. 99, 197-204 (1952).

29. Mallett, M. W., A. F. Gerds and D. A. Vaughn, "Uranium Sesquicarbide", J. Electrochem. Soc. 98, 505-509 (1951).

30. Moissan, H., Compt. Rend. 122, 274 (1896).

31. Mukaibo, T. and K. Naito, "On the Thermochemical Properties of Uranium Carbides", J. Atomic Energy Soc. Japan 5, 601-8 (1963).

32. Mukaibo, T., K. Naito, K. Sato and T. Uchijima, "The Measurement of the Specific Heats of Uranium Carbides Above Room Temperature", Symposium on the Thermodynamics of Nuclear Materials, International Atomic Energy Agency, Vienna, May 21-25, 1962.

33. Norman, J. H. and P. Winchell, "Mass Spectrometry-Knudsen Cell Studies of the Vaporization of Uranium Dicarbide", J. Phys. Chem. 68, 3802-5 (1964).

34. Pattoret, A., S. Smoes and J. Drowart, "Thermodynamic Studies by Mass Spectrometry - Thermodynamic Study of the Uranium-Oxygen System by Mass Spectrometry: The Heat of Sublimation of Uranium", EURATOM Report EUR 2458, Dounreay Translation 224, 1965.

35. Piazza, J. R. and M. J. Sinnott, "High Temperature Phase Equilibria in the System Carbon-Oxygen-Uranium", J. Chem. Eng. Data 7, 451-7 (1962).

36. Rand, M. H. and O. Kubaschewski, "The Thermochemical Properties of Uranium Compounds", Report AERE-R 3487, 1960.

37. Rauh, E. G. and R. J. Thorn, J. Chem. Phys. 22, 1414, 1954.

38. Rice, P. A., D. V. Ragone and R. E. Balzhiser, "Thermodynamics of the Uranium-Bismuth System", Symposium on Thermodynamics of Nuclear Materials, International Atomic Energy Agency, Vienna, May 21-25, 1962.

39. Robinson, W. C. and P. Chiotti, "Reactions of Uranium Carbide in a Fused KCl-LiCl/Zinc System", Report 1S-1061, 1964.

40. Storms, E. K., "A Mass Spectrometric Study of the Vapor Pressure of U(g) and UC_2(g) over Various Compositions in the Uranium-Carbon System", Report LA-DC-6953, 1965.

41. Storms, E. K., "A Critical Review of Refractories", Report No. LA 2942, 1964.

42. Tien, L. C., K. J. Guion and R. D. Pehlke, Symposium on Thermodynamics, International Atomic Energy Agency, Vienna, 1965.

43. "The Uranium Carbon and Plutonium-Carbon Systems, A Thermochemical Assessment", A Panel Report, International Atomic Energy Agency, Technical Report Series No. 14, Vienna, October 8-12, 1962.

44. The Fourth Uranium Carbide Conference, East Hartford, Connecticut, May 20-21, 1963, Report No. TID-7676.

45. Vozzella, P.A., A.D. Miller and M.A. De Crescente, Report No. PWAC-378, 1963.

46. Volk, W., "Applied Statistics for Engineers", McGraw-Hill Book Company, Inc., New York, 1958.

47. Wagner, C., "Thermodynamics of Alloys", Addison-Wesley Publishing Company, Inc., Reading, Massachusetts, 1952.

48. Westrum, E.F., Jr., "Cryothermal Properties of Uranium Nitride, Carbides and Chalcognides", International Symposium on Compounds of Interest in Nuclear Reactor Technology, Colorado, 1964.

49. Westrum, E.F., Jr., E. Suits and H.K. Lonsdale, "Uranium Monocarbide and Hypostoichiometric Dicarbide. Heat Capacities and Thermodynamic Properties from 5 to 350°K", Third Symposium on Thermophysical Properties, Purdue University, March 22-26, 1965.

50. Wilhelm, H.A., P. Chiotti, A.I. Snow and A. Daane, J. Chem. Soc. 1949, (Suppl. Issue No. 2), S 318-21.